T.R.
GEBZE TECHNICAL UNIVERSITY
GRADUATE SCHOOL OF NATURAL AND APPLIED SCIENCES

RICINOLEIC ACID-BASED FUNCTIONAL POLYMERS

MAGDALENA MARİA TONTA
A THESIS SUBMITTED FOR THE DEGREE OF
DOCTOR OF PHILOSOPHY
DEPARTMENT OF CHEMISTRY

GEBZE
2019

T.R.

GEBZE TECHNICAL UNIVERSITY

GRADUATE SCHOOL OF NATURAL AND APPLIED SCIENCES

RICINOLEIC ACID-BASED FUNCTIONAL POLYMERS

MAGDALENA MARİA TONTA

A THESIS SUBMITTED FOR THE DEGREE OF

DOCTOR OF PHILOSOPHY

DEPARTMENT OF CHEMISTRY

THESIS SUPERVISOR

PROF. DR. AYŞE GÜL GÜREK

II. THESIS SUPERVISOR

ASSOC. PROF. DR. SERDAR SEZER

GEBZE

2019

T.C.
GEBZE TEKNİK ÜNİVERSİTESİ
FEN BİLİMLERİ ENSTİTÜSÜ

RİSİNOLEİK ASİT BAZLI FONKSYONEL POLİMERLER

MAGDALENA MARİA TONTA

DOKTORA TEZİ
KİMYA ANABİLİM DALI

TEZ DANIŞMANI
PROF. DR. AYŞE GÜL GÜREK
TEZ II. DANIŞMANI
DOÇ. DR. SERDAR SEZER

GEBZE
2019

GEBZE TEKNİK ÜNİVERSİTESİ	**DOKTORA JÜRİ ONAY FORMU**

GTÜ Fen Bilimleri Enstitüsü Yönetim Kurulu'nun 03/07/2019 tarih ve 2019/30 sayılı kararıyla oluşturulan jüri tarafından 12/07/2019 tarihinde tez savunma sınavı yapılan Magdalena Maria TONTA'ın tez çalışması Kimya Anabilim Dalında DOKTORA tezi olarak kabul edilmiştir.

JÜRİ

ÜYE (TEZ DANIŞMANI)	: Prof. Dr. Ayşe Gül GÜREK
ÜYE	: Prof. Dr. Hayal BÜLBÜL SÖNMEZ
ÜYE	: Dr. Öğr. Üyesi Semra YILMAZER KESKİN
ÜYE	: Dr. Öğr. Üyesi İlke ANAÇ
ÜYE	: Prof. Dr. Mehmet Atilla TAŞDELEN

ONAY

Gebze Teknik Üniversitesi Fen Bilimleri Enstitüsü Yönetim Kurulu'nun

...../...../2019 tarih ve 2019/..... sayılı kararı.

SUMMARY

Ricinoleic acid is a component of various bio-based copolymers. However, synthesis and properties of high-molecular-weight polyricinoleate homopolymers are not widely investigated due to high cost of monomer and catalysts.

In the first part of this thesis, low cost approach for the synthesis of high-molecular-weight polyricinoleate is presented by preparation large amount of pure monomer and use commercial lipase Lipozyme TL IM as catalyst. Polymerization conditions were optimized and comparative study of medium-molecular-weight polyricinoleate (PRA-M) of M_w = 30 000 $gmol^{-1}$ and high-molecular-weight polyricinoleate (PRA-H) of M_w = 72 000 $gmol^{-1}$ properties was conducted. Next, polyepoxyricinoleate (PER) Mw = 74 000 $gmol^{-1}$ was prepared from PRA-H. Polyricinoleates and polyepoxyricinoleate were characterized by ^{1}H NMR, ^{13}C NMR, FT-IR, GPC, DSC and TGA.

In the second part of this thesis, coating and rheological properties, *in vitro* degradation, antibacterial activity, lap-shear adhesion strength and cytotoxicity of synthesized polymers were investigated.

Key Words: Ricinoleic Acid, Polyricinoleate, Polyepoxyricinoleate, Lipozyme TL IM, Polycondensation.

ÖZET

Risinoleik asit, çeşitli biyo-bazlı kopolimerlerin bir bileşenidir. Fakat, yüksek molekül ağırlıklı polirisinoleat homopolimerlerinin sentezi ve özellikleri, monomer ve katalizörlerin maliyetli olmasından dolayı geniş bir şekilde araştırılmamaktadır.

Bu tezin ilk bölümünde, yüksek molekül ağırlıklı polirisinoleat sentezi için düşük maliyetli yaklaşım, büyük miktarda saf monomerin hazırlanmasıyla ve ticari lipaz Lipozyme TL IM kullanılmasıyla gösterildi. Polimerizasyon koşulları optimize edildi ve orta molekül ağırlıklı (PRA-M) (M_w = 30 000 $gmol^{-1}$) ve yüksek molekül ağırlıklı (PRA-H) (M_w = 72 000 $gmol^{-1}$) polirisinoleat'ın karşılaştırılmalı incelemesi yapıldı.

Daha sonra, poliepoksirisinoleat (PER) M_w = 74 000 $gmol^{-1}$, PRA-H'den hazırlandı. Polirisinoleat'lar ve poliepoksirisinoleat, ^{1}H NMR, ^{13}C NMR, FT-IR, GPC, DSC ve TGA ile karakterize edildi. Bu tezin ikinci bölümünde, sentezlenen polimerlerin, kaplama ve reolojik özellikleri, *in vitro* degradasyon, antibakteriyel aktivite, yapışma gücü ve sitotoksisite gibi özellikleri araştırıldı.

Anahtar Kelimeler: Risinoleik Asit, Polirisinoleat, Poliepoksirisinoleat, Lipozyme TL IM, Polikondansasyon.

ACKNOWLEDGEMENTS

Firstly, I would like to express my sincere gratitude to my advisor Prof. Dr. Ayşe Gül Gürek for her continuous support and valuable guaidance during my PhD study. I would like to thank my co-advisor Assoc. Prof. Dr. Serdar Sezer whose expertise was invaluable in the formulating of my research topic and who was always serving advice. Special thanks to Dr. Ümran Aydemir Sezer for her patience, time and valuable guidance and suggestions during all stages of my thesis.

I would also like to thank my thesis steering committee members, Prof. Dr. Hayal Bülbül Sönmez and Dr. Semra Yılmazer Keskin for their time and guidance.

I gratefully acknowledge the financial support of this thesis by Gebze Technical University (2017-A102-14 Project).

I would like to thank my friend Zeynep M. Şahin for providing me with unfailing support and continuous encouragement throughout years of study and through the process of researching and writing this thesis.

I owe special thanks to İsa Şahin for his constant help with laboratory experiments and support with solving problems. I would like to thank Başak Aru for support with blood clotting time and cytotoxicity experiments.

I would also like to extend my gratitude to my laboratory mates Dr. Sümeyra Bayır and Figen Aynalı for their friendship and great memories.

Lastly, I would like to thank my family for all their love and encouragement. For my parents, who raised me with a love of science and supported me in all my pursuits. And most of all for my loving, supportive, encouraging, and patient husband Gürkan Tonta whose faithful support during all stages of this Ph.D. is so appreciated. Thank you.

TABLE of CONTENTS

	Page
SUMMARY	v
ÖZET	vi
ACKNOWLEDGEMENTS	vii
TABLE of CONTENTS	viii
LIST of ABBREVIATIONS and ACRONYMS	xi
LIST of FIGURES	xiii
LIST of TABLES	xvi
1. INTRODUCTION	1
2. VEGETABLE/PLANT OILS	2
2.1. Castor Plant (Ricinus communis) and Obtaining of Castor Oil	4
2.2. Castor Oil	7
2.3. Plant Oil Based Polymers	9
2.3.1. Plant Oil Based Polymers Obtained in Free Radical Polymerization	9
2.3.1.1. Unmodified Plant Oils Used As Monomers	10
2.3.1.2. Plant Oils after Double Bond Modifications Used as Monomers	11
2.3.1.3. Plant Oils with Triglyceride Ester Modifications Used as Monomers	17
2.3.2. Plant Oil Based Polymers Obtained by Cationic Polymerization	18
2.3.2.1. Plant Oil Based Vinyl Monomers in Cationic Polymerization	18
2.3.2.2. Plant Oils Epoxides in Cationic Polymerization	19
2.3.3. Olefin Metathesis in Polymerization of Plant Oil Based Monomers	20
2.3.4. Acyclic Diene Metathesis Polymerization (ADMET) in Polymerization of Plant Oil Based Monomers	21
2.3.5. Ring-Opening Metathesis Polymerization (ROMP) in Polymerization of Plant Oil Based Monomers	22
2.3.6. Condensation Polymerization of Plant Oil Based Monomers	24
2.3.6.1. Plant Oil Based Polyesters	24
2.3.6.2. Plant Oil Based Polyamides	26
2.3.6.3. Plant Oil Based Polyurethanes	27

2.4. Castor Oil and Ricinoleic Acid Based Polymers 28
3. RESEARCH OBJECTIVE 30
4. EXPERIMENTAL 31
4.1. Materials 31
4.2. Instrumentation 31
4.3. Monomer Preparation 34
4.3.1. Esterification of Ricinoleic Acid (>80%) 34
4.3.2. Conversion of Ricinoleic Acid (>80%) into FAME 35
4.3.3. Isolation of Methyl Ricinoleate from FAME 36
4.4. Enzymatic Polymerization of Methyl Ricinoleate 39
4.4.1. Selection of Lipase Catalyst 40
4.4.2. Effect of Reaction Temperature on Molecular Weight of Polyricinoleate 41
4.4.3. Effect of Enzyme Concentration on Molecular Weight of Polyricinoleate 41
4.4.4. Effect of Reaction Time on Molecular Weight of Polyricinoleate 42
4.4.5. Reusability of Lipozyme TL IM Enzyme 42
4.5. Synthesis of Polyepoxyricinoleate 43
4.6. Preparation of Pure Ricinoleic Acid 44
4.7. Characterization Methods 45
4.7.1. Preparation of Polymer Films 45
4.7.2. Antibacterial Activity Test 45
4.7.2.1. Preparation of the Inoculum 45
4.7.2.2. Colony Counting Method 46
4.7.3. *In vitro* Degradation Study 46
4.7.4. Mechanical Testing 46
4.7.4.1. Lap-Shear Adhesion Test on Glass, Aluminium, Paper and PET 46
4.7.4.2. Lap-Shear Adhesion Test on Ovine Skin 47
4.7.5. Quantification of Whole Blood Clotting Time 47
4.7.6. Analysis of Cell Viability by the Modified Lactate Dehydrogenase (LDH) Assay 48
5. RESULTS AND DISCUSSION 49
5.1. Enzymatic Polymerization of Methyl Ricinoleate 49
5.1.1. Selection of Lipase Catalyst 49
5.1.1.1. Screening of Enzymes Activity at 50ºC 49

5.1.1.2. Screening of Enzymes Activity at 70ºC 50
5.1.2. Effect of Reaction Temperature on Molecular Weight of Polyricinoleate 52
5.1.3. Effect of Enzyme Concentration on Molecular Weight of Polyricinoleate 53
5.1.4. Effect of Reaction Time on Molecular Weight of Polyricinoleate 54
5.1.5. Reusability of Lipozyme TL IM Enzyme 55
5.2. Characterization of Polymers PRA-M, PRA-H and PER 56
5.2.1. GPC Analysis of PRA-M, PRA-H and PER 56
5.2.2. NMR Spectroscopy of PRA-M, PRA-H and PER 58
5.2.3. FT-IR Spectroscopy of PRA-M, PRA-H and PER 61
5.2.4. DSC Analysis of PRA-M, PRA-H and PER 63
5.2.5. TGA Analysis of PRA-M, PRA-H and PER 64
5.2.6. Rheology Measurements of RA, PRA-M, PRA-H and PER 66
5.2.6.1. Frequency Sweep – Measurement of Complex Viscosity 66
5.2.6.2. Amplitude Sweep – Measurement of Storage and Loss Modulus 67
5.3. Coating Properties of RA, PRA-M and PRA-H 69
5.3.1. SEM Observation of RA, PRA-M and PRA-H Films 70
5.3.2. AFM Observation of RA, PRA-M and PRA-H Films 71
5.4. Antibacterial Properties of RA, PRA-M and PRA-H 72
5.5. Lap-Shear Adhesion Test 74
5.5.1. Lap-Shear Adhesion Test on Glass, Aluminium, Paper and PET 74
5.5.2. Lap-Shear Adhesion Test on Ovine Skin 76
5.6. *In Vitro* Degradation Study of PRA-M, PRA-H and PER 78
5.7. Whole Blood Clotting Time 79
5.8. LDH Cytotoxicity Test 81
6. CONCLUSIONS 82

REFERENCES 84
BIOGRAPHY 93
APPENDICES 94

LIST of ABBREVIATIONS and ACRONYMS

Abbreviations and Acronyms		**Explanation**
cfu	:	colony-forming unit
cm	:	centimetre
DDW	:	double distilled water
E. coli	:	*Escherichia coli*
g	:	gram
G’	:	storage modulus
G’’	:	loss modulus
h	:	hour
kPa	:	kilopascal
log	:	logarithm
m	:	metre
MHz	:	megahertz
mg	:	milligram
mL	:	millilitre
mm	:	millimetre
min	:	minute
M_n	:	number average molecular weight
M_w	:	weight average molecular weight
N	:	newton
nm	:	nanometre
Pa	:	pascal
PER	:	polyepoxyricinoleate
ppm	:	parts per million
PRA	:	polyricinoleate
PRA-H	:	medium-molecular-weight polyricinoleate
PRA-M	:	medium-molecular-weight polyricinoleate
RA	:	ricinoleic acid

rad	:	radian
rpm	:	revolutions per minute
s	:	second
S. aureus	:	*Staphylococcus aureus*
TLC	:	thin layer chromatography
T_g	:	glass transition temperature
wt. %	:	weight per cent

LIST of FIGURES

Figure No:		Page:
2.1:	Chemical structure of triglyceride. R1, R2, R3 – fatty acid chains.	2
2.2:	(a) Castor plant, (b) Castor plant leaves and fruits (c) Castor beans.	5
2.3:	Schematic representation of castor oil extraction procedure.	7
2.4:	Structure of 12-hydroxy-cis-9-octadecenoic acid (ricinoleic acid).	8
2.5:	Possible chemical modification sites (A) ester; (B) double bond; (C) hydroxyl group modification; and reactions in castor oil.	9
2.6:	Drying oil autooxidation reaction in oxygen atmosphere.	10
2.7:	Synthesis of Acrylated Epoxidized Soybean Oil.	12
2.8:	Acrylated Epoxidized Fatty Methyl Ester.	13
2.9:	Reaction of AESO with (a) maleic acid and (b) cyclohexane dicarboxylic acid.	14
2.10:	One-step acrylation of soybean oil.	15
2.11:	Synthesis of acrylate sunflower oil and hydrogenated acrylate sunflower oil by singlet O_2.	16
2.12:	Polymerization reaction of soybean oil with monoglyceride maleate.	17
2.13:	Reaction ofcationic polymerization of soybean oil with ST and DVB.	19
2.14:	Mechanism of olefin metathesis reaction.	20
2.15:	Plant oil-based polymers obtained from ADMET polymerization.	21
2.16:	Structure of Dilulin and ML 189.	22
2.17:	VO sourced monomers for Ring Opening Metathesis reaction.	23
2.18:	Possible routes of polyester synthesis (a) reaction of a diacid and a diol, (b) reaction of hydroxyl acid, and (c) ring opening polymerization of a lactone.	25
2.19:	Synthesis of HNME from castor oil.	25
2.20:	Structure of poly-3-hydroxyalkanoates (PHAs).	26
2.21:	Plant oils based polyols.	27
2.22:	Synthesis of azelaic acid and diisocyanate from oleic acid.	28
4.1:	Esterification reaction of ricinoleic acid (~80%).	34

4.2: TLC spots from the left: ricinoleic acid (~80%) and methyl ricinoleate (~80%). 35
4.3: Isolation of pure methyl ricinoleate from mixture of FAME. 37
4.4: TLC monitoring of mobile phases after passing three stationary phases. 38
4.5: Schematic representation of isolation of methyl ricinoleate from FAME by counter current distribution. 38
4.6: Synthesis of polyricinoleate in the presence of lipase catalyst. 39
4.7: Synthesis of polyepoxyricinoleate from polyricinoleate. 43
4.8: Synthesis of pure ricinoleic acid. 44
5.1: (a) Polyricinoleate M_w (■), $M_wM_n^{-1}$ (▲) and yield (♦) as a function of reaction temperature catalysed by Lipozyme TL IM for 7 days. 100 wt. % of enzyme relative to monomer, for 7 days. 52
5.2: Polyricinoleate M_w (■), $M_wM_n^{-1}$ (▲) and yield (♦) as a function of enzyme load to monomer ratio polymerized by Lipozym TL IM, at 80ºC for 7 days. 53
5.3: Polyricinoleate M_w (■), $MwMn^{-1}$(▲) and yield (♦) as a function of reaction time at 100 wt. % Lipozyme TL IM load at 80°C. 54
5.4: Polyricinoleate M_w (■), $M_wM_n^{-1}$(▲) and yield (♦) as a function of reusability cycle. Each cycle was performed for at 100 wt. % Lipozyme TL IM load at 80°C for 7 days. 55
5.5: GPC traces of PRA-M and PRA-H. 57
5.6: GPC traces of PRA-H and PER. 57
5.7: ^{1}H NMR spectra of PRA-M and PRA-H. 58
5.8: ^{13}C NMR spectra of PRA-M and PRA-H. 59
5.9: ^{1}H NMR spectrum of polyepoxyricinoleate. 60
5.10: ^{13}C NMR spectrum of polyepoxyricinoleate. 61
5.11: FT-IR spectra of PRA-M and PRA-H. 62
5.12: FT-IR spectrum of polyepoxyricinoleate. 62
5.13: DSC scans of PRA-M and PRA-H polyricinoleates (2nd run). 63
5.14: DSC scan of PER (2nd) run. 64
5.15: TGA scans of PRA-M and PRA-H polyricinoleates. 65
5.16: TGA scan of polyepoxyricinoleate (PER). 66
5.17: Frequency dependence of complex viscosity values. 67

5.18: Amplitude sweep results of RA PRA-M, PRA-H and PER. 68
5.19: Frequency sweep of PRA-H and PER and calculated cross-over points. 69
5.20: Preparation of RA, PRA-M and PRA-H films by solvent casting method. 69
5.21: Glass plate covered with colourless PRA-H film. 70
5.22: SEM micrographs of RA, PRA-M and PRA-H films on (a) glass cover slips and on (b) stainless steel plates. 71
5.23: AFM images of RA, PRA-M and PRA-H coated stainless steel surfaces. 72
5.24: (a) Plates of S. aureus after 24 h of incubation at 37°C: Control, RA, PRA-M, PRA-H, (b) plates of E. coli after 24 h of incubation at 37°C: Control, RA, PRA-M, PRA-H, antibacterial activity against, (c) S. aureus, and (d) E. coli after 24 h of incubation at 37°C. 73
5.25: Lap shear strength of PRA-M, PRA-H and PER on different substrates. 75
5.26: Schematic representation of Van der Waals interaction of adhesive polymer and substrate. 75
5.27: Lap-shear adhesion test of PRA-H on glass plates. 76
5.28: Lap shear adhesion test of PER on ovine skin. 77
5.29: Lap shear strength of PRA-M, PRA-H and PER on ovine skin. 78
5.30: In vitro degradation of PRA-M, PRA-H and PER. 79
5.31: Blood clotting experiment on glass plates covered with polymer (PRA-H sample). 80
5.32: Average blood coagulation time in contract with RA, PRA-M, PRA-H and PER. 80
5.33: Cell viability after 1 and 3 days. 81

LIST of TABLES

Table No:		Page No
2.1:	Formulas and structures of the most important fatty acids.	3
2.2:	Composition and properties of most common plant oils.	4
2.3:	Typical composition of fatty acids in castor oil.	8
4.1:	Compounds and corresponding retention factors (R_f).	35
5.1:	Polymerization of methyl ricinoleate using various lipases at 50°C for 7d.	49
5.2:	Polymerization of methyl ricinoleate using various lipases at 70°C for 7d.	50

1. INTRODUCTION

Over the last few decades, in both academia and industry, there is increasing interest in obtaining novel bio-based materials that could compete with petroleum-derived chemicals in the future. Petroleum-based plastics have many advantages such as long durability or disposability. On the other hand, petroleum resources are limited and its prices are continuously rising.

Moreover, constant production of petroleum-based plastics and their disposal contribute to global warming and environmental pollution problems. For this reason there is need for development of new bio-based materials [1].

Greater awareness among customers is also significant factor increasing demand for products based on natural resources. Main advantages of bio-based resources are their world-wide abundance, low toxicity, inherent biodegradability and presence of reactive groups that can be modified. Polysaccharides (such as cellulose and starch), wood and proteins are commonly used natural raw materials but vegetable oils (VOs) are the most promising ones [2].

2. VEGETABLE/PLANT OILS

Vegetable oils (VOs) are natural resources derived from various plants. The name of VO is given by its source e.g. cotton oil or palm oil. Chemically, VOs are triglycerides (tri-esters of glycerol and various fatty acids) (Figure 2.1) with composition of fatty acids characteristic for each plant but also varying with the season, the crop and the growing conditions [2,3]. Most important fatty acids are listed in Table 2.1. [3]. Length of the fatty acids carbon chain, degree of unsaturation and stereochemistry of the double bond in fatty acids chain are key factors affecting chemical and physical properties of plant oils [3,4].

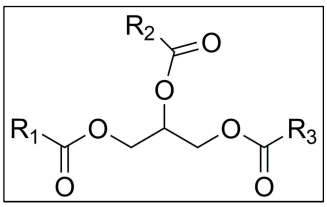
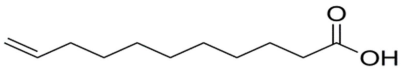
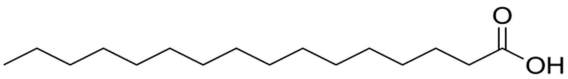
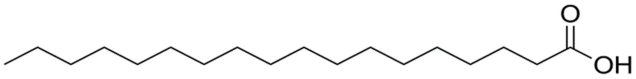
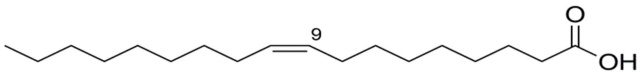
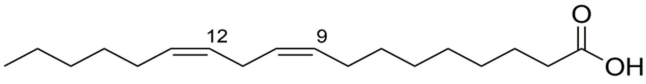
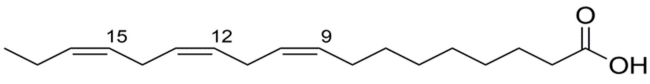
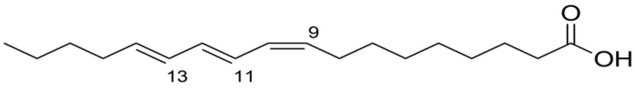
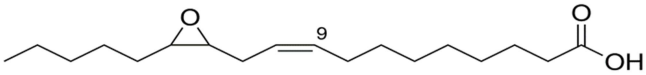
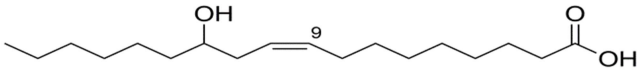
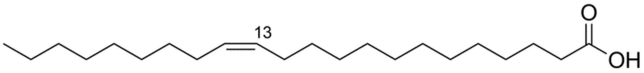


Figure 2.1: Chemical structure of triglyceride. R1, R2, R3 – fatty acid chains.

One of the most important factors that influence properties of VOs is their degree of unsaturation that can be described by iodine value (IV). Iodine value is expressed as amount of iodine (in mg) that reacts with double bond in 100g f of VO.

Table 2.1: Formulas and structures of the most important fatty acids.

Fatty acid	Formula	Structure
10-undecenoic	$C_{11}H_{20}O_2$	
Palmitic	$C_{16}H_{32}O_2$	
Stearic	$C_{18}H_{36}O_2$	
Oleic	$C_{18}H_{34}O_2$	
Linoleic	$C_{18}H_{32}O_2$	
Linolenic	$C_{18}H_{30}O_2$	
α-Eleostearic	$C_{18}H_{30}O_2$	
Vernolic	$C_{18}H_{32}O_3$	
Ricinoleic	$C_{18}H_{34}O_3$	
Erucic	$C_{22}H_{42}O_2$	

The higher the iodine value, the higher the unsaturation degree of plant oil. Vegetable oils are classified into three groups according to their IV. When IV>130 oil belongs to drying oils category. For IV in the range 100-130 semi-drying oils and for IV<100 non-drying oils terms are used. The fatty acids composition and properties of VOs are summarized in Table 2.2.

Table 2.2: Composition and properties of most common plant oils.

Vegetable oil	Double bonds[a]	Iodine value[b]/mg per 100 g	Fatty acids (%)				
			Palmitic	Stearic	Oleic	Linoleic	Linolenic
Palm	1.7	44–58	42.8	4.2	40.5	10.1	—
Olive	2.8	75–94	13.7	2.5	71.1	10.0	0.6
Groundnut	3.4	80–106	11.4	2.4	48.3	31.9	—
Rapeseed	3.8	94–120	4.0	2.0	56.0	26.0	10.0
Sesame	3.9	103–116	9.0	6.0	41.0	43.0	1.0
Cottonseed	3.9	90–119	21.6	2.6	18.6	54.4	0.7
Corn	4.5	102–130	10.9	2.0	25.4	59.6	1.2
Soybean	4.6	117–143	11.0	4.0	23.4	53.3	7.8
Sunflower	4.7	110–143	5.2	2.7	37.2	53.8	1.0
Linseed	6.6	168–204	5.5	3.5	19.1	15.3	56.6

[a] Average number of double bonds per triglyceride. [b] The amount of iodine (mg) that reacts with the double bonds in 100 g of VO

2.1. Castor Plant (Ricinus communis) and Obtaining of Castor Oil

Tropical regions of Asia and Africa are natural habitat of castor oil plant. Nowadays, it is often grown in other regions of the world mainly in temperate zones. The world's largest exporter of castor oil is India, sharing 70% of total exports. Other influential exporters of castor oil are China, Brazil and Thailand. Major importers are USA, Russia and Japan [5].

Depending on the climate, the castor plant is a large shrub or tree and can grow up to 12 meters in height. However, when cultivated in temperate zones it is much smaller. Castor plant has hollow and pale green or sometimes reddish stems. Leaves are large (about 10-40 cm long), red or brown in colour and veins are visible. Castor oil plant is in leaf all year and flowers from July to September. From September to November seeds of castor plant ripen and are dispersed by the wind. Castor beans contain approximately 40-60% of castor oil, but they also contain ricin, a water soluble toxin. [5]. Castor plant tree, leaves, fruits and beans are shown in Figure 2.2.

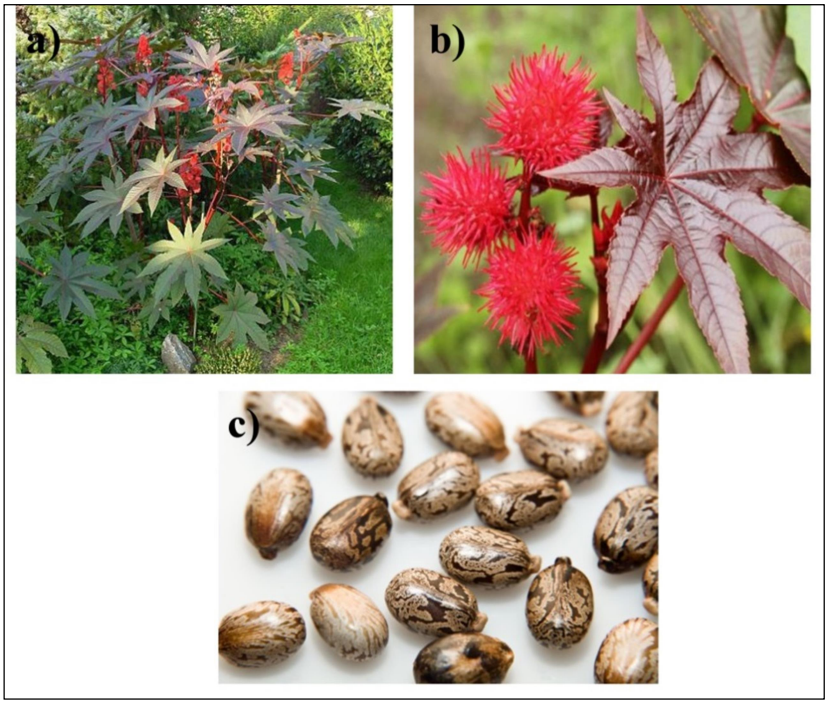


Figure 2.2: (a) Castor plant, (b) Castor plant leaves and fruits (c) Castor beans.

In order to obtain pure castor oil, it has to be extracted from the bean by a series of processes.

First of all, the castor beans have to undergo various preparation steps as preparation for extraction, such as *clearing step*: castor beans are separated from dirt and any foreign materials; *drying step*: beans are dried at 60 ºC for several hours to reach splitting of casing and shedding the seeds; *winnowing step*: shells are separated from the beans; *grinding step*: beans are grinded into cake (paste) to break the cell walls and release the castor oil for extraction (see Figure 2.3.) [5].

The mechanical isolation of oil from beans is commonly more preferable compared to solvent extraction method because it is more cost effective. Lower investment and operation costs are required and the mechanical isolation process is also much safer for the environment. But because in this process low yield is reached; therefore, subsequent solvent extraction is usually applied in order to extract remaining oil [5,6]. Very effective solution is application of two methods. For example, hot pressing performed by hydraulic press, followed by solvent extraction. Since the extracted castor oil is not pure and contains small amounts of impurities such e.g. free fatty acids, phospholipids, protein degradation products, waxes, mono and diacylglycerols, hydrocarbons, moisture, dirt, and other contaminants, a refining

process has to be carried out before oil derivatization. Typically refining of oil consists of the following steps: degumming, neutralization, bleaching, deodorization, and optionally winterisation. Degumming step helps to remove the phospholipids and the metal content from crude oil by mixing it with water and an acid. Depending on the applied neutralisation method used to remove the free fatty acids, refining process can be divided into chemical and physical refining methods. Physical refining is based on vacuum distillation and is more environmentally friendly compared to chemical refining based on alkaline treatment because less water is required.

The next applied step is bleaching. This is adsorption process used to eliminate pigments, traces of soap and phospholipids by natural clays. Finally, deodorisation process is applied to avoid undesired characteristic flavours and odours caused by the presence of minor amounts of free fatty acids, aldehydes, ketones, and other compounds. However this process may cause undesirable double bond isomerization (from *cis* to *trans*) or oil degradation due to polymerization. When necessary, winterization step is applied to remove oil components that solidify at low temperatures (e.g. waxes) [5,7].

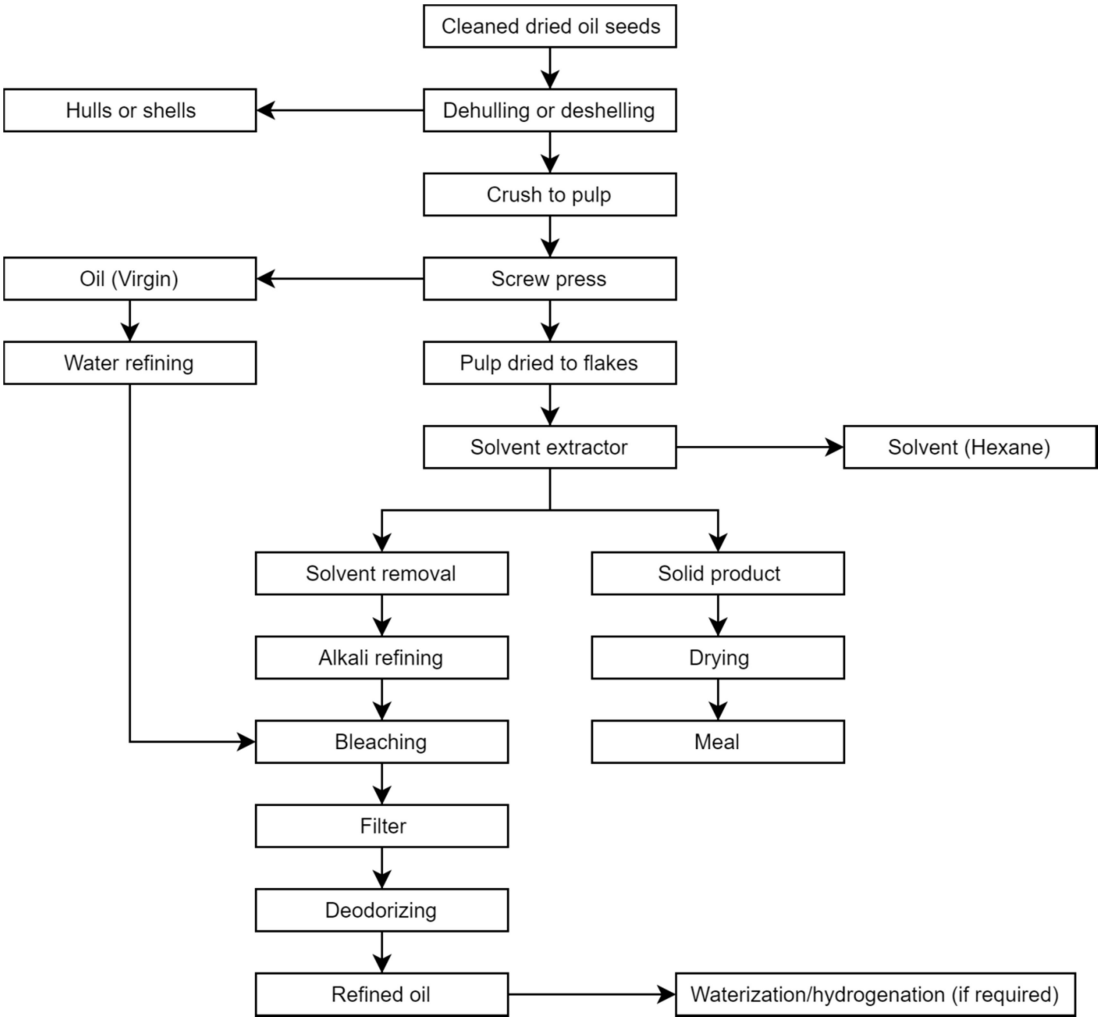


Figure 2.3: Schematic representation of castor oil extraction procedure.

Castor cake which is residue after extraction and refining process cannot be used as livestock feed because it contains toxic compounds – ricin (up to 1.5%), ricinine (0.15-0.23%) and an allergen. In order to detoxify castor cake a number of chemical and physical methods must be applied [5,8].

2.2. Castor Oil

Castor oil (or *Oleum Palmae Christi*), extracted from beans of *Ricinus communis* plant was first mentioned for its medical properties in the Ebers papyrus of ancient Egypt (~3500 years ago). Its primary use was as purgative/laxative agent. Moreover it has an ability to activate prostaglandin EP_3 receptors and hasten uterine contractions and in the past it was prescribed by many doctors and midwives to

induce labour. However, it is classified as nonedible oil due to its nauseating properties [9].

Castor oil can have various physical and chemical properties. On the other hand, its chemical composition remains relatively constant regardless of its country of origin or season in which it was grown (Table 2.3) [5].

Table 2.3: Typical composition of fatty acids in castor oil.

Fatty acid	**Molecular formula**	**Percentage (%)**
Palmitic	$C_{16}H_{32}O_2$	0.8 – 1.2
Stearic	$C_{18}H_{36}O_2$	0.7 - 1.0
Oleic	$C_{18}H_{34}O_2$	2.2 - 3.3
Linoleic	$C_{18}H_{32}O_2$	4.0 - 4.7
Linolenic	$C_{16}H_{30}O_2$	0.5 - 0.7
Ricinoleic	$C_{16}H_{34}O_3$	87.8 - 90.3

Similarly to other VOs, castor oil is a triacylglycerol composed of various fatty acids and glycerol. However, among other vegetable oils, it is distinguished by a highly homogeneous composition of fatty acids. Approximately, 87-95% of fatty acids content in castor oil is ricinoleic acid (12-hydroxy-9-cis-octadecenoic acid). Structure of ricinoleic acid is presented in Figure 2.4. Ricinoleic acid belongs to small group of naturally available bifunctional fatty acids which can be used as monomers for polymerization without preliminary modification. This high homogeneity as well as presence of reactive groups make castor oil/ricinoleic acid perfect building block for synthesis of novel bio-based materials. Figure 2.5. shows possible modifications of different reactive sites present in castor oil [5,9].

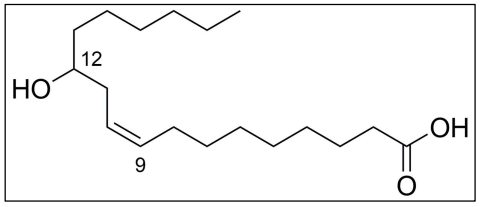


Figure 2.4: Structure of 12-hydroxy-cis-9-octadecenoic acid (ricinoleic acid).

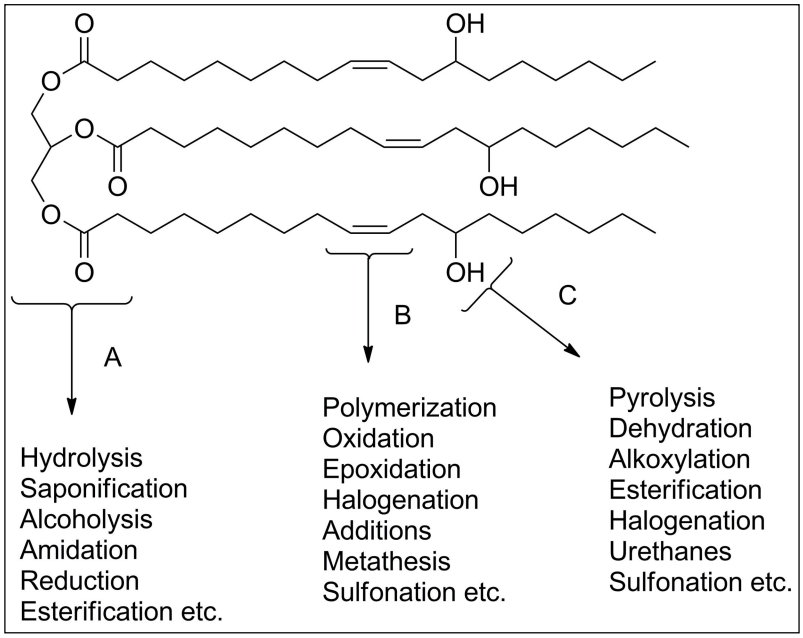


Figure 2.5: Possible chemical modification sites (A) ester; (B) double bond; (C) hydroxyl group modification; and reactions in castor oil.

Before description of castor oil/ricinoleic based polymers some general information on VOs as raw material for polymer synthesis is given below.

2.3. Plant Oil Based Polymers

In the last few decades, a variety of VOs based polymers have been developed. Unmodified and modified VOs have been used to prepare polymers by various polymerization methods, such as radical, cationic, acyclic diene metathesis, ring opening, olefin metathesis or condensation polymerization. In this section various VOs based monomers as well as different methods of polymerization are described.

2.3.1. Plant Oil Based Polymers Obtained in Free Radical Polymerization

Both unmodified and modified plant oils can undergo radical polymerization reaction.

2.3.1.1. Unmodified Plant Oils Used As Monomers

The –C=C- bonds present in VOs can undergo free radical polymerization. For example, drying oils (see Section 1.1) can undergo autoxidation in oxygen atmosphere. Formed peroxides (Figure 2.6), can cause crosslinking of oils by radical recombination and cause formation of branched polymers. Therefore they are used as binders and film formers in paint formulations [10].

For example, Hazer *et. al.* applied this phenomenon to prepare VOs based free-radical macroinitiators, which then could initiate polymerization of methyl methacrylate (MMA) or n-butyl methacrylate (nBMA), resulting in polymeric linseed oil (PLO) and polymeric soybean oil (PSB). It was found that VOs can not only make synthesized PMMA and PnBMA partially biocompatible and biodegradable but they also act as plasticizers [11–13].

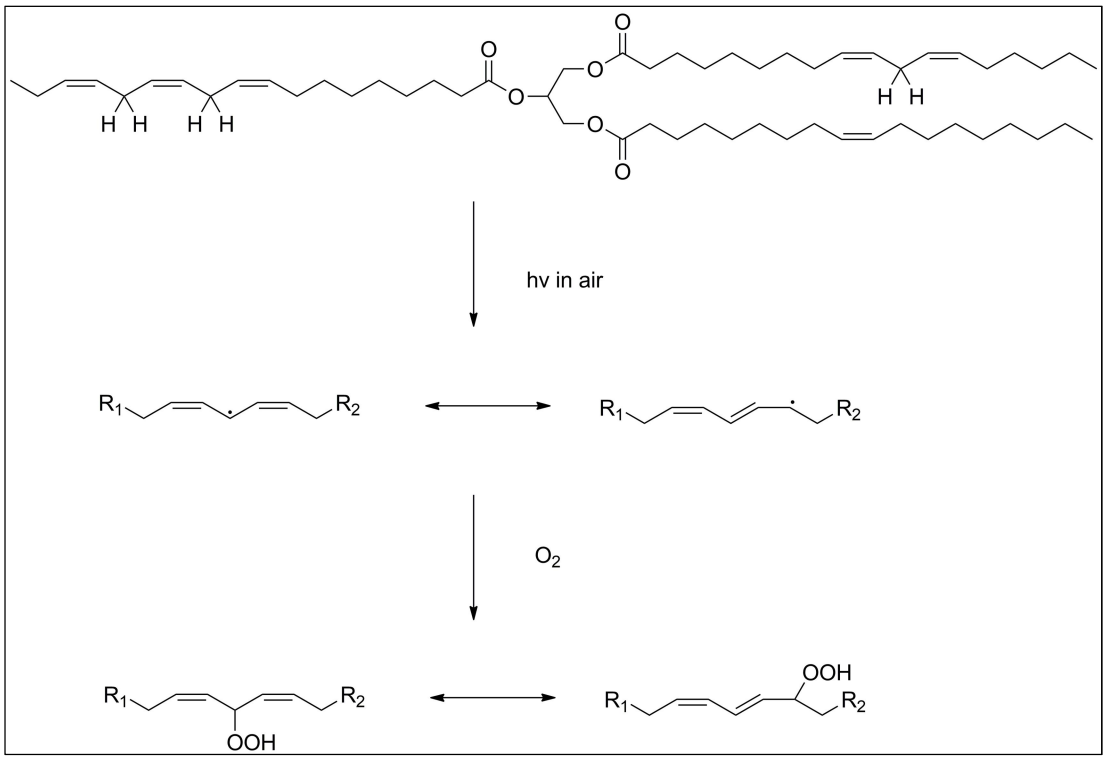


Figure 2.6: Drying oil autoxidation reaction in oxygen atmosphere.

In another study, polysoybean oil (polySOY) prepared by free radical polymerization have been melt blended with isotactic poly(L-lactide) (PLLA) to

increase its the toughness. Prepared PLLA/polySOY blends had tensile toughness four times greater than that of PLLA before modification [14].

Tung oil obtained from the nut of the tung tree (*Vernicia fordii*) has unique composition. Approximately 84% of fatty acids in tung oil consist of α-eleostearic acid, which is naturally occurring conjugated triene. Due to high unsaturation and conjugation of double bonds, this oil is readily polymerizable. Larock *et al.* prepared tung oil-styrene(ST)-divinylbenzene(DVB) with tung oil content 30-70 wt.% These fully cured thermoset (90-100% of cross-linked materials) had properties from rubbery to rigid plastics and T_g from -2°C to 116°C. It was found that addition of Co, Ca and Zr salts as catalyst can accelerate thermal copolymerization [15].

2.3.1.2. Plant Oils after Double Bond Modifications Used as Monomers

In order to enhance reactivity of VOs, various modifications of their –C=C- bonds in the fatty acid chains can be performed. Most common modification is appending of polymerizable acrylate functionality. The most widely studied functionalized VOs based modified monomer is acrylated epoxidized soybean oil (AESO) which is synthesized in the reaction between epoxidized soybean oil and acrylic acid (see Figure 2.7) [16]. AESO is commercially available and is produced e.g. by UCB Chemicals under the brand name Ebceryl 860 [3].

When blended with reactive diluents, e.g. styrene (ST), AESO improves their processability and suitable AESO-ST composites and thermosets for structural applications can be obtained [17]. By changing the acrylate level in AESO and amount of styrene, polymer properties can be controlled resulting in a range of materials with various properties.

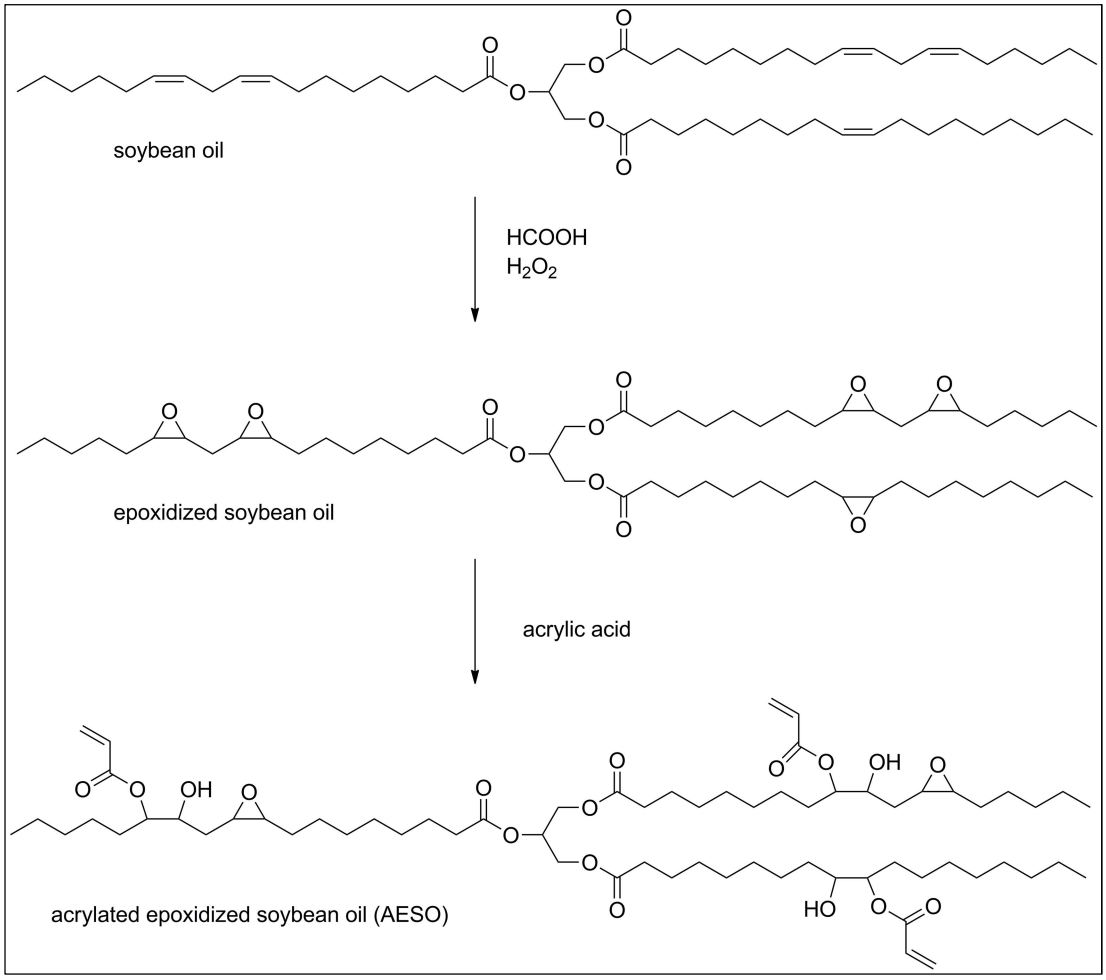


Figure 2.7: Synthesis of Acrylated Epoxidized Soybean Oil.

In another study, styrene was replaced by novel reactive diluent, namely acrylated epoxidized fatty methyl ester (AFAME) (see Figure 2.8) in the reaction with AESO [18]. This replacement made new materials more biorenewable and help reduce dangerous air pollutants as well as health and environmental risks.

AESO/CO_2 was used to prepare thermosetting foams with mechanical properties that were comparable to semi-rigid industrial foams [19].

Similarly to AFAME, acrylated epoxidized methyl oleate was prepared and undergoes free radical emulsion polymerisation to obtain polymer that could be used as pressure sensitive adhesive [20].

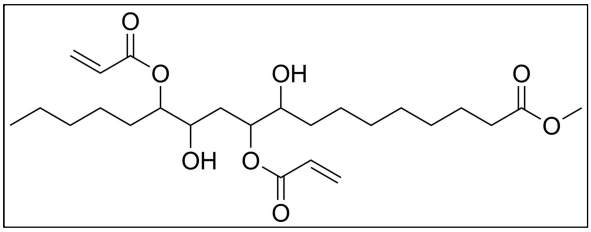


Figure 2.8: Acrylated Epoxidized Fatty Methyl Ester.

Because in AESO both residual unreacted epoxy groups and newly formed hydroxyl groups are present, they can be used for further modifications.

For example, as presented in Figure 2.9a, reacting AESO with maleic anhydride resulted in more –C=C- double bonds but also formation of oligomers that can rise entanglement density of biopolymers. The MAESO-ST thermosets had higher crosslink density, higher T_g and improved storage moduli at room temperature compared to AESO-ST thermosets. Also reacting AESO with cyclohexanedicarboxylic acid (see Figure 2.9b) forms oligomers, and introduce rigid cyclic rings into the structure [16,21].

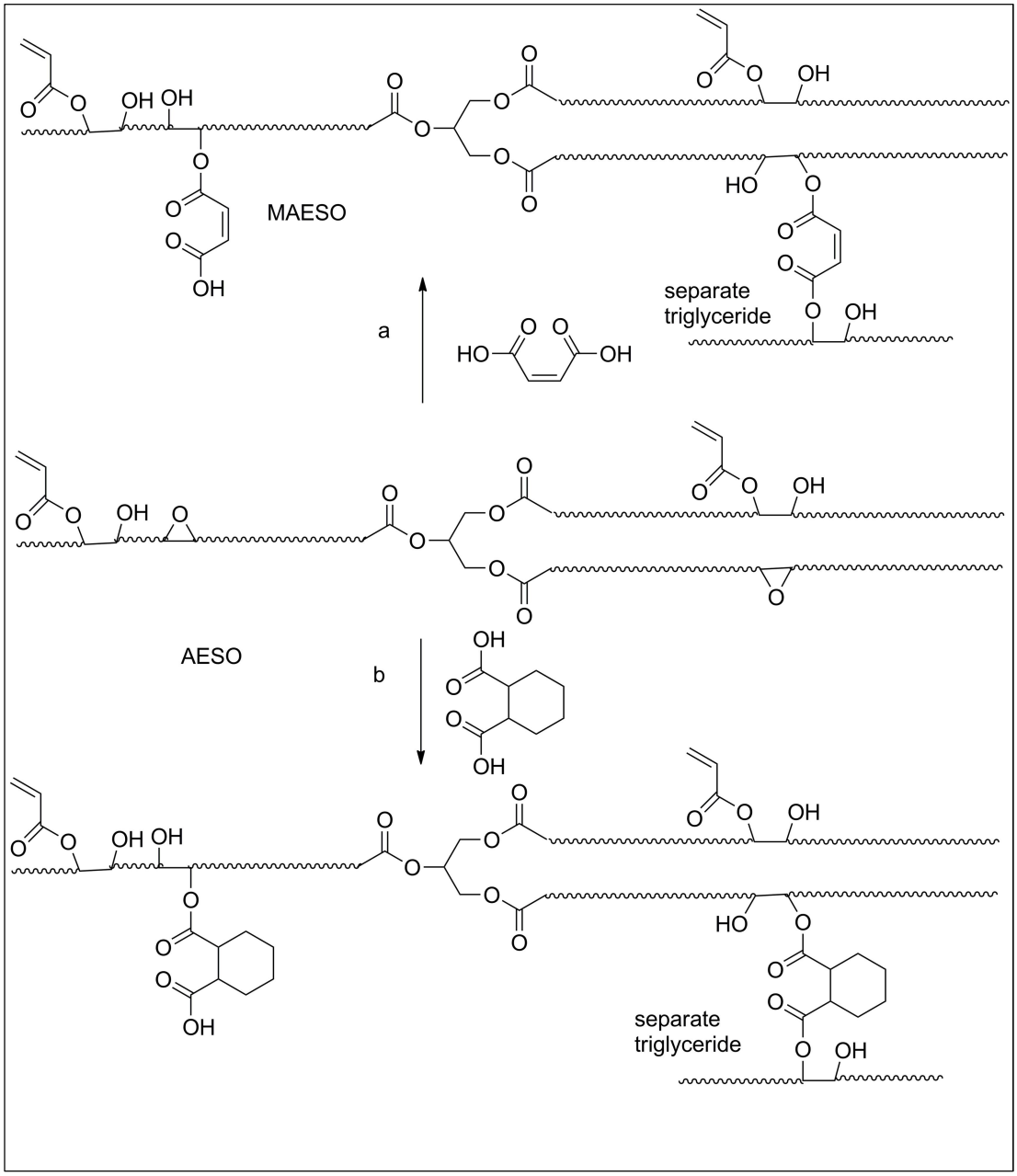


Figure 2.9: Reaction of AESO with (a) maleic acid and (b) cyclohexane dicarboxylic acid.

Triglycerides containing acrylate group can be also prepared in different way by an “ene” reaction with singlet oxygen. As shown in Figure 2.11a, photooxygenation by singlet oxygen and reduction resulted in secondary allylic alcohols (HSO) mixture. Synthesized unsaturated HSO can be later reduced to saturated alcohols (HSO[H]). Both HSO and HSO[H] can be functionalized with acrylate group (see Figure 2.11b) [22–25].

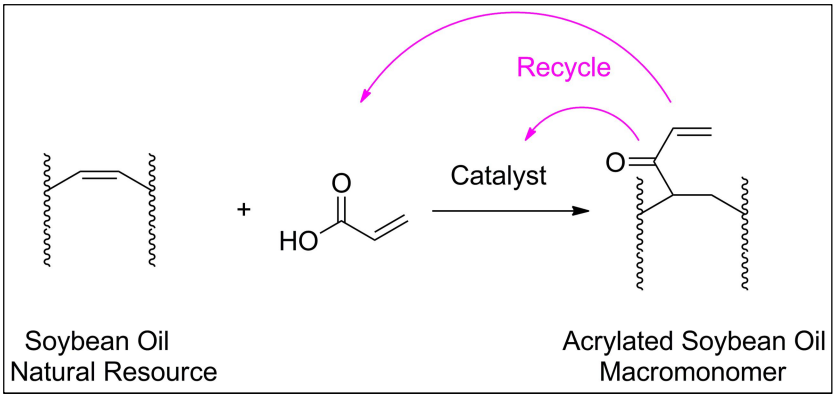


Figure 2.10: One-step acrylation of soybean oil.

Recently, a method of one-step acrylation of soybean oil was demonstrated by Zhang et al. [26] (see Figure 2.10). In this research, acrylated soybean oil (ASO) was synthesized directly from the addition reaction of acrylic acid and soybean oil in the presence of various catalysts, but $BF_3 \cdot Et_2O$ was the most effective catalyst for this addition reaction.

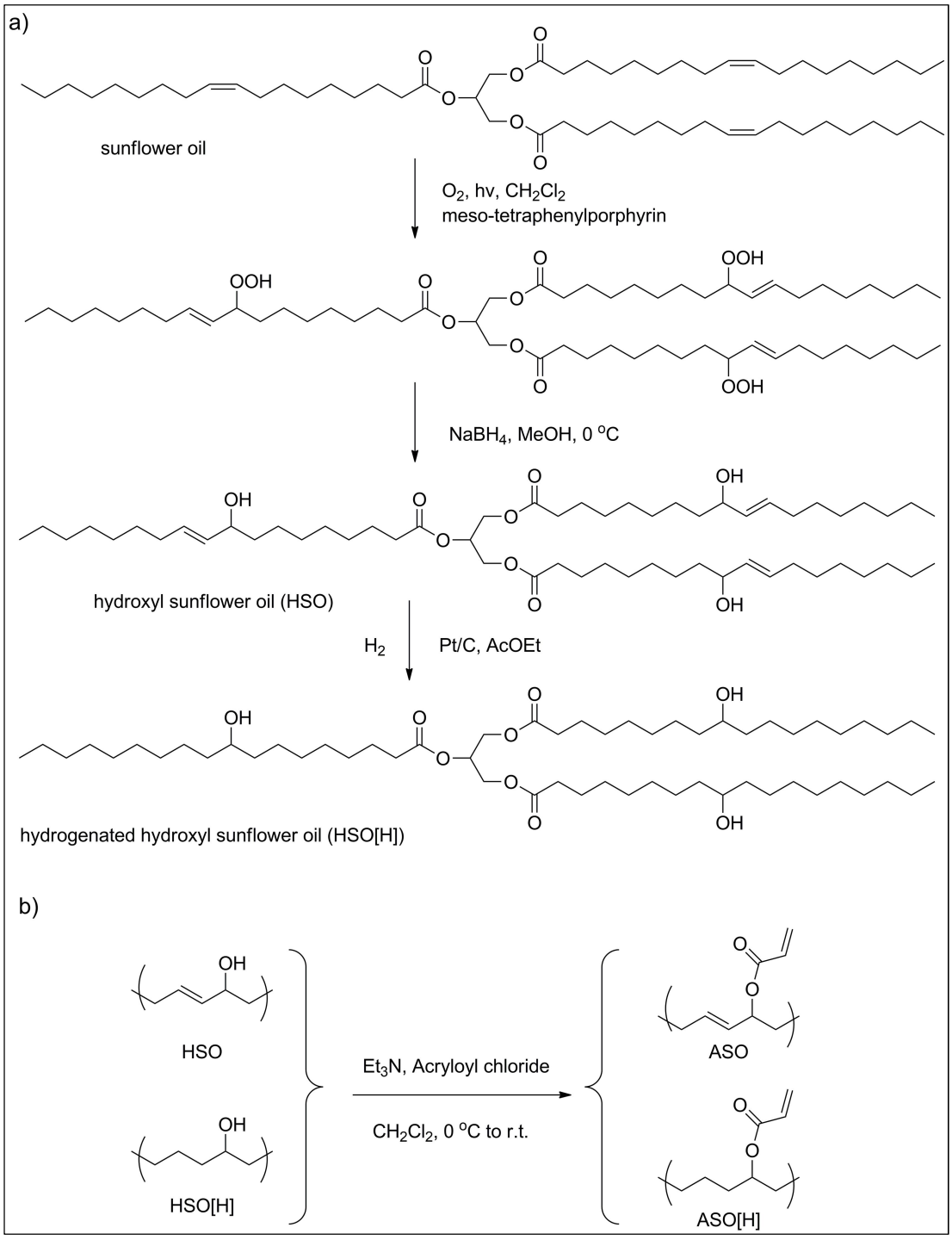


Figure 2.11: Synthesis of acrylate sunflower oil and hydrogenated acrylate sunflower oil by singlet O_2.

2.3.1.3. Plant Oils with Triglyceride Ester Modifications Used as Monomers

Another approach to increase reactivity of VOs is incorporation of more reactive –C=C- bonds by modifications of ester group in triglyceride. Wool *et. al.* [27] prepared a series of rigid thermoset polymers by copolymerization of VOs monoglyceride maleates with ST. In Figure 2.12 preparation and polymerization of soybean oil monoglyceride (SOMG) maleate half esters is demonstrated. SOMG were prepared in transesterification reaction of soybean oil and glycerol. Next, reaction with maleic anhydride resulted in obtaining SOMG maleate half esters, which copolymerized with 35 wt% of styrene gave thermoset, rigid polymer with glass transition temperature of 135°C and storage modulus of 0.92 GPa. These polymers are promising materials for replacement of conventional petroleum-based plastics. Further studies on SOMG included reaction with neopentyl glycol and bisphenol A to improve their mechanical properties [28].

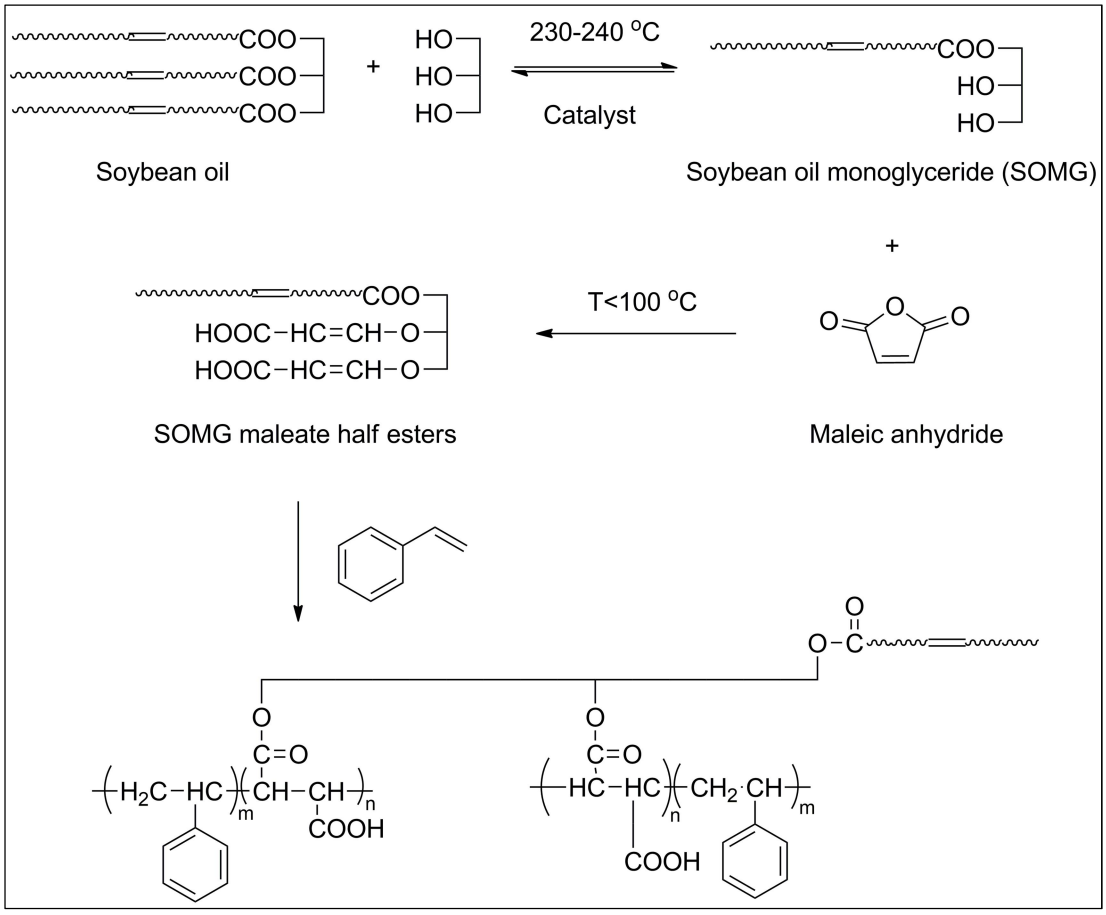


Figure 2.12: Polymerization reaction of soybean oil with monoglyceride maleate.

2.3.2. Plant Oil Based Polymers Obtained by Cationic Polymerization

Plant oil based vinyl monomers and oil epoxides are suitable starting materials for cationic polymerization.

2.3.2.1. Plant Oil Based Vinyl Monomers in Cationic Polymerization

Vinyl monomers can be polymerized cationically under relatively mild conditions e.g. in the presence of Lewis acid such as $AlCl_3$, $TiCl_4$, $SnCl_4$, $ZnCl_2$ and $BF_3 \cdot OEt_2$ (BFE) that acts as an initiator. BFE has been proven to be the most effective among these initiators and is widely used in alkenes cationic polymerization [3]. Vinyl monomers have to be sufficiently nucleophilic to undergo protonation and polymerization. In monomers such as ethylene and propylene, -C=C- bond can undergo cationic polymerization. However, only oligomers can be obtained because carbocations formed are relatively unstable and secondary reactions (such as elimination, proton transfer, chain transfer and isomerization) are favoured instead of chain propagation. In VOs, -C=C- are more nucleophilic compared to ethylene and propylene. Additionally, cationic intermediates formed in conjugated plant oils are stabilized by adjacent -C=C- bond. For this reason, tung oil, which contains conjugated triene, is very reactive towards cationic polymerization when BFE initiator is applied [29]. Plant oils are generally cationically polymerizable. Each unsaturated fatty acid in branched triglyceride structure can take part in the cationic reaction which leads to cross-linking and formation of three-dimensional polymeric network.

Larock *et al.* [30,31] studied cationic polymerization of several types of soybean oils: regular soybean oil (SOY), low-saturation soybean oil (LSS) and conjugated LoSatSoy oil (CLS). They found that polymerization of soybean oil alone, leads to low molecular weights oils or soft rubber like materials with limited utility. In order to improve mechanical properties of thermoset, styrene (ST) and divinyl benzene (DVB) has been cationically polymerized with soybean oil (Figure 2.13) to afford thermosets [32].

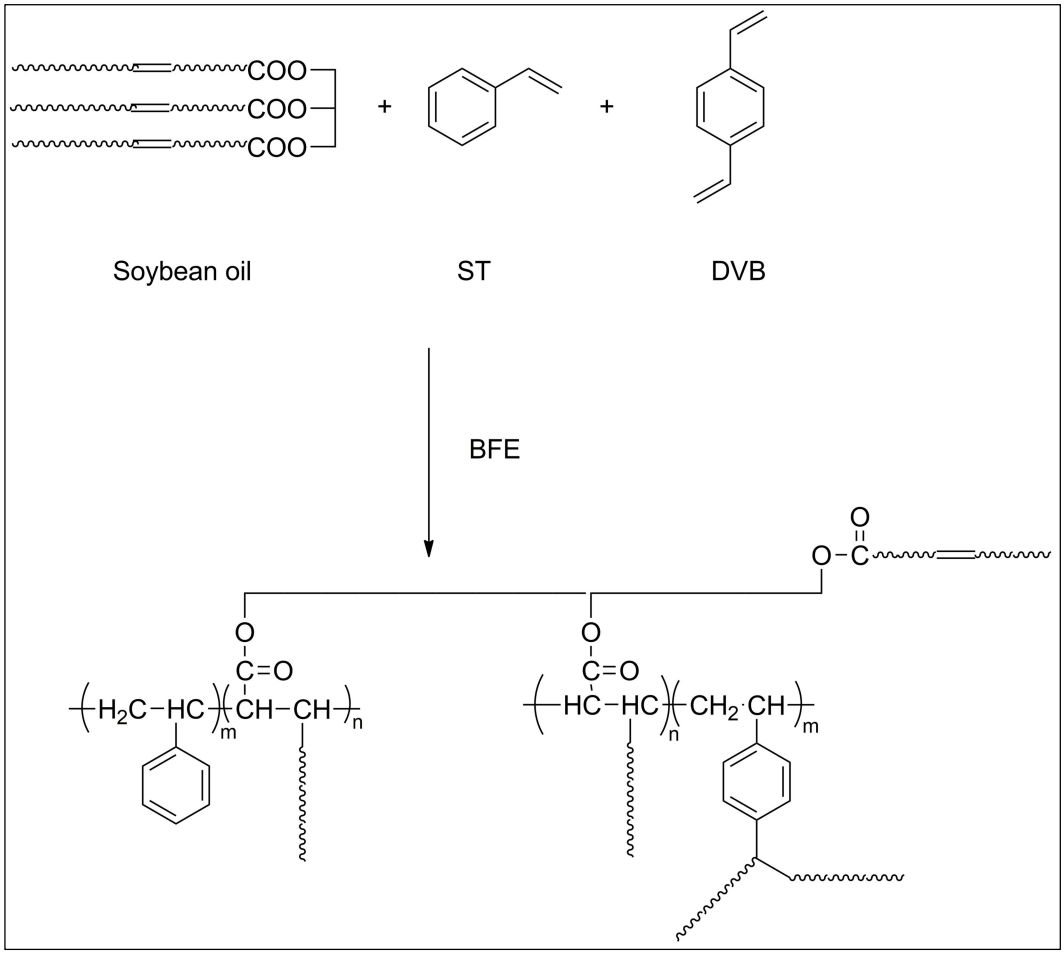


Figure 2.13: Reaction of cationic polymerization of soybean oil with ST and DVB.

Also corn oil and has been copolymerized cationically with styrene and divinylbenzene. Obtained thermosets showed commercially viable thermophysical and mechanical properties [33]. The same cationic polymerization of ST, DVB and VO reaction was performed for olive, peanut, sesame, canola, corn, soybean, grapeseed, sunflower, low-saturation soy, safflower, walnut, and linseed oils. The physical, thermal and mechanical properties of these various plant based thermosets have been investigated as a function of the VO reactivity [34].

2.3.2.2. Plant Oils Epoxides in Cationic Polymerization

Also epoxidized VOs can be polymerized cationically. In the literature mainly "latent initiators", which enable controlled polymerization have been used. These

types of initiators stay inactive under normal conditions and may be activated to initiate polymerization (e.g. benzylpyrazinium salt) [35].

Epoxidized soybean oil (ESO) and epoxidized castor oil (ECO) have been polymerized cationically with *N*-benzylpyrazinium hexafluoroantimonate (BPH) latent thermal catalyst. Cured ESO and ECO samples had glass transition temperatures of 24°C and 38°C respectively and low coefficient of thermal expansion [36]. Cationic copolymerization of ESO and ECO with diglycidyl ether of bisphenol A (DGEBA) resulted in obtaining materials with better mechanical properties. [37]

2.3.3. Olefin Metathesis in Polymerization of Plant Oil Based Monomers

Discovered in 1964, olefin metathesis reaction involves redistribution of fragments of alkene (olefin) by the scission and regeneration of carbon-carbon double bonds. It occurs through a metallacyclobutane intermediate formed between a metal alkylidene and an olefin (see Figure 2.14) [38]. In early years, transition metal salts together with main group organometallic reagents or deposited on solid supports, such as WC_{l6}/Bu_4Sn, $WOCl_4/EtAlCl_2$, MoO_3 /SiO_2 or Re_2 O_7/Al_2O_3 were used as catalysts for olefin metathesis reaction [39]. However production of these catalysts was difficult and their activity was low. Schrock et al. [40] developed highly reactive molybdenum and tungsten alkylidenes with common formula $(ArN)(R'O)_2M{=}CHR$. Drawback of these catalysts was their extreme sensitivity to moisture and air. Later in the mid-1990's, well-defined ruthenium alkylidenes (e.g. $(Cy_3P)_2Cl_2Ru{=}CHPh$) catalysts were developed by Grubbs *et al.* [41]. These new catalysts were stable in air and moisture and could tolerate most functional groups. They are generally called first-generation Grubbs catalysts (G1).

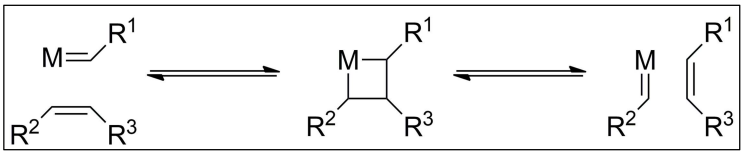


Figure 2.14: Mechanism of olefin metathesis reaction.

Second-generation Grubbs catalysts (G2) were obtained by monosubstitution of PCy_3 with N-heterocyclic carbine in G1. G2 catalysts had higher activity and improved thermal stability [42].

Since 1972, olefin metathesis reaction of plant oils derivatives (e.g. fatty acids) has been investigated [43,44]. By means of olefin metathesis reaction many useful chemicals have been obtained from unsaturated fatty acid esters and contributed to green chemical industry. Various catalysts have been employed for these processes, such as heterogeneous supported rhenium oxide catalysts or homogeneous ruthenium catalysts. Besides synthesis of various chemicals, olefin metathesis has been applied to synthesize VOs polymers, mainly by acyclic diene metathesis polymerization (ADMET) and ring-opening metathesis polymerization (ROMP).

2.3.4. Acyclic Diene Metathesis Polymerization (ADMET) in Polymerization of Plant Oil Based Monomers

Soybean oil in the presence of G1 catalyst has been polymerized by ADMET process. Obtained products were in the range of sticky oils to rubbery materials [45].

High molecular weight polymers has been prepared by ADMET polymerization of VO based derivative, aliphatic α,ω-diene (see Figure 2.15) [46] Molecular weight of these polymers could be controlled by changing the monomer to chain stopper ratio.

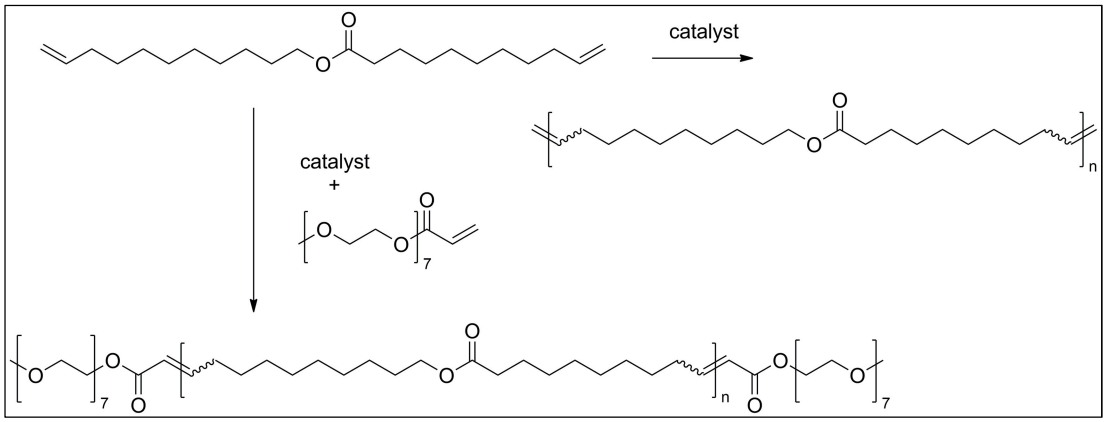


Figure 2.15: Plant oil-based polymers obtained from ADMET polymerization.

Chain stoppers with different functionalities can be used to obtain telechelic polymers. For example, ADMET polymerization of phosphorous-containing α,ω-dienes affords polymers with flame retardant properties [47, 48].

2.3.5. Ring-Opening Metathesis Polymerization (ROMP) in Polymerization of Plant Oil Based Monomers

Monomers that contain strained rings e.g. norborene units can be polymerized by ROMP reaction. Introduction of such strained rings to VOs is necessary before ROMP reaction of these compounds. For example, Dilulin or ML 189, which are norbornene-containing linseed oils (see Figure 2.16), has been copolymerized with dicyclopentadiene by ROMP to give a various thermosets [49].

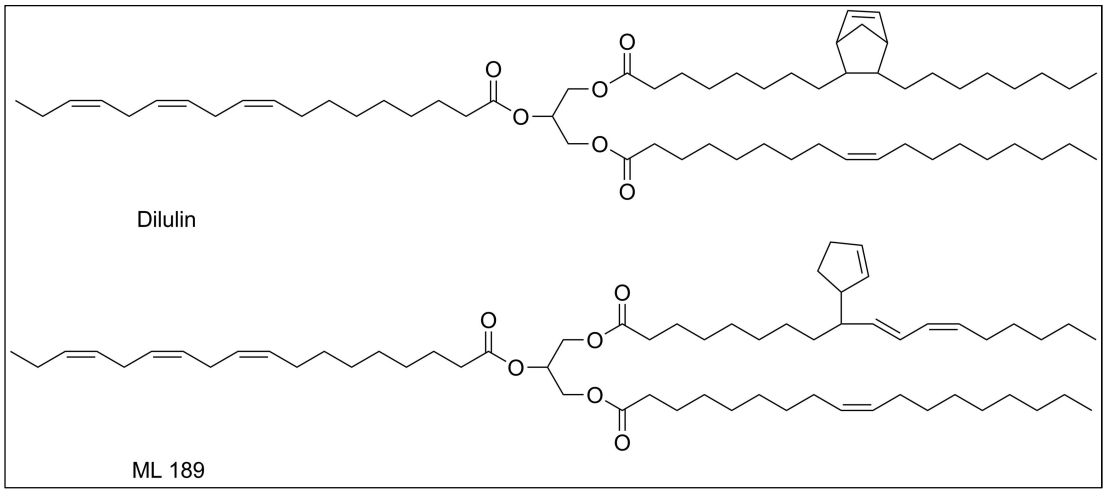


Figure 2.16: Structure of Dilulin and ML 189.

Examples of VO-based monomers for ROMP polymerization are given in Figure 2.17 [3].

Norbornenyl-functionalised bicyclic castor oil derivative (BCO) (Figure 2.17a) has been prepared by reacting castor oil with a commercially bicyclic anhydride bicycle-2.2.1-hept-5-ene-2,3-dicarboxylic anhydride. BCO copolymerized with cyclooctene and catalysed by of the G2 catalyst, gave transparent rubbery thermosets with T_g values in the range from -14°C to 1°C. [50].

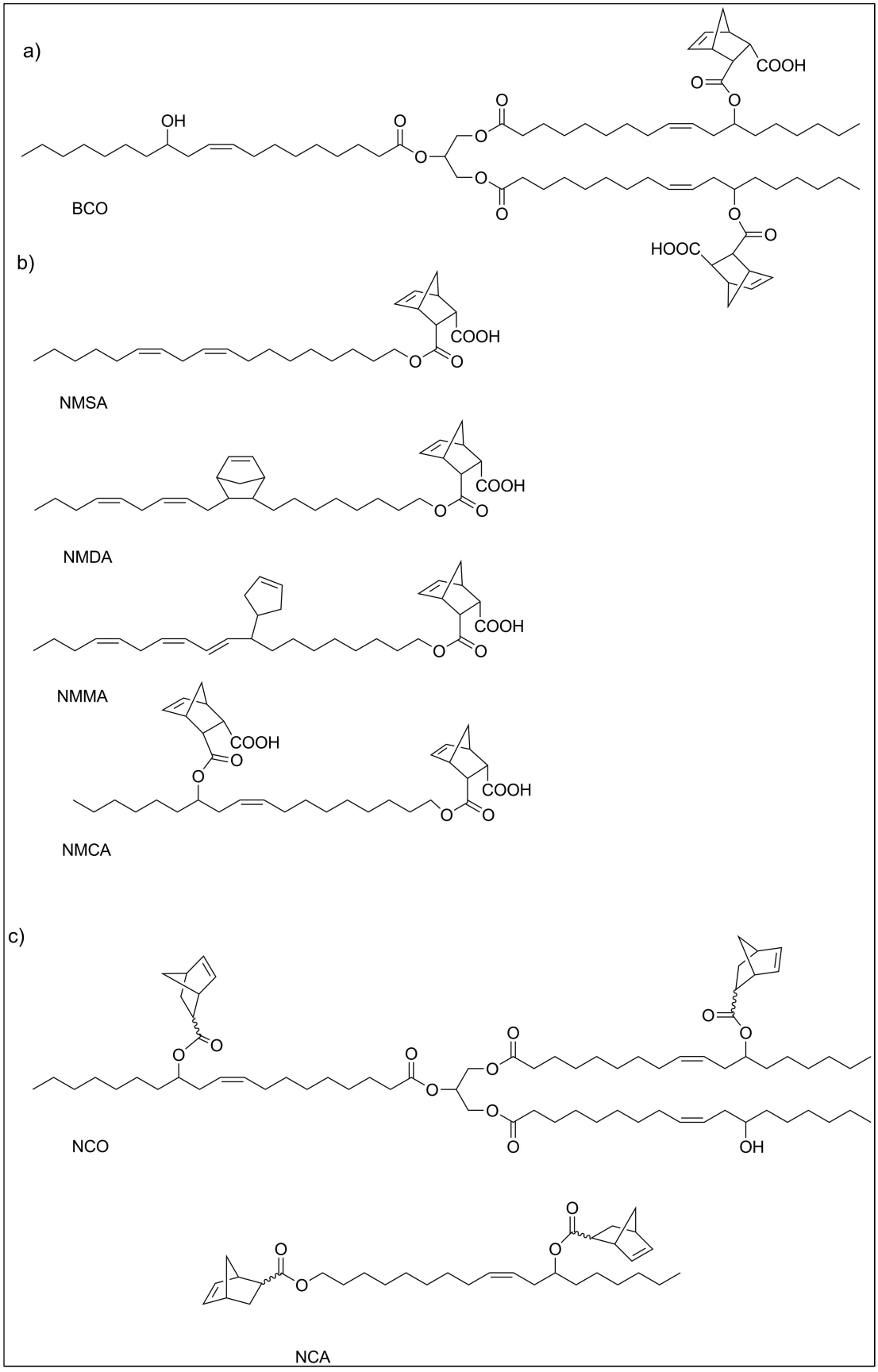


Figure 2.17: VO sourced monomers for Ring Opening Metathesis reaction.

Norbornenyl-functionalized fatty alcohols obtained from soybean oil (NMSA), Dilulin (NMDA), ML189 (NMMA) and castor oil (NMCA) (see Figure 2.17b), have been polymerized with the G2 catalyst. Different functional groups attached to the fatty acid chains of these monomers influenced both propagation process and final properties of polymers [51].

Original castor oil-based systems, norbornenyl-functionalized castor oil (NCO) and norbornenyl functionalized castor fatty alcohol (NCA), were prepared in order to eliminate the adverse effect of the free carboxylic acid groups on ROMP (see Figure 2.17c). The ROMP reaction of NCO/NCA in different ratios with the G2 catalyst (0.125 wt%) resulted in rubbery to rigid plastics. Obtained polymers had crosslink densities ranging from 318 to 6028 mole/m^3 [52].

2.3.6. Condensation Polymerization of Plant Oil Based Monomers

Condensation polymerization is the most common route of preparation of VO-based polymers. This type of polymerization enables to obtain e.g. VO-based polyesters, polyamides and polyurethanes.

2.3.6.1. Plant Oil Based Polyesters

There are three main routes that can be utilized to obtain VOs based polyesters; polycondensation of a diacid and a diol, polycondensation of hydroxy acids or by ring-opening polymerization (Figure 2.18).

For example, VOs monoglyceride, like SOMG (see Figure 2.12), can react with phthalic or maleic anhydride to afford polyesters that could potentially replace industrial resins [53].

High molecular weight polyester was prepared by Petrovic *et al.* [54] from methyl ester of 9-hydroxynonamic acid (HNME). HNME was prepared from ozonolysis and methanolysis of castor oil (Figure 2.19).

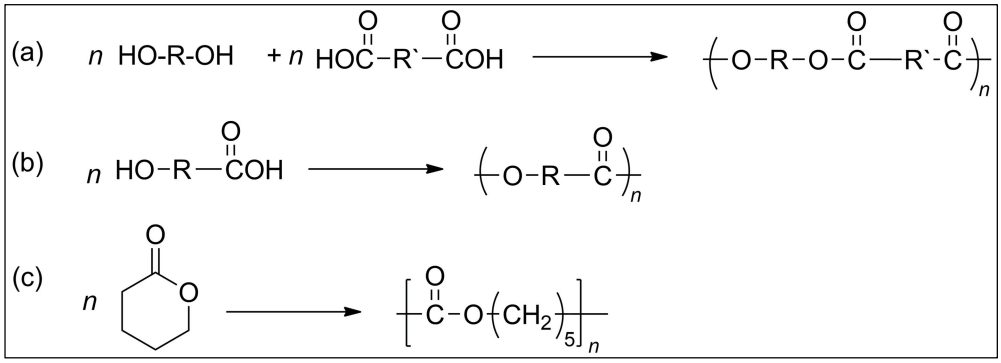


Figure 2.18: Possible routes of polyester synthesis (a) reaction of a diacid and a diol, (b) reaction of hydroxyl acid, and (c) ring opening polymerization of a lactone.

Polymers prepared by self-transesterification of HNME were completely bio-based and obtained polyester is an analogue of polycaprolactone (PCL), but with longer hydrocarbon chain between ester groups.

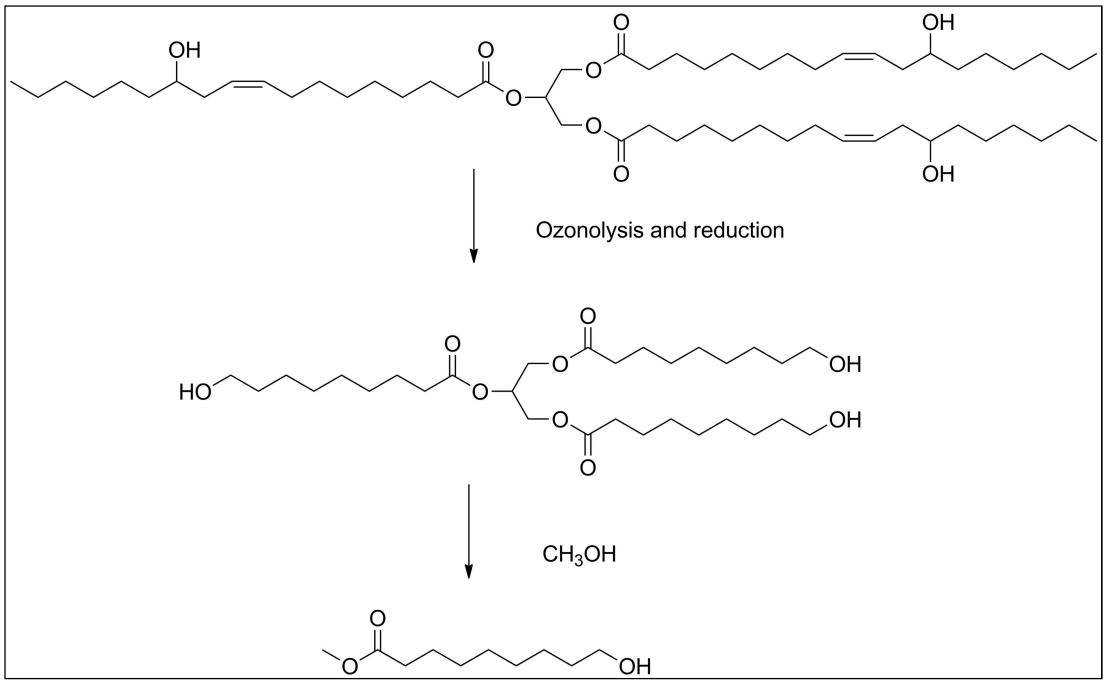


Figure 2.19: Synthesis of HNME from castor oil.

In the literature there are many examples of castor oil or ricinoleic acid based polyesters prepared mainly by thermal polycondensation or transesterification. They will be discussed in details in Section 1.5. Also numerous examples of castor oil or

ricinoleic acid based polyesters are presented in great review prepared by Domb *et al.* [9].

Poly-3-hydroxyalkanoates (PHAs) are separate class of polyesters produced by some bacteria strains when subjected to metabolic stress (see Figure 2.20) [55].

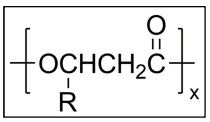


Figure 2.20: Structure of poly-3-hydroxyalkanoates (PHAs).

If carbon-carbon double bond is present in -R side chain of PHAs it can be further cross-linked in autoxidation process to give PHA based elastomers [56].

Above are mentioned only few examples of VO-based polyesters. There are many examples on this topic in scientific literature and several reviews cover the subject in more details [2,9,57]

2.3.6.2. Plant Oil Based Polyamides

Plant-oil based polyamides have been applied in paint and ink productions. For example, soy oil-based (SO) polyamides have been made and applied into dual-component toners which exhibit printing performance similar to that of commercial toners [58].

SO based dimer acids, diamines and amino acids were used to obtain copolyamides. Type and the content of the amino acid in the copolymer affected the chain morphology, crystalline physical properties of the copolyamides [59].

Nylon 11 is important polyamide developed from castor oil. Monomer for synthesis of Nylon 11 polyamide is 11-amino-undecanoic acid (10-undeceoic acid is obtained from pyrolysis of castor oil). Area of Nylon 11 application include but is not limited to metal coatings for noise reduction and protection against UV, wire sheathing, in textiles through brush bristles, filters, or woven and technical fabrics [3].

2.3.6.3. Plant Oil Based Polyurethanes

VOs after conversion into polyols, can react with diisocyanates to afford polyurethanes (PUs). Castor oil or ricinoleic acid may be used for PUs synthesis directly or after modifications. Castor oil derived PUs have good mechanical properties, similar to those of petrochemical PUs and could can be applied as wood adhesives, flexible foams or hard elastomers [60–62].

Plant oils other than castor oil should be first modified to obtain polyols before reaction with isocyanates. Polyols can be prepared by variety of methods e.g. ring opening of epoxidized VOs (see Figure 2.21) [63]. For example, polyols prepared from different oils have been polymerized with diphenylmethane diisocyanate (MDI) to give PUs with different properties. It was discovered that these differences in PUs networks originate from different crosslink densities rather than from the position of the reactive sites in the fatty acids. For example oils with higher functional oil -based polyols afforded PUs with higher crosslink densities and higher mechanical properties [64].

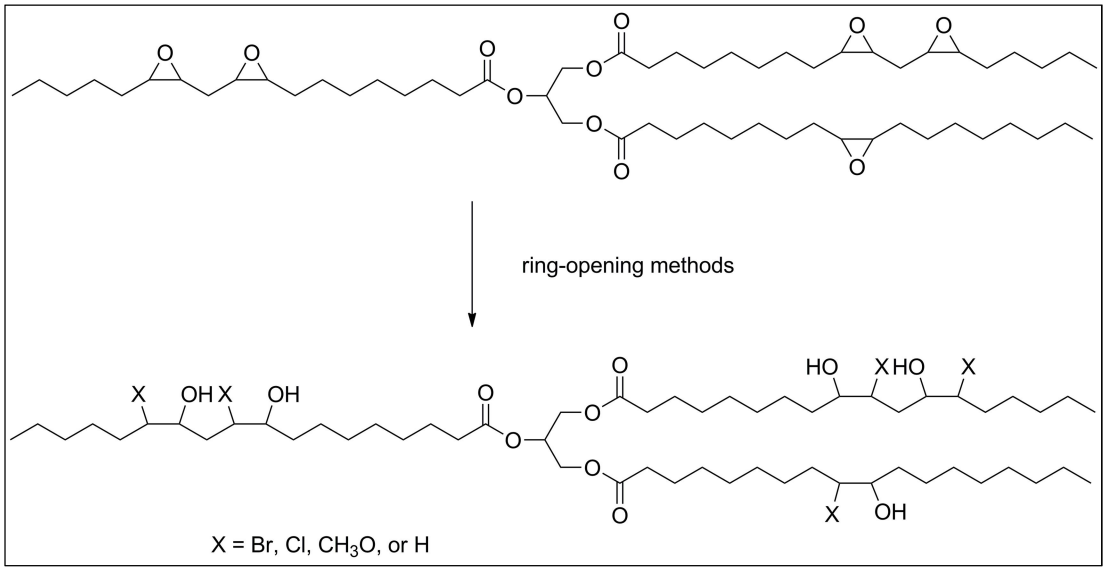


Figure 2.21: Plant oils based polyols.

In another study, VOs derived polyols with various hydroxyl numbers have been prepared by hydroformylation, reduction and partial esterification reaction of

the hydroxyl groups with formic acid. Prepared polyols have been polymerized with MDI to afford PUs to obtain polymers with different crosslink densities [65].

Also the diisocyanate part of polyurethane can be VOs originated. Narine *et. al.* performed ozonolysis and oxidation of oleic acid to obtain azelaic acid. Next, azelaic acid has been transformed to the 1,7-heptamethylene diisocyanate (HPMDI) via Curtius rearrangement (see Figure 2.22) [66].

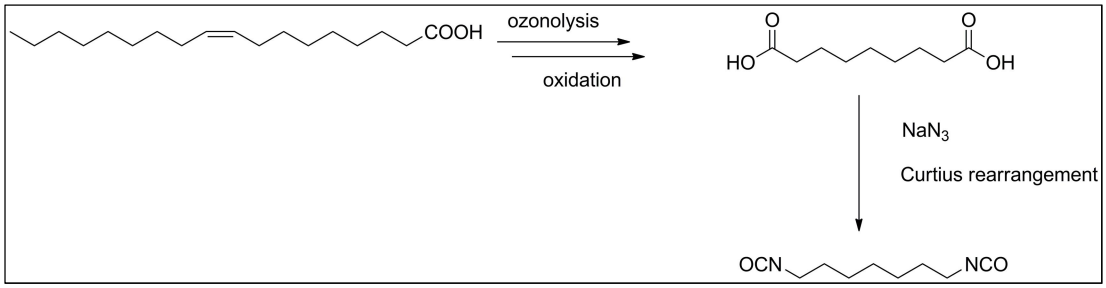


Figure 2.22: Synthesis of azelaic acid and diisocyanate from oleic acid.

PUs synthesized from HPDMI had properties similar to PUs prepared with commercially available diisocyanate 1,6-hexamethylene diisocyanate (HDI) [67].

Similarly to VOs based polyesters, VOs-based polyurethanes have been widely studied and only few examples of thereof were given in this section.

2.4. Castor Oil and Ricinoleic Acid Based Polymers

There is large amount of scientific data on the synthesis of castor oil and ricinoleic acid based copolymer materials. Some of them have potential application in biomedical field, such as drug delivery systems, implants or tissue engineering materials [68–72]. For example, copolymers of ricinoleic and lactic acid, with molecular weight of M_w = 3 000–13 000 gmol^{-1}, were synthesized by ring opening polymerization, melt condensation or transesterification. In drug release and degradation studies, these copolyesters showed almost zero-order weight loss kinetics and structure dependent release of hydrophobic drug [73,74]. Branched castor oil/citric acid copolyesters (M_w = 11 000 gmol^{-1}) can be used as soft tissue augmentation and castor oil/sebacic acid/citric acid/mannitol copolyesters (M_w = 8 223 gmol^{-1}) had perfect properties for drug delivery [75–77]. Poly(ester-anhydrides)

with random nature, prepared by melt polycondensation of poly(sebacic acid) oligomers and ricinoleic acid (M_w = 2000-60000 $gmol^{-1}$) were used as drug carriers [78]. Series of pasty biodegradable poly(ester-anhydrides) were obtained by reacting ricinoleic acid or polyricinoleic acid (M_n = 3000 $gmol^{-1}$) with alkane dicarboxylic acids (from C6 to C12). Poly(ester anhydrides) prepared with ricinoleic acid and adipic, suberic, sebacic or dodecanoic acid had injectable nature (and M_w = 5000-6700 $gmol^{-1}$), while these monomers prepared with polyricinoleic acid were viscous and non-injectable (M_w = 5000-13000 $gmol^{-1}$) [71]. On the other hand, relatively few studies focus on preparation of polyricinoleate homopolymer (PRA). Poly(ricinoleic acid) with M_w = 5600 $gmol^{-1}$ was prepared by thermal polymerization of ricinoleaic acid [73,74]. Ring opening polymerization of ricinoleic acid lactone by Sn(Oct) catalyst yielded poly(ricinoleic acid) with M_w = 5700 $gmol^{-1}$ [79]. High molecular weight polyricinoleate (M_w = 100600 $gmol^{-1}$) was first obtained by Ebata et al. [80] by polycondensation of methyl ricinoleate using immobilized lipase from *Pseudomonas cepeacia* as catalyst in bulk at 80ºC for 7 days. This polymer was reported to be soft material at room temperature, with T_g = -74.8°C, exhibited no crystallinity and was readily biodegraded by activated sludge. Cross-linking of these high molecular weight polyricinoleate with dicumyl peroxide and sulphur curatives yielded rubber-like thermosetting elastomers [81]. In another study, high molecular weight polyepoxyricinoleate (M_w = 272000 $gmol^{-1}$) was prepared by enzymatic polycondensation of methyl epoxyricinoleate using immobilized lipase from *Burkholderia cepeacia* for 7 days, at 80°C. Polyepoxyricinoleate was later cured by maleic and succinic anhydride to obtain biodegradable films [82].

3. RESEARCH OBJECTIVE

Ricinoleic acid and castor oil has been widely used in preparation of various polymers, however their application is limited to copolymers or low molecular weight homopolymer synthesis. Main obstacle in high-molecular-weight polyricinoleate homopolymer synthesis is cost of pure monomer and catalyst.

In this thesis, first we intended to introduce cost-effective synthesis of high-molecular-weight polyricinoleate. High amount of pure monomer (methyl ricinoleate) was obtained from inexpensive ricinoleic acid (80%) in few simple steps (esterification, liquid-liquid extraction and purification). Additionally, the use of commercial enzyme Lipozyme TL IM for synthesis of high-molecular-weight polyricinoleate resulted in further cost reduction. Next, synthesis of polyepoxyricinoleate from high molecular-weight-polyricinoleate was performed by simple reaction with m-chloroperbenzoic acid without any degradation of polymer.

In the second part of this work various properties of polyricinoleates and polyepoxyricinoleate were tested in order to verify their potential use in biomedicine (e.g. for *in vivo* application). Following chemical characterization, film forming properties, morphological characteristics after coating, in vitro degradation, antibacterial activity, adhesive properties and cytotoxicity of synthesized polymers were tested.

4. EXPERIMENTAL

4.1. Materials

Ricinoleic acid (>80%) was obtained from TCI Co., Inc. (Tokyo, Japan). 2,2-dimethoxypropane (>97%) was bought from Merck. Sulfuric acid (95-97%, ACS reag.), hydrochloric acid (37%, ACS reag.), 2,2-dimethoxypropane (98%), m-chloroperbenzoic acid ≤77% and molecular sieves 4 Å (beads, 8-12 mesh) were purchased from Sigma-Aldrich. All solvents and salts were analytical grade from Sigma-Aldrich or Merck and were used as received. Lipozyme TL IM from *Thermomyces lanuginosus* immobilized on silica gel (250 $IUNg^{-1}$) and Novozym 40086 from *Rhizomucor miehei* immobilized on a resin carrier (275 $IUNg^{-1}$) were donated by Novozymes (Bagsvaerd, Denmark). Lipase A *Candida antarctica*, recombinant from *Aspergillus oryzae* immobilized on Immobead 150 (>500 Ug^{-1}), Amano Lipase PS IM, from *Burkholderia cepacia* immobilized on diatomaceous earth (>500 Ug^{-1}), Amano Lipase PS-C I, from *Burkholderia cepacia* (immobilized on ceramic) and Amano Lipase PS-C II, from *Burkholderia cepacia*, (immobilized on ceramic) were purchased from Sigma-Aldrich. The enzymes were dried in a vacuum over P_2O_5 at 25°C for 3 h.

4.2. Instrumentation

- Nuclear Magnetic Resonance (NMR)

^{1}H (600 MHz) and ^{13}C NMR (150 MHz) spectra were recorded with a Varian INOVA 600 spectrometer, using tetramethylsilane (TMS) as an internal standard. Samples were dissolved in deuterated chloroform.

- Gas Chromatography (GC)

Gas chromatography (GC) Perkin Elmer Auto System XL with SP™ -2380 (100 m length x 0.25 mm with a 0.25 μm film thickness) column and flame ionization detector (FID) was used for analysis of fatty acids composition. The temperature of injector and detector was 280°C and 260°C, respectively. The oven

temperature was programmed to increase from 120◦C to 220◦C at 5◦C min^{-1}. Helium was the carrier gas.

- Fourier-Transform Infrared Spectroscopy (FTIR)

FTIR spectra were recorded with Perkin Elmer Spectrum One spectrometer on KBr pellet in the 4000–450 cm^{-1} range.

- Gel Permeation Chromatography (GPC)

Gel permeation chromatography (GPC) Agilent 1100 apparatus equipped with PLgel 5μm MIXED-D column (Agilent, USA) and refractive index detector MODEL (Agilent 1100, USA) was used for measurements of molecular weights (M_n, M_w) and polydispersity ($M_wM_n^{-1}$). THF was used as an eluent with flow rate 0.5 mL min^{-1}. Polystyrene (PS) with narrow molecular weight was used as a calibration standard (Agilent, USA).

- Thin Layer Chromatography (TLC)

Thin layer chromatography (TLC) was performed on TLC silica gel 60 aluminium sheets from Merck with hexane:acetone (9:1) mobile phase.

- Thermogravimetric Analysis (TGA)

Thermogravimetric analysis (TGA) was determined on Perkin Elmer Pyris 1TGA from 25ºC to 700ºC at a heating rate of 10 °C min^{-1} under nitrogen atmosphere.10 mg of polymer sample was used for measurements.

- Differential Scanning Calorimetry (DSC)

Differential scanning calorimetry (DSC) was determined on DSC Q2000 (TA Instruments, USA). 10 mg of polymer sample was used for measurements. In the first run samples were cooled to -90°C and then heated to 200ºC. Samples were then cooled again to -90°C and second run was performed by heating samples to 200ºC. Cooling and heating rates were 10ºCmin^{-1}.

- Scanning Electron Microscopy (SEM)

Scanning electron microscope (SEM) TESCAN VEGA 3 SBH (Czech Republic) was used for morphological characterization of the prepared film samples. Before SEM investigations samples were sputter-coated by Au-Pd thin film.

- Atomic Force Microscopy (AFM)

Surface topographies of the films were analysed using an atomic force microscope (AFM, Nanomagnetics Instruments, Oxford, UK) in the tapping mode. The surface roughness was evaluated by root mean square (RMS) based on 20×20 μm scan area.

- Rheology

An Anton Paar, MCR 302 Rheometer with parallel plate system (∅ 15mm) and P-PTD (lower plate with Peltier temperature control) with passive hood was used for rheological measurements. The amplitude sweep has been carried out at a constant angular frequency of 10 $rads^{-1}$ at a strain range from 0.01% to 100%. A constant temperature of 37°C was chosen. The frequency sweep has been carried out at a constant strain of 1% (which is within the linear viscoelastic range) and at an angular frequency range from 400 $rads^{-1}$ to 0.1 $rads^{-1}$. A constant temperature of 37°C was chosen.

- Mechanical Testing

Adhesive strength of polymers was determined in lap-shear by tension loading (Lloyd Instrument, Fareham, UK), equipped with a 50-N load cell, with a cross-head speed of 2 mm/min.

- UV-Vis

In LDH cytotoxicity assay the absorbance of the wells was read at 490 nm on Epoch Microplate Reader (BioTek Instruments, Inc., USA).

4.3. Monomer Preparation

4.3.1. Esterification of Ricinoleic Acid (>80%)

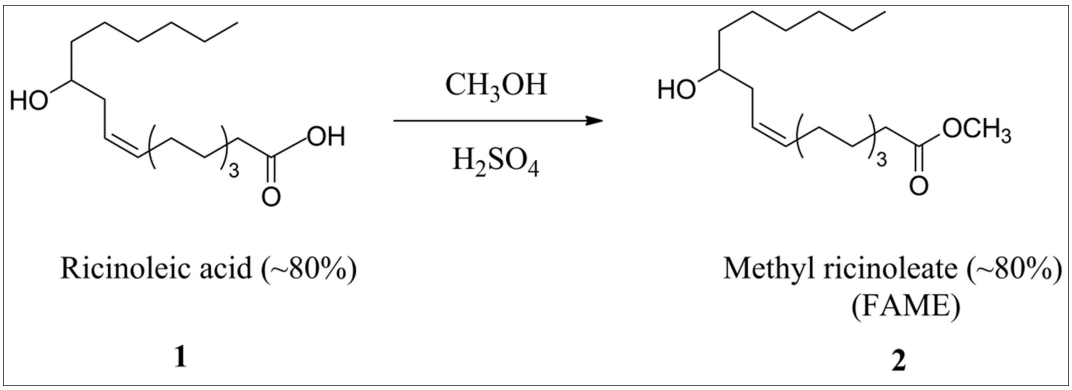


Figure 4.1: Esterification reaction of ricinoleic acid (~80%).

Experimental procedure: Ricinoleic acid (>80%) (100g) was mixed with 2 vol% H_2SO_4 methanolic solution (100 mL) in 500 mL round-bottomed flask with magnetic stirrer. Next, 2,2-dimethoxypropane (50 mL) was added and reaction mixture was refluxed at 60°C with TLC monitoring every 10 min. After 30 min. fatty acids were reaction was completed (see Figure 4.2 and Table 4.1), the mixture was transferred to the separatory funnel, hexane (200 mL) and water (100 mL) were added and the mixture was shaken for about 1 min. Bottom phase was discarded and hexane phase was shaken with 5 wt% sodium bicarbonate solution (100 mL) and then dried over anhydrous sodium sulfate, filtered and evaporated to obtain fatty acid methyl esters (FAME) (101.4g). Conversion (~100%) of ricinoleic acid to methyl ester was confirmed by measuring acid value of FAME. FAME composition analysed by GC showed 79.6% ricinoleic acid and 20.4% other esters. For GC analysis, ^{1}H NMR, ^{13}C NMR and FT-IR spectra of FAME see Figure B1.1 – B1.4 in Appendix B.



Figure 4.2: TLC spots from the left: ricinoleic acid (~80%) and methyl ricinoleate (~80%).

Table 4.1: Compounds and corresponding retention factors (R_f).

Code	Compound name	R_f	Compound
1	Ricinoleic acid (~80%)	0.05	Ricinoleic acid
		0.14	Non-hydroxy fatty acids
2	FAME	0.27	Methyl ricinoleate
		0.64 – 0.73	Non-hydroxy fatty acids methyl esters

4.3.2. Conversion of Ricinoleic Acid (>80%) into FAME

Conversion of ricinoleic acid into FAME can be calculated from the equation 4.1:

$$C(\%) = \frac{AV_0 - AV_f}{AV_0} \quad (4.1)$$

Where:

- AV_0 – acid value of ricioleic acid (~80%)
- AV_f – acid value of FAME

Acid values of ricinoleic acid (~80%) and FAME were measured experimentally.

Experimental procedure: Approximately 0.5 g of ricinoleic acid (~80%) or FAME was placed in 250 mL Erlenmayer flask and 50 mL of hot neutralised ethanol was added. After that phenolphthalein (1mL) was added to the mixture and boiled for about 5 min. Solution was titrated with 0.1M NaOH until pale pink colour appeared and remained for more than 1 min. Procedure was repeated in triplicate for each parallel sample and average value was determined. Acid value was then calculated from the equation 4.2:

$$AV = \frac{56.1 \times \mathrm{V} \times N}{W} \tag{4.2}$$

Where:

- V - volume of standard solution of sodium hydroxide used
- N - normality of sodium hydroxide solution
- W - weight of the sample

Results:

$AV_0 = 149.4 \pm 1.5$

$AV_f \sim 0$ (changed colour after one drop of 0.1 M NaOH)

Conversion of ricinoleic acid into FAME ~100%.

4.3.3. Isolation of Methyl Ricinoleate from FAME

Methyl ricinoleate was isolated from FAME mixture by counter current distribution according to the method described by Berdeaux *et al.* [83]. The purpose of this method is to obtain pure methyl ricinoleate (see Figure 4.3).

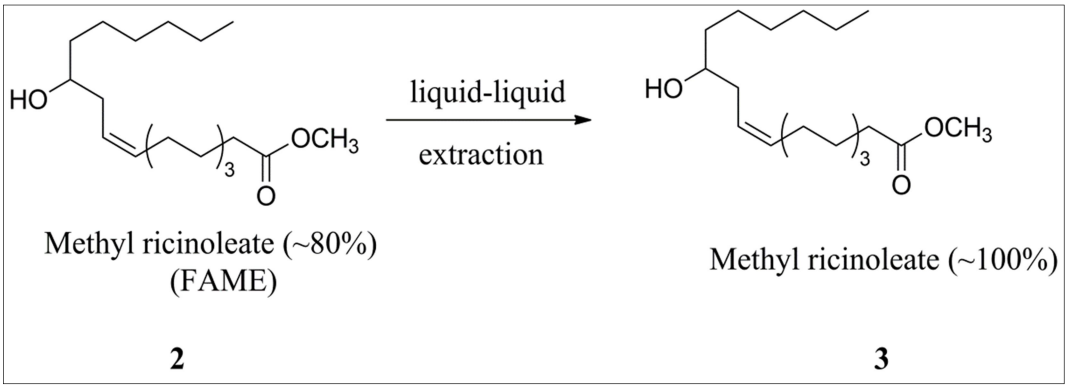


Figure 4.3: Isolation of pure methyl ricinoleate from mixture of FAME.

Experimental procedure: Isolation was performed in three separatory funnels with hexane as a stationary phase (3×600 mL) and 90 vol% aqueous methanol as a mobile phase (10×300 mL). FAME (100 g) was dissolved in 600 mL of hexane in first separatory funnel and shaken with first portion of methanolic mobile phase. After layers reach to equilibration, mobile phase was removed and consecutively passed thought second and third stationary phases (Figure 4.5). Procedure was continued with remaining mobile phases and separation was monitored by TLC analysis (Figure 4.4). First 8 methanolic phases were combined and concentrated on rotary evaporator until formation of turbid oil. The oil was dissolved in hexane (500 mL), washed with water (800 mL) and saturated brine (300 mL). Hexane phase was dried over anhydrous sodium sulfate and evaporated to give 71.4 g of esters, containing 99.7% of pure methyl ricinoleate and 0.3% other esters.

For GC analysis, ^{1}H NMR, ^{13}C NMR and FT-IR spectra of FAME see Figure B1.5 – B1.8 in Appendix B.

FTIR (KBr): ν (cm^{-1}) = 3444 (-OH), 3007, 1655 (-C=C-), 2928 (-CH_2), 1741 (C=O, ester).

^{1}H NMR (600 MHz, $CDCl_3$): δ (ppm) = 0.87 (3H, t, C18 –CH_3), 1.29 (16H, m, C4-7 and C14-17), 1.45 (2H, m, C13 –CH_2), 1.61 (2H, m, C3 –CH_2), 2.03 (2H, m, C3 –CH_2), 2.20 (2H, t, C11 –CH_2), 2.29 (2H, t, C2 –CH_2), 3.60 (1H, m, C12 HC-O-), 3.65 (3H, s, -OCH_3), 5.53-5.40 (m, 2H, C9-10, -CH=CH-).

^{13}C NMR (150 MHz, $CDCl_3$): δ (ppm) = 14.19 (C18, -CH_3), 22.73 (C17, -CH_2), 25.03 (C3, -CH_2), 25.83 (C14, -CH_2), 29.19 (C4, 7 and 15 -CH_2), 29.47 (C5, -CH_2),

29.68 (C6, -CH_2), 31.95 (C16, -CH_2), 34.19 (C2, -CH_2), 35.47 (C11, -CH_2), 36.97 (C13, -CH_2), 51.54 (-OCH_3), 71.61 (C12, -CH), 125.36 (C10, -CH), 133.38 (C9, -CH), 174.41 (C1, C=O).

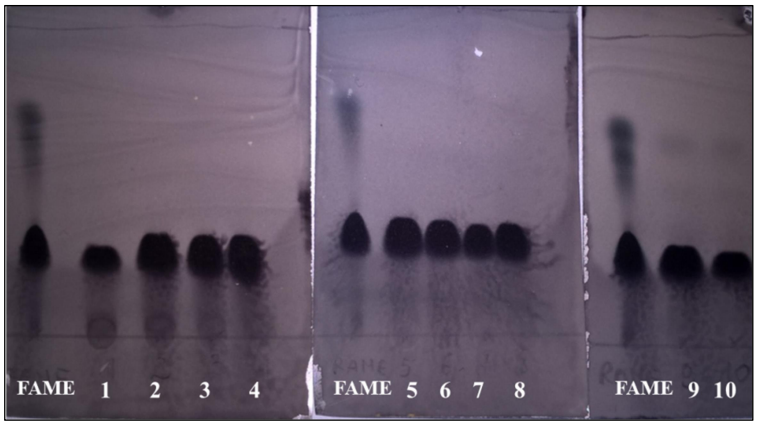


Figure 4.4: TLC monitoring of mobile phases after passing three stationary phases.

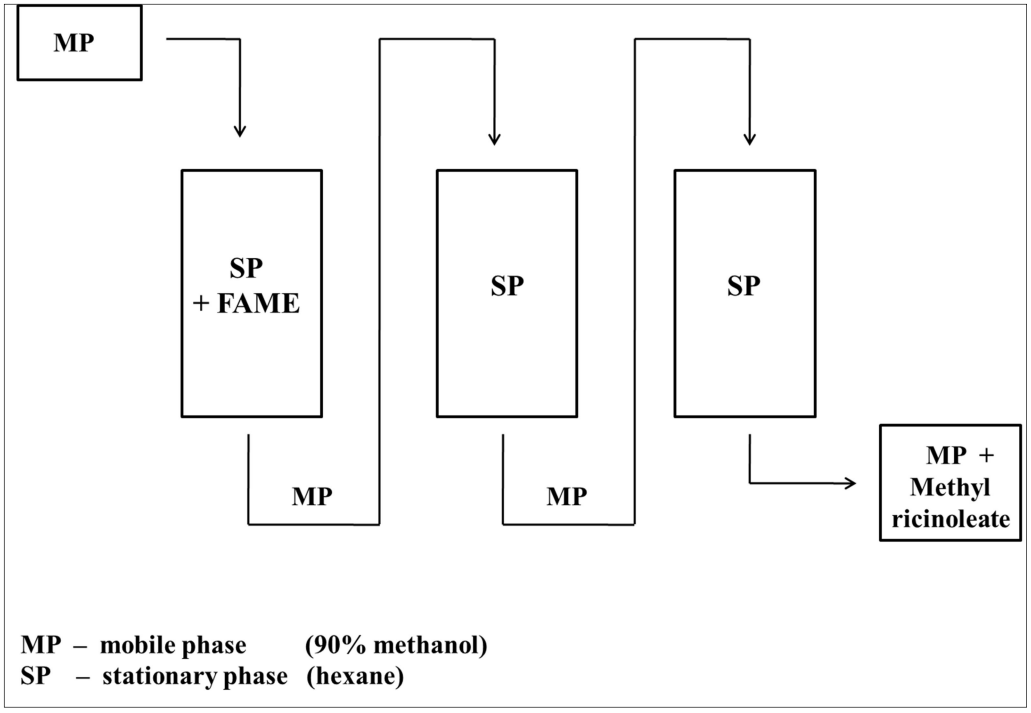


Figure 4.5: Schematic representation of isolation of methyl ricinoleate from FAME by counter current distribution.

4.4. Enzymatic Polymerization of Methyl Ricinoleate

Procedure for synthesis of high molecular weight polyricinoleate with Lipase TL IM is given as representative example.

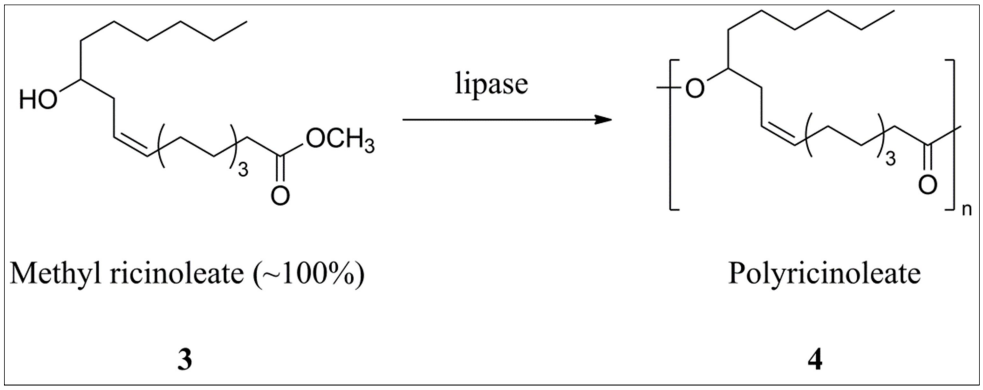


Figure 4.6: Synthesis of polyricinoleate in the presence of lipase catalyst.

Experimental procedure: Pure methyl ricinoleate (0.5 g) was gently mixed with lipase enzyme (0.5 g) in 5 mL glass vial. Vial was then placed in flat-bottomed flask filled with activated 4 Å molecular sieves. Flask was sealed and placed in oven preheated to 80ºC without any mixing or shaking for 7 days. After polymerization was completed, the polymerization mixture from vial was dissolved in chloroform (30 mL), insoluble enzyme was filtered out and solvent was evaporated to obtain the polymer. Unreacted monomer was removed by reprecipitation with methanol – chloroform mixture. The number-average molecular weight (M_n), weight-average molecular weight (M_w) and polydispersity index ($M_wM_n^{-1}$) of the polymers were determined by GPC. The molecular structure was analysed by FTIR, ^{1}H NMR and ^{13}C NMR spectroscopy. Spectral data for PRA-H of M_w = 72 000 gmol^{-1} are given as a representative example.

FTIR (KBr): ν (cm^{-1}) = 3447 (-OH, small residual peak), 3011, 1657 (-C=C-), 2928 (-CH_2), 1732 (C=O, ester).

^{1}H NMR (600 MHz, $CDCl_3$): δ (ppm) = 0.87 (3H, t, C18 –CH_3), 1.29 (16H, m, C4-7 and C14-17), 1.52 (2H, m, C13 –CH_2), 1.60 (2H, m, C3 –CH_2), 2.00 (2H, m, C8 –CH_2), 2.26 (4H, m, C2, C11 –CH_2), 4.87 (1H, m, C12 HC-O-), 5.44-5.32 (m, 2H, C9-10, -CH=CH-).

^{13}C NMR (150 MHz, $CDCl_3$): δ (ppm) = 14.20 (C18, $-CH_3$), 22.71 (C17, $-CH_2$), 25.25 (C3, $-CH_2$), 25.49 (C14, $-CH_2$), 27.50 (C8, $-CH_2$), 29.28 (C4, 7 and 15 $-CH_2$), 29.38 (C5, $-CH_2$), 29.70 (C6, $-CH_2$), 31.89 (C16, $-CH_2$), 32.13 (C2, $-CH_2$), 33.77 (C11, $-CH_2$), 34.80 (C13, $-CH_2$), 73.81 (C12, -CH), 124.44 (C10, -CH), 132.64 (C9, -CH), 173.65 (C1, C=O).

4.4.1. Selection of Lipase Catalyst

Six lipase catalysts were screened at two different temperatures (50ºC and 70ºC) with respect to polymerization activity at 100 wt. % of enzyme (with respect to monomer) for 7 days.

Screened lipase catalyst:

- Lipozyme TL IM
- Novozym 40086
- Lipase A *Candida antarctica*
- Lipase PS IM
- Lipase PS CI
- Lipase PS CII

Experimetal procedure: Each lipase catalyst (0.5g) was gently mixed with pure methyl ricinoleate (0.5g) in 5 mL glass vial. Vials were then placed in flat-bottomed flasks, each filled with activated 4 Å molecular sieves. Flask was sealed and placed in oven preheated to 50ºC or 70ºC for 7 days without any mixing or shaking. Work-up was as in general polymerization procedure.
Lipozyme TL IM was selected as most active and low-cost enzyme for further investigation.

4.4.2. Effect of Reaction Temperature on Molecular Weight of Polyricinoleate

Efficiency of Lipozyme TL IM was tested at different temperatures (40ºC, 50ºC, 60ºC, 70ºC, 80ºC and 90ºC) in order to select optimal conditions for polyricinoleate synthesis. Experiments were performed at 100 wt. % enzyme concentration for 7 days.

Experimental procedure: Pure methyl ricinoleate (0.5 g) was gently mixed with Lipozyme TL IM enzyme (0.5 g) in 5 mL glass vial. Vial was then placed in flat-bottomed flask filled with activated 4 Å molecular sieves. Flask was sealed and placed in oven preheated to selected temperature (from the range 40ºC-90ºC) for 7 days without any mixing or shaking. Work-up was as in general polymerization procedure.

Temperature of **80ºC** was the most favourable for synthesis of polyricinoleate.

4.4.3. Effect of Enzyme Concentration on Molecular Weight of Polyricinoleate

Effect of Lipozyme TL IM concentration on molecular weight of polyricinoleate was established. For this purpose polyricinoleates were synthesized at 50 wt. %, 100 wt. % and 150 wt. % concentration of enzyme at 80ºC for 7 days.

Experimental procedure: Pure methyl ricinoleate (0.5g) was gently mixed with different amounts of Lipozyme TL IM enzyme (0.25g, 0.5g and 0.75g) in 5 mL glass vial. Vials were then placed in flat-bottomed flask filled with activated 4 Å molecular sieves. Flasks were sealed and placed in oven preheated to 80ºC for 7 days without any mixing or shaking. Work-up was as in general polymerization procedure.

100 wt. % concentration of enzyme resulted in highest molecular weight of polyricinoleate.

4.4.4. Effect of Reaction Time on Molecular Weight of Polyricinoleate

Influence of reaction time on polyricinoleate molecular weight was established by polymerization of methyl ricinoleate with 100 wt. % of Lipozyme TL IM at 80ºC for different periods of time (1, 3, 5, 7 and 9 days).

Experimental procedure: Pure methyl ricinoleate (0.5g) was gently mixed with Lipozyme TL IM enzyme (0.5g) in 5 mL glass vial. Vial was then placed in flat-bottomed flask filled with activated 4 Å molecular sieves. Flask was sealed and placed in oven preheated to 80ºC for different periods of time (from 1 to 9 days) without any mixing or shaking. Work-up was as in general polymerization procedure.
The highest molecular weight was obtained after **7 days** of polymerization.

4.4.5. Reusability of Lipozyme TL IM Enzyme

Lipozyme TL IM was used in repeatedly after reaction in order to check its potential ability for repeated use. Each cycle was performed at 100 wt. % of enzyme, at 80ºC for 7 days. Retention of Lipozyme TL IM activity after repeated use was assessed in terms of molecular weight after each cycle.

Experimental procedure: Pure methyl ricinoleate (0.5g) was gently mixed with Lipozyme TL IM enzyme (0.5g) in 5 mL glass vial. Vial was then placed in flat-bottomed flask filled with activated 4 Å molecular sieves. Flasks were sealed and placed in oven preheated to 80ºC for 7 days without any mixing or shaking. After polymerization was completed, the polymerization mixture from vial was dissolved in chloroform (30 mL), insoluble enzyme was filtered out and solvent was evaporated to obtain the polymer. Unreacted monomer was removed by reprecipitation with methanol – chloroform mixture. After each cycle enzyme was additionally washed with chloroform (2×30 mL) for 10 min. to remove any monomer/polymer residues. Chloroform was filtered out and enzyme was dried over P_2O_5 for 3 h before next cycle.

4.5. Synthesis of Polyepoxyricinoleate

Polyepoxyricinoleate was synthesized to increase adhesive force of polyricinoleate polymer.

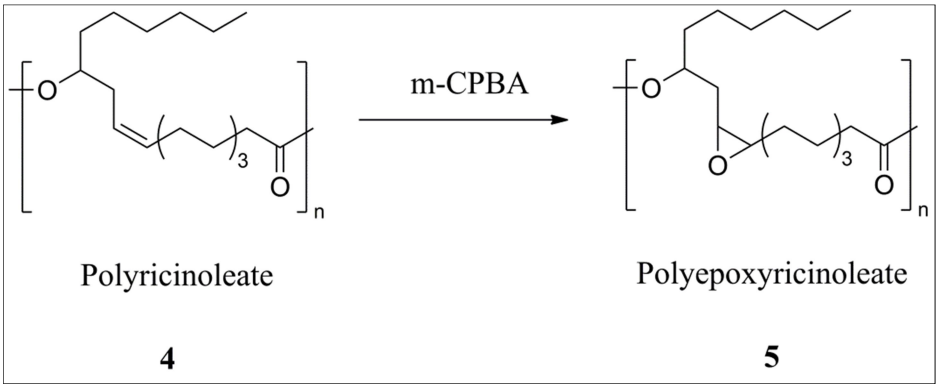


Figure 4.7: Synthesis of polyepoxyricinoleate from polyricinoleate.

Experimental procedure: Polyricinoleate (1g) was stirred with chloroform (20 mL) and $NaHCO_3$ (0.7g) in 100 mL round bottomed flask until complete dissolution of polymer. Next, flask was placed in an ice bath and solution of m-chloroperbenzoic acid (1.7g dissolved in 40 mL of chloroform) was added dropwise within 15 min. After that ice bath was removed and stirring was continued for 3h at room temperature with reaction monitoring every 1h by TLC. Reaction is presented in Figure 4.7. Then, reaction mixture was filtered and filtrate was transferred to separatory funnel (250 mL). Organic phase was washed with 10% Na_2SO_3, 5% $NaHCO_3$ and three times with warm water. Then, organic phase was dried over anhydrous Na_2SO_4, filtered and solvent was evaporated to dryness. 0.920 g of polyepoxyricinoleate (PER) was obtained (yield 89.6 %).

FTIR (KBr): ν (cm^{-1}) = 3447 (-OH, small residual peak), 2928 (-CH_2), 1732 (C=O, ester), 830 (-C-O-C- epoxy).

^{1}H NMR (600 MHz, $CDCl_3$): δ (ppm) = 0.88 (3H, t, C18 –CH_3), 1.32-1.80 (24H, m, C3-8, C11, C13-17 –CH_2), 2.30 (2H, m, C2 –CH_2), 2.85 (1H, m, C9 HC-O), 2.94 (1H, m, C10 HC-O), 5.06 (1H, m, C12 HC-O-).

^{13}C NMR (150 MHz, $CDCl_3$): δ (ppm) = 14.20 (C18, -CH_3), 22.69 (C17, -CH_2), 25.13 (C3, -CH_2), 25.36/25.49 (C14, -CH_2), 26.73 (C7, -CH_2), 28.07/28.14 (C8, -

CH_2), 29.18 (C4, -CH_2), 29.24 (C15, -CH_2), 29.39 (C5, -CH_2), 29.50 (C6, -CH_2), 31.84 (C16, -CH_2), 32.96/32.93 (C11, -CH_2), 34.31/34.50 (C13, -CH_2), 34.70 (C2, -CH_2), 53.83/53.98 (C10, HC-O), 56.28/56.92 (C9, HC-O), 72.27/72.37 (C12, -CH), 173.63 (C1, C=O).

4.6. Preparation of Pure Ricinoleic Acid

Pure ricinoleic acid (RA) was synthesized for comparative antibacterial study as it is known antibacterial agent [84].

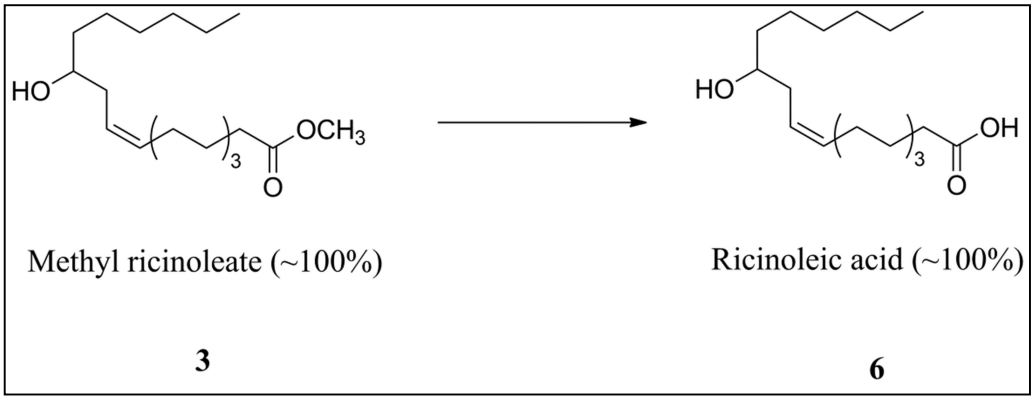


Figure 4.8: Synthesis of pure ricinoleic acid.

Experimental procedure: pure methyl ricinoleate (10 g) was hydrolyzed (refluxed) at 50◦C in methanol:alkaline water 1:1 solution (100 mL) for 30 min and monitored by TLC every 10 min. Next, DDW was added to dilute the mixture and pH was adjusted to 2 with concentrated HCl solution. Ricinoleic acid was extracted to ethyl acetate, dried over anhydrous sodium sulphate, filtered and evaporated to obtain 8.76 g of (91.72 yield %).

FTIR (KBr): ν (cm^{-1}) = 3399 broad (-OH and carboxylic acid), 3011 (-C=C-), 2927 (-CH_2), 1710 (C=O, ester).

^{1}H NMR (600 MHz, $CDCl_3$): δ (ppm) = 0.87 (3H, t, C18 –CH_3), 1.30(16H, m, C4-7 and C14-17), 1.45 (2H, m, C13 –CH_2), 1.61 (2H, m, C3 –CH_2), 2.02 (2H, m, C3 –CH_2), 2.20 (2H, t, C11 –CH_2), 2.32(2H, t, C2 –CH_2), 3.62 (1H, m, C12 HC-O-), 5.52-5.39 (m, 2H, C9-10, -CH=CH-).

^{13}C NMR (150 MHz, $CDCl_3$): δ (ppm) = 14.19 (C18, -CH_3), 22.73 (C17, -CH_2), 24.78 (C3, -CH_2), 25.78 (C14, -CH_2), 27.45 (C8, -CH_2), 29.15 (C4, 7 and 15 -CH_2), 29.47 (C5, -CH_2), 29.62 (C6, -CH_2), 31.95 (C16, -CH_2), 34.15 (C2, -CH_2), 35.35 (C11, -CH_2), 36.84 (C13, -CH_2), 71.80 (C12, -CH), 125.28 (C10, -CH), 133.36 (C9, -CH), 179.51 (C1, C=O).

Disappearance of peak at 3.65 ppm in ^1H NMR and 51.54 ppm in ^{13}C NMR confirms complete conversion of methyl ester into carboxylic acid.

^1H NMR, ^{13}C NMR and FT-IR spectra of pure ricinoleic acid are presented in see Figure B1.9-B1.11- in Appendix B.

4.7. Characterization Methods

4.7.1. Preparation of Polymer Films

Polymer films for investigation of coating properties and surface characterization by SEM and AFM were prepared on round glass or stainless steel plates with ∅15 mm. Polymer films for antibacterial tests were prepared on glass plates with ∅15 mm. Films were prepared by solvent casting method. 85 μL of 5 wt. % THF solution of RA, PRA-M or PRA-H was pipetted onto the plate and left for 2 h at room temperature for drying.

4.7.2. Antibacterial Activity Test

This study was designed to assess the antibacterial effect of the RA, PRA-M and PRA-H samples on *Staphylococcus aureus* and *Escherichia coli*, based on the colony counting method.

4.7.2.1. Preparation of the Inoculum

The bacterial cultures of *S. aureus* ATCC 25923 (Gram-positive) and *E.coli* ATCC 25922 (Gram-negative) were grown on nutrient agar slants and stored at 4°C. A loop full of bacteria from the agar slant was transferred into 15 mL tryptic soy broth (TSB) in a sterile centrifuge tube and incubated at 37°C for 24 h.

4.7.2.2. Colony Counting Method

For the quantitative assessment of the antibacterial activity against gram positive and gram negative bacteria, the cultures of *S. aureus* and *E. coli* were diluted to a concentration of 10^4-10^5 cfu/mL to obtain the test suspension. The glass plates ∅15 mm coated with the RA, PRA-M and PRA-H were aseptically transferred into separate sterile petri dishes. Then, each of the test discs was inoculated with either 50 µL of *S. aureus* or *E. coli* suspension. The bacterial suspension was spread out over the disc surface evenly, preventing any overflow from the surface. The plates were covered and incubated at 37°C overnight. Then all of the discs were separately transferred into 50 mL sterile centrifuge tubes. After addition of 1 mL of peptone water, they were vortexed rigorously for 1 min.

For colony counting, Baird-Parker agar plates were used for *S. aureus* and 3M total plate count slides were used for *E. coli*. Serial dilutions from each sample were inoculated on Baird-Parker or 3M plates. The plates were incubated at 37°C for 24h before the colonies were counted. The experiments were triplicated. Data points were expressed as means ± standard deviations. Differences between the means were analysed using Student's *t*-test, taking $p<0.05$ as statistically significant.

4.7.3. *In vitro* Degradation Study

100 mg of polymer sample (PRA-M, PRA-H and PER) was placed in 5 mL PBS buffer solution (pH = 7.4) at 37ºC with orbital shaking (100 rpm). Degradation medium was replaced at pre-determined time intervals; sample was washed with double distilled water (DDW) and dried in oven at 60°C under vacuum until obtaining constant weight.

4.7.4. Mechanical Testing

4.7.4.1. Lap-Shear Adhesion Test on Glass, Aluminium, Paper and PET

Plates of different materials with dimensions 2.5×10 cm^2 were washed with acetone to remove any impurities 10 ± 1 mg of sample was spread on 1×2.5 cm^2 overlap area

of. Next, surfaces covered with sample were overlapped and placed into mechanical tester for shear testing by tensile loading with strain rate 2 mm/min. Adhesion strength was calculated by dividing the maximum load by overlapping area.

4.7.4.2. Lap-Shear Adhesion Test on Ovine Skin

Lap-shear adhesion test for measurement of adhesive performance was adapted from F 2255-05 ASTM standard. Fresh ovine skin, purchased from local butcher shop was used for the adhesion test. First, epidermal layer of the skin was removed with a dermatome and 2.5×10 cm^2 skin specimens were cut with scalpel blade using glass template. 10mg ± 1mg of sample was spread on 1×2.5 cm^2 overlap area of one end of tissue strip. Next, surfaces covered with sample were overlapped and placed into mechanical tester for shear testing by tensile loading with strain rate 2 mm/min. Adhesion strength was calculated by dividing the maximum load by overlapping area.

4.7.5. Quantification of Whole Blood Clotting Time

All experiments performed with humans were carried out in accordance with World Medical Association Declaration of Helsinki: Ethical Principles for Medical Research Involving Human Subjects published in 2013 and a copy of declaration was signed by all researchers. Local scientific committee of Yeditepe University (Istanbul, Turkey), has approved the research protocol. Informed consent forms were signed by all of the healthy volunteers. Two millilitres of blood taken from each of five healthy adult female volunteers was drawn into sodium citrate tubes. Cover slips with polymer films were placed into a Co® 96 well tissue culture plate in triplicates. 50 μL blood and 5 μL 0.1 M $CaCl_2$ was added to each well, and thrombus formation was observed in time. Control group was performed without any polymer sample.

4.7.6. Analysis of Cell Viability by the Modified Lactate Dehydrogenase (LDH) Assay

In this study, CytoSelect™ LDH Cytotoxicity Assay Kit (Germany, Sigma) was used. Bottoms of a 96 well tissue culture plate was coated with materials and sterilized with UV exposure for 2h. 3T3 mouse fibroblasts cultured in DMEM High Glucose medium supplemented with 10% fetal bovine serum and 1% penicillin streptomycin antibiotic solution were seeded in coated culture plate wells as triplicates. Cells were incubated with materials for 1 or 3 days. Culture medium was removed and fresh 190 µL medium containing 10 µL lysis solution provided with the kit was added to wells and incubated for 30 min. to lyse cells. Untreated cells were used as control. Viability was measured on day 1 and 3. For measuring viability, 200 µL of culture medium was transferred to another 96 well tissue culture plate, 20 µL LDH assay reagent was added to wells and incubated in the cell culture incubator for 2h. For control, cells were lysed to obtain highest possible absorbance. Absorbance was measured with Epoch spectrophotometer, and cell viability was calculated according to the equation 4.3:

$$Cell\ viability\ (\%) = \frac{Sample\ OD\ (490\ nm)}{Control\ OD\ (490\ nm)} \times 100\% \qquad (4.3)$$

5. RESULTS AND DISCUSSION

5.1. Enzymatic Polymerization of Methyl Ricinoleate

In this section optimization steps of methyl ricinoleate polymerization are discussed.

5.1.1. Selection of Lipase Catalyst

For synthesis of polyricinoleate, Lipozyme TL IM, Novozym 40086, Lipase A *Candida antarctica*, Lipase PS IM, Lipase PS CI and Lipase PS CII have been screened for their catalytic activity at two different temperatures.

5.1.1.1. Screening of Enzymes Activity at 50ºC

First, six lipases were screened at 50°C with enzyme concentration 100 wt. % relative to monomer for 7 days. Blank test was performed in order to compare polymerization degree at tested conditions without presence of catalyst. Results of polymerization are given in Table 4.1.

Table 4.1: Polymerization of methyl ricinoleate using various lipases at 50°C for 7 d.

Code	Enzyme[a)]	Yield (%)	M_w ($gmol^{-1}$)	$M_wM_n^{-1}$
E1-50	Lipozyme TL IM	91	48 900	1.5
E2-50	Novozym 40086	94	37 300	1.5
E3-50	Lipase A *Candida antarctica*	94	1 700	1.0
E4-50	Lipase PS IM	91	53 200	1.4
E5-50	Lipase PS C I	98	34 600	1.6
E6-50	Lipase PS C II	95	22 500	1.4
B-50	Blank	96	~400	1.0

[a)] enzyme concentration: 100 wt.% relative to monomer

The highest molecular weight polyricinoleate was obtained in the presence of Lipase PS IM catalyst and slightly lower M_w was catalysed by Lipozyme TL IM.

Reactions with Lipase PS CI and Lipase PS CII showed moderate molecular weight. Only Lipase A *Candida antarctica* showed low activity toward polymerization of methyl ricinoleate at 50ºC. Without addition of any enzyme (blank test) no polymerization occurred.

5.1.1.2. Screening of Enzymes Activity at 70ºC

In the second experiment, six lipases were screened at 70°C with enzyme concentration 100 wt. % relative to monomer for 7 days. Again, blank test was performed in order to compare polymerization degree at tested conditions without presence of catalyst. Results of polymerization are given in Table 4.2.

Table 4.2: Polymerization of methyl ricinoleate using various lipases at 70°C for 7d.

Code	Enzyme[a)]	Yield (%)	M_w (gmol^{-1})	$M_wM_n^{-1}$
E1-70	Lipozyme TL IM	92	63 200	1.5
E2-70	Novozym 40086	92	64 100	1.5
E3-70	Lipase A *Candida antarctica*	95	1 700	1.0
E4-70	Lipase PS IM	97	32 300	1.3
E5-70	Lipase PS C I	91	64 500	1.4
E6-70	Lipase PS C II	97	31 400	1.4
B-70	Blank	91	~ 400	1.0

a) enzyme concentration: 100 wt % relative to monomer

Polymerization reaction performed at 70°C resulted in different trends for various lipase catalysts compared to reactions carried out at 50ºC. Increase of temperature from 50ºC to 70ºC, resulted in decrease of molecular weight for reaction catalysed by enzyme Lipase PS IM from 53 200 gmol^{-1} to 32 300 gmol^{-1}. This indicated decrease of this enzyme activity at higher temperature.

Activity of Lipase A *Candida antarctica* did not change with increase of temperature, as the molecular weight stays equal to 1 700 gmol^{-1}. In case of lipase PS CI molecular weight was almost doubled from 34 600 gmol^{-1} to 64 500 gmol^{-1}.

Lipase PS CII catalysed polyricinoleate with molecular weight 31 400 $gmol^{-1}$ which is approximately 150% increase compared to the result at 50ºC.

Polymerization catalysed by Novozym 40086 resulted in polyricinoleate with molecular weight of 64 100 $gmol^{-1}$. Finally, reaction catalysed by Lipozyme TL IM showed molecular weight of 63 200 $gmol^{-1}$.

At both 50°C and 70°C blank experiments gave almost the same and very low molecular weight ~400 $gmol^{-1}$, which indicated that no polymerization has occurred. However, normally it is well known for a chemical reaction that the higher the temperature, the higher the reaction rate. In case of polyricinoleates synthesis, these results were expected and are similar to other findings in the literature. Ebata *et al.* [80] obtained molecular weight <700 $gmol^{-1}$ for blank experiment at 60°C for 7 days with extra stirring. However, when we consider that monomer unit has molecular weight of 312.5 $gmol^{-1}$, our polymerization results are not very different.

Both our and literature findings confirm that at the tested conditions no significant polymerization takes place without addition of enzymes. Additionally to the best of our knowledge only enzymatic polymerization of methyl ricinoleate gives high molecular weight and even to obtain low molecular weight polymer more harsh conditions are required.

For example, thermal polycondensation in bulk, at 180°C in vacuum for 15 h gives polyricinoleic acid of Mw = 3400 $gmol^{-1}$ [85]. Polycondensation at 180ºC for 3h gives Mw = 1600 $gmol^{-1}$ and continuation of polymerization in vacuum overnight resulted in polyricinoleic acid of 5600 $gmol^{-1}$ [74]. Slightly higher molecular weight (Mw = 8000 $gmol^{-1}$) was obtained by polycondensation of ricinoleic acid at 230ºC for 4 h 45 min in the presence of titanium tetrabutoxide catalyst [86].

Thus, we can assume that in the range of activity of our enzyme 40-80°C effect of temperature alone can be negligible. Yield of blank reaction at 50°C is slightly higher than for reaction at 70°C. This might come from some extra losses during purification process that was performed also for blank samples.

In summary, polyricinoleates with various molecular weights were synthesized by various lipase catalysts with yields higher than 90% and polydispersity index $MwMn^{-1}$ in the range 1.0-1.6.

For further investigation, Lipozyme TL IM was chosen due to high activity at both lower and higher temperature and competitive price compared to other enzymes.

5.1.2. Effect of Reaction Temperature on Molecular Weight of Polyricinoleate

In order to test the influence of temperature on polyricinoleate molecular weight, polymerization at different temperatures from the range 40°C - 90°C was carried out. Results are presented in Figure 5.1.

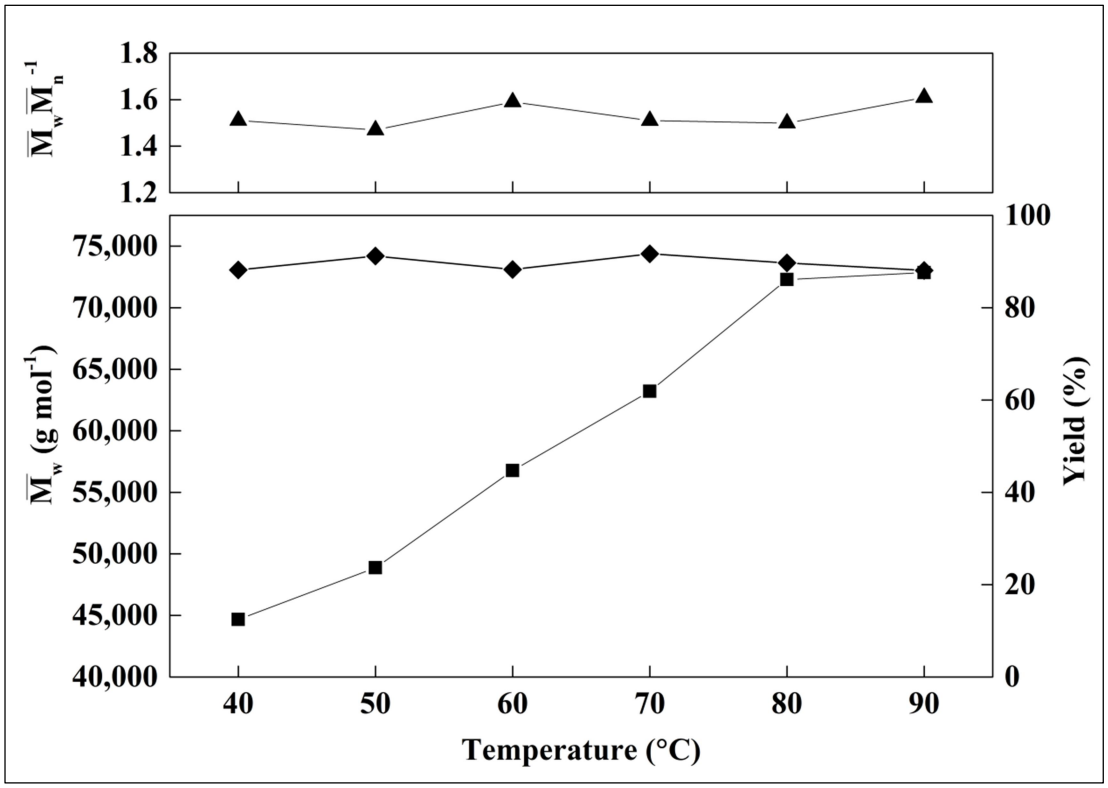


Figure 5.1: (a) Polyricinoleate M_w (■), $M_wM_n^{-1}$ (▲) and yield (♦) as a function of reaction temperature catalysed by Lipozyme TL IM for 7 days. 100 wt. % of enzyme relative to monomer, for 7 days.

The molecular weight of polyricinoleate increased gradually from lowest to highest temperature. At 40°C, molecular weight reached 44 700 gmol^{-1} and increased slightly by 9% to 48 900 gmol^{-1} at 50°C.

Further increase of polymerization temperature resulted in molecular weight rise by 27% (M_w = 56 800 $gmol^{-1}$) at 60°C, 41% (M_w = 63 200 $gmol^{-1}$) at 70°C. Finally, the highest molecular weight polyricinoleate was obtained at 80°C (M_w= 72 000 $gmol^{-1}$). Increase of polymerization temperature from 80ºC to 90°C did not result in significant rise of polymer chain. Molecular weight increased only by ~1% (M_w= 72 800 $gmol^{-1}$). For this reason 80°C was chosen as the optimum temperature for polyricinoleate synthesis.

5.1.3. Effect of Enzyme Concentration on Molecular Weight of Polyricinoleate

After selection of optimum temperature for polyricinoleate synthesis, a set of experiment was performed to select most advantageous amount of enzyme necessary to synthesize the highest molecular weight polyricinoleate. Polymerization was performed at 80ºC for 7 days with 50%, 100% and 150 % weight load of enzyme relative to monomer (Figure 5.2)

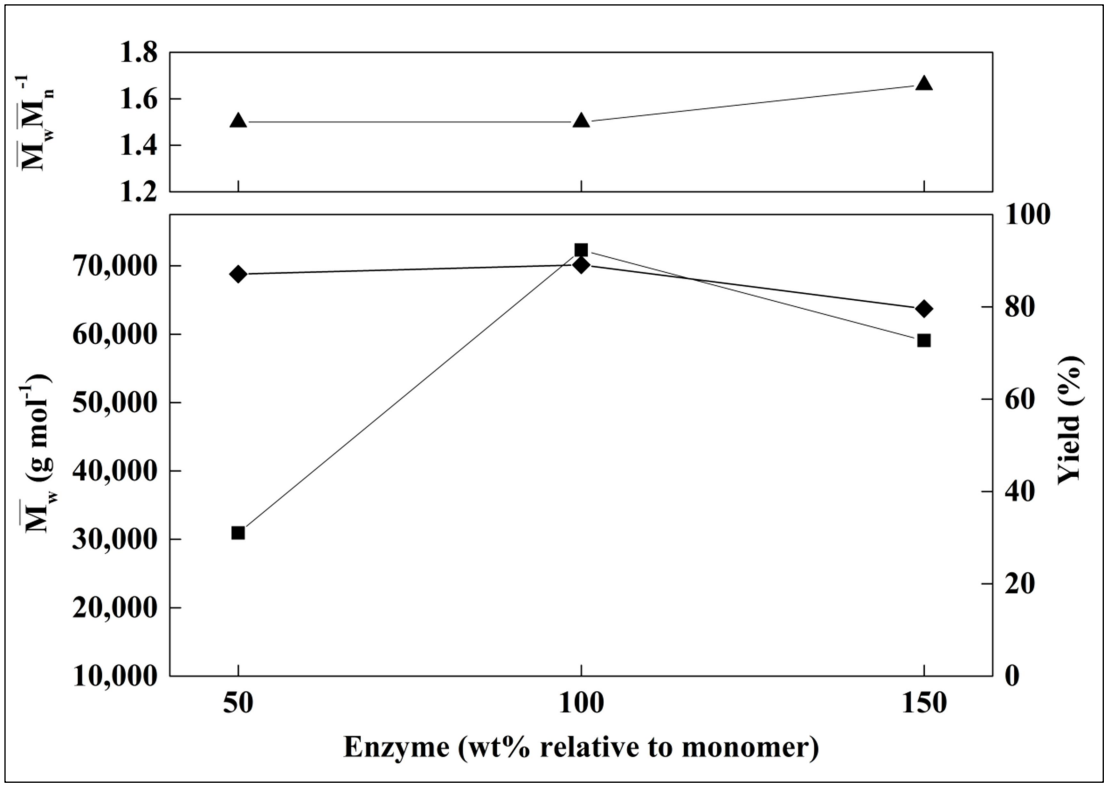


Figure 5.2: Polyricinoleate M_w (■), $M_wM_n^{-1}$ (▲) and yield (♦) as a function of enzyme load to monomer ratio polymerized by Lipozym TL IM, at 80ºC for 7 days.

Medium molecular weight (M_w = 31 000 $gmol^{-1}$) was obtained at 50 wt. % of enzyme, at 80ºC for 7 days. At 100 wt. % enzyme molecular weight reached the highest value (M_w = 72 000 $gmol^{-1}$), however at 150 wt. % of enzyme decreased to 59 000 $gmol^{-1}$. This effect could be explained by the fact that the amount of solid enzyme capable to mix with the liquid monomer is limited in bulk polymerization. Additionally, extra solid catalyst (non-wetted by monomer) could cause steric hindrance for both monomer and forming polymer chains during polymerization, resulting in lower molecular weight.

5.1.4. Effect of Reaction Time on Molecular Weight of Polyricinoleate

In the last stage of optimization, reaction time influence on the molecular weight of polyricinoleate was examined. Parallel reactions were performed at 80ºC with 100 wt. % of Lipozyme TL IM for 1, 3, 5, 7 and 9 days. Results are presented in Figure 5.3.

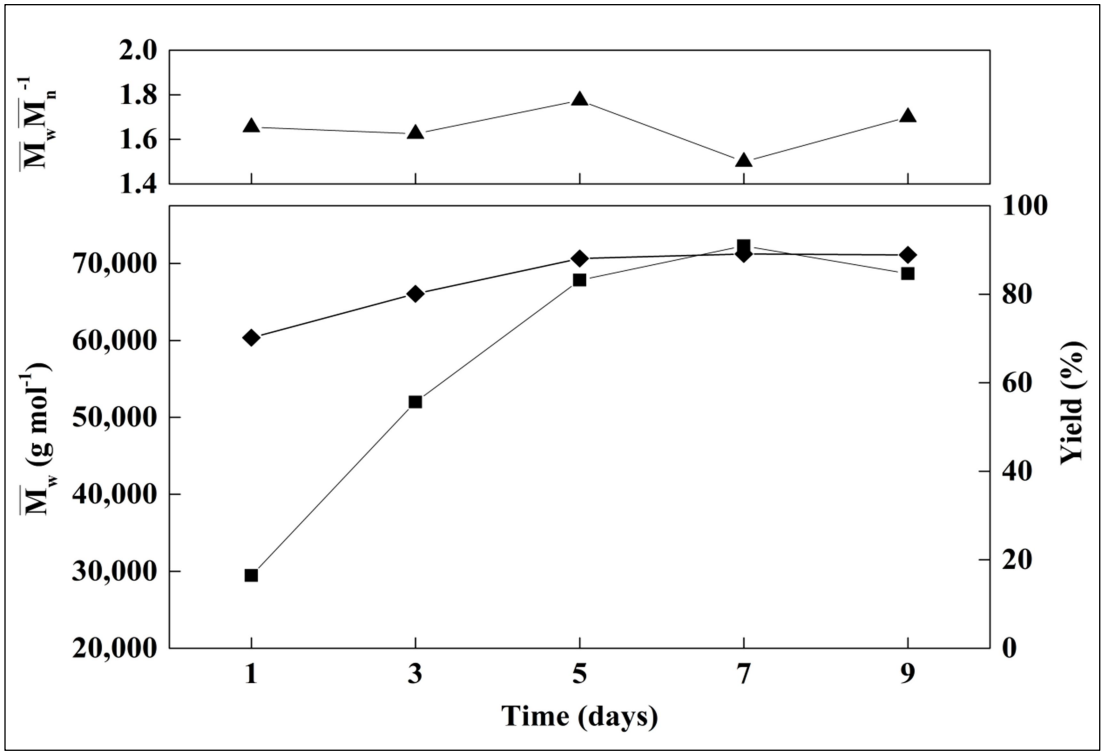


Figure 5.3: Polyricinoleate M_w (■), $MwMn^{-1}$(▲) and yield (♦) as a function of reaction time at 100 wt. % Lipozyme TL IM load at 80°C.

After only one day of reaction, medium-molecular-weight (M_w = 30 000 $gmol^{-1}$) of polyricinoleate was already reached. Maximum molecular weight was reached after 7 days of polymerization (72 000 $gmol^{-1}$). Prolonged polymerization to 9 days did not resulted in increase of molecular weight.

5.1.5. Reusability of Lipozyme TL IM Enzyme

Lipozyme TL IM is a lipase from *Thermomyces lanuginosus* immobilized on silica gel. Previously some authors reported that this enzyme can be reused several times in order to reduce cost of catalysed reaction [87].

Activity of Lipozyme TL IM after repeated use for polyricinoleate synthesis has been tested. Results of polyricinoleate synthesis after multiple uses (7 cycles) of Lipozyme TL IM enzyme are presented in Figure 5.4.

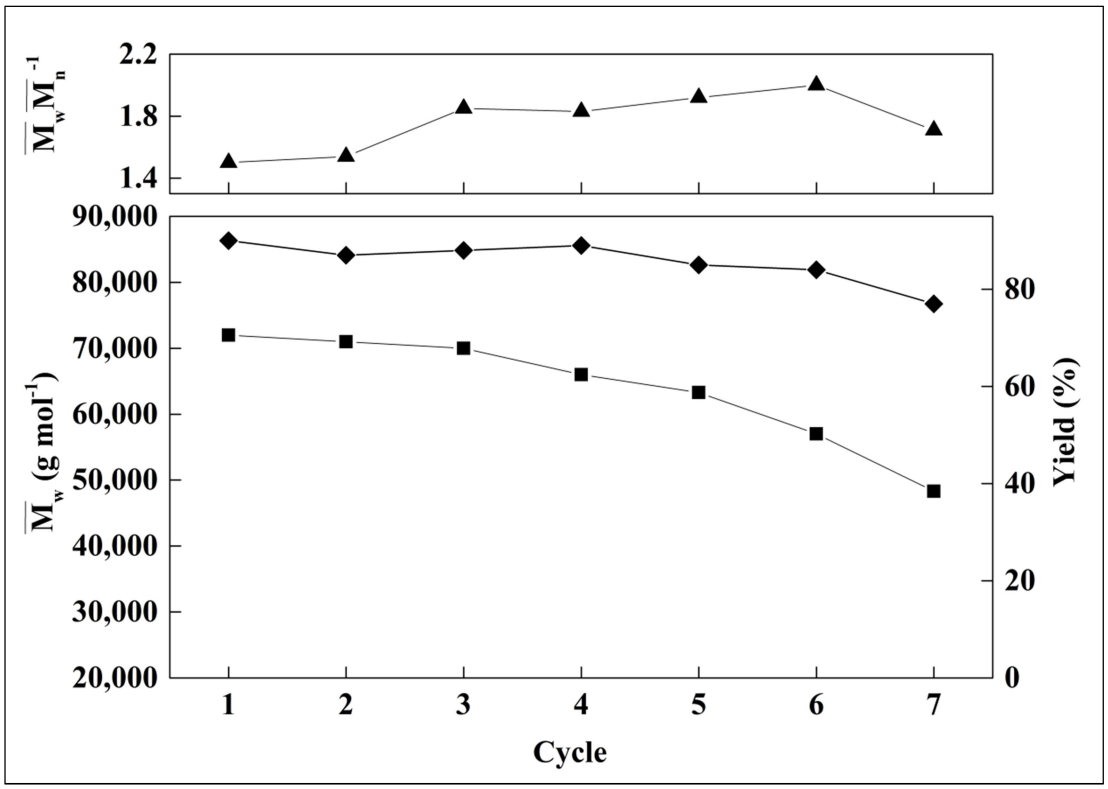


Figure 5.4: Polyricinoleate M_w (■), $M_wM_n^{-1}$(▲) and yield (♦) as a function of reusability cycle. Each cycle was performed for at 100 wt. % Lipozyme TL IM load at 80°C for 7 days.

Molecular weight of polyricinoleate almost did not change significantly in the first three polymerization cycles (72 000 $gmol^{-1}$ in first cycle, 71 000 $gmol^{-1}$ in second cycle and 70 000 $gmol^{-1}$ in third cycle). Polydispersity remained at 1.5 $M_wM_n^{-1}$ for the first two cycles but increased to 1.8 in third cycle. In the next cycles, molecular weight decreased continuously from 66 000 $gmol^{-1}$ in fourth cycle to 48 300 $gmol^{-1}$ in seventh cycle. This decrease of molecular weight could be caused by reduction of enzyme activity or gradual deposition of monomer or polymer over the pores of enzymes, which could block the access of substrates to active sites of lipase [87].

Lipozyme TL IM could be used repeatedly for polymerization of methyl ricinoleate at least 2-3 times without any significant decrease in molecular weight. However even in at least 7 cycles it is possible to obtain relatively high or moderate molecular weight polyricinoleate.

5.2. Characterization of Polymers PRA-M, PRA-H and PER

For comparative study on properties of polyricinoleates, medium-molecular-weight polyricinoleate (PRA-M), high-molecular-weight polyricinoleate (PRA-H) and polyepoxyricinoleate (PER) were selected.

- PRA-M of Mw = 30 000 $gmol^{-1}$ was synthesized by Lipozyme TL IM (100 wt. %) at 80ºC for 1 day.
- PRA-H of Mw = 72 000 $gmol^{-1}$ was synthesized by Lipozyme TL IM (100 wt. %) at 80ºC for 7 days.
- PER of Mw = 74 000 $gmol^{-1}$ was synthesized from PRA-H.

5.2.1. GPC Analysis of PRA-M, PRA-H and PER

Molecular weight of PRA-M and PRA-H was determined by GPC. Figure 5.5 shows typical chromatogram of two different molecular weight polymers with PRA-H eluting faster than PRA-M.

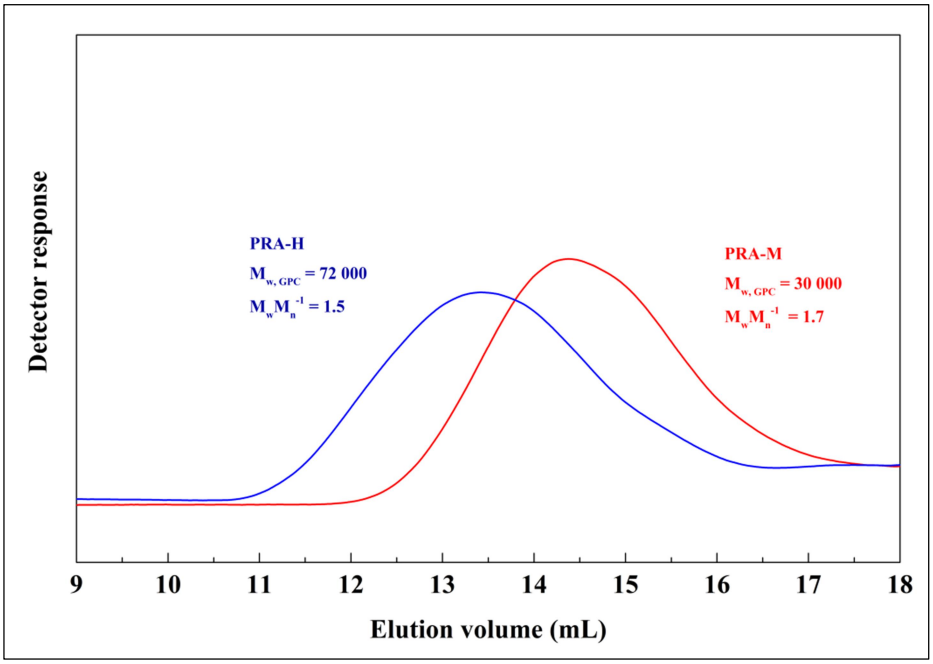


Figure 5.5: GPC traces of PRA-M and PRA-H.

Figure 5.6. represents GPC chromatograms of PRA-H and PER polymers. Due to epoxidation of double bond, PER polymer elutes slightly faster than PRA-H.

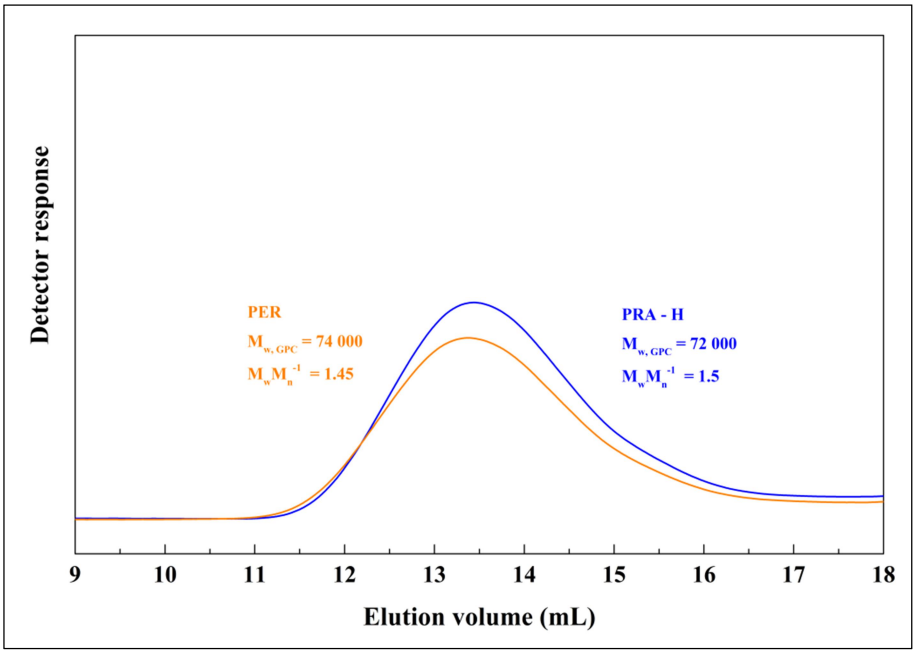


Figure 5.6: GPC traces of PRA-H and PER.

5.2.2. NMR Spectroscopy of PRA-M, PRA-H and PER

^{1}H and ^{13}C NMR spectra were taken in order to confirm the polyester structure of PRA-M and PRA-H. Full spectra are shown in Figure 5.7 and Figure 5.8.

^{1}H NMR spectrum shows typical spectrum of fatty acid based compound. Signal at 0.87 ppm belongs to $–CH_3$ at the end of the dangling aliphatic side chain. A group of signals at around 1.29 ppm represents protons at $–CH_2$- groups on C4-7 and C14-17 which are both at polymer main chain and dangling chain. Other $–CH_2$- groups, on C2, C11, C8, C and C13 are shifted to the lower filed due to their proximity of deshielding groups on polymer chain. Two multiplets at 5.44-5.32 ppm correspond to unsaturation at –C=C- bond. In both spectra we can observe almost complete disappearance of $–OCH_3$ peak at 3.65 ppm which confirms high degree of polymerization.

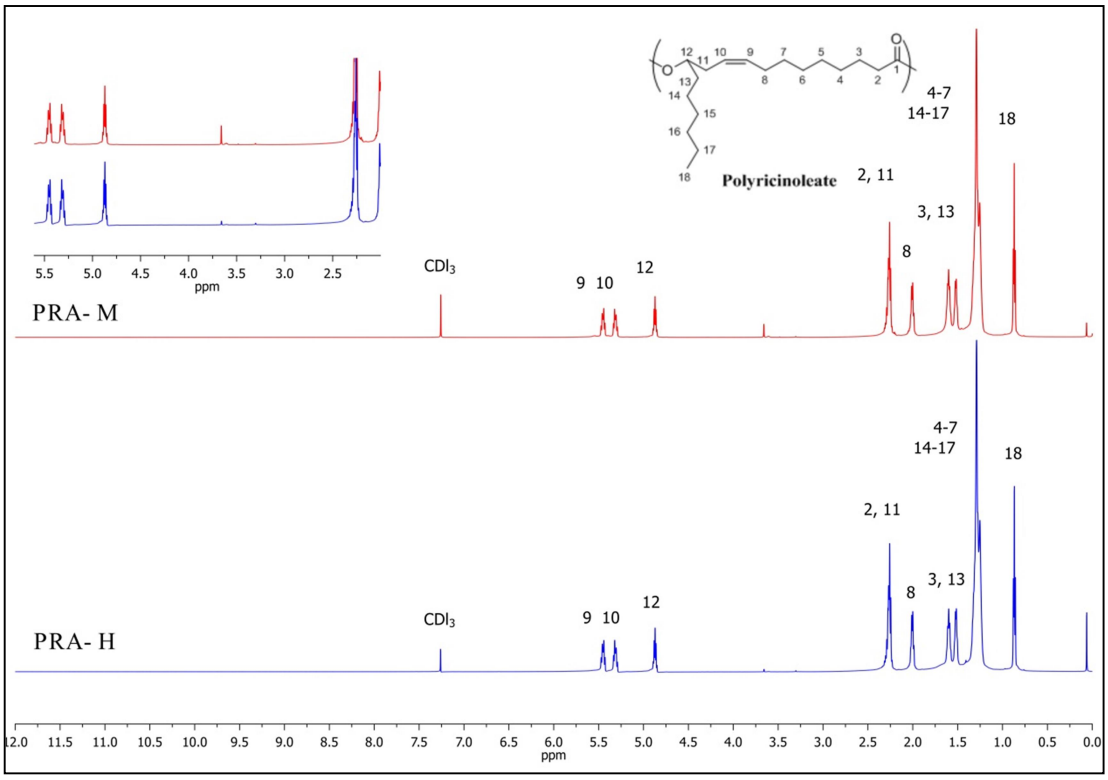


Figure 5.7: ^{1}H NMR spectra of PRA-M and PRA-H.

^{13}C NMR spectrum also confirms the structure of the polyricinoleate. Signal of C1 that belongs to carbon of carboxylate group appears at 173.65 ppm. Signals at

124.44 ppm and 132.64 ppm are assigned to C10 and C9 carbons at double bond in polyester main chain. C12 near the ester bond appears at 73.81 ppm. A group of peaks in the range from 22.71 to 34.80 ppm are signals of $–CH_2-$ carbons in the aliphatic main chain (C2-8, C11) and side dangling chain (C13-17). At 14.20, the peak of $–CH_3$ (C18) at the end of side dangling chain can be observed. Again, peak that corresponding to carbon of $–OCH_3$ in the monomer at 51.54 ppm almost completely disappeared.

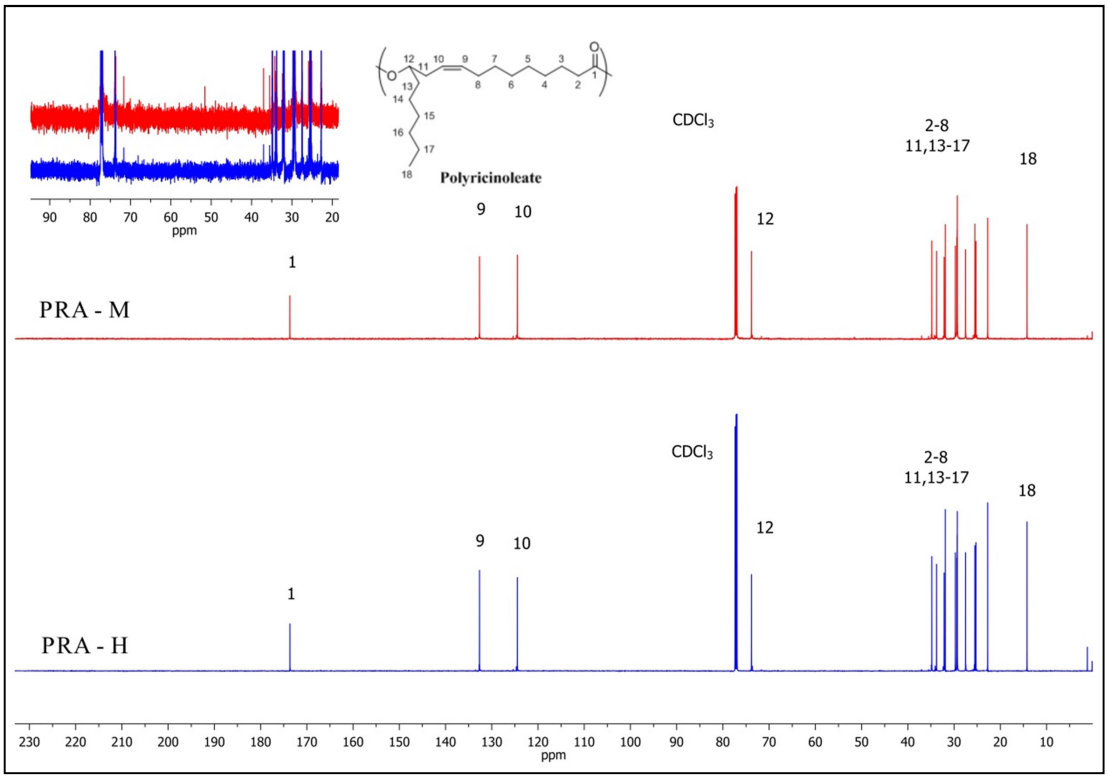


Figure 5.8: ^{13}C NMR spectra of PRA-M and PRA-H.

Also structure of polyepoxyricinoleate is confirmed by ^{1}H NMR spectrum (Figure 5.9). Signal of protons at –C=C- unsaturation disappeared and signals of protons at –C-O-C- (epoxide) appeared at 2.85 and 2.94 ppm. Similarly to polyricinoleate, signals of protons at polymer aliphatic main and side chains are visible as groups of multiplets in the 0.88-2.30 ppm region and multiplet at 5.06 ppm is assigned to proton at C12 near the ester bond.

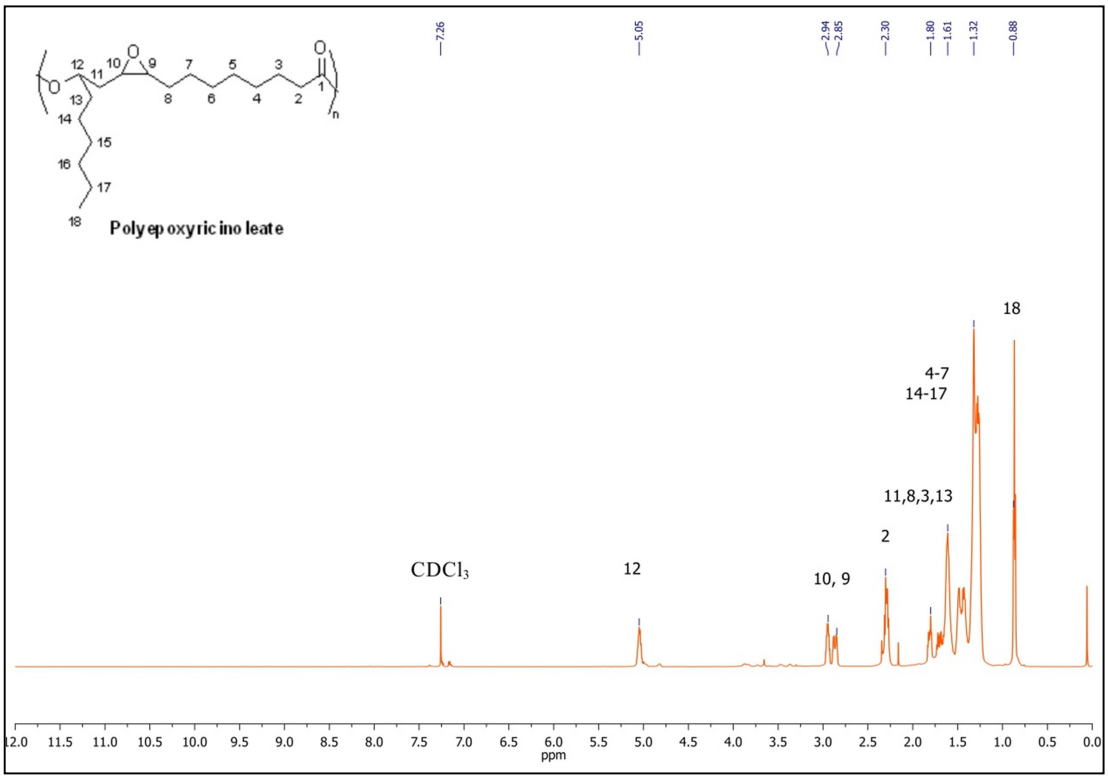


Figure 5.9: ^{1}H NMR spectrum of polyepoxyricinoleate.

Also ^{13}C NMR spectrum corresponds to polyepoxyricinoleate structure (Figure 5.10). New signals at 53.83/53.98 and 56.28/56.92 ppm belong to carbon of epoxide ring with simultaneous disappearance of carbon –C=C- signals at 124.44 ppm and 132.64 ppm.

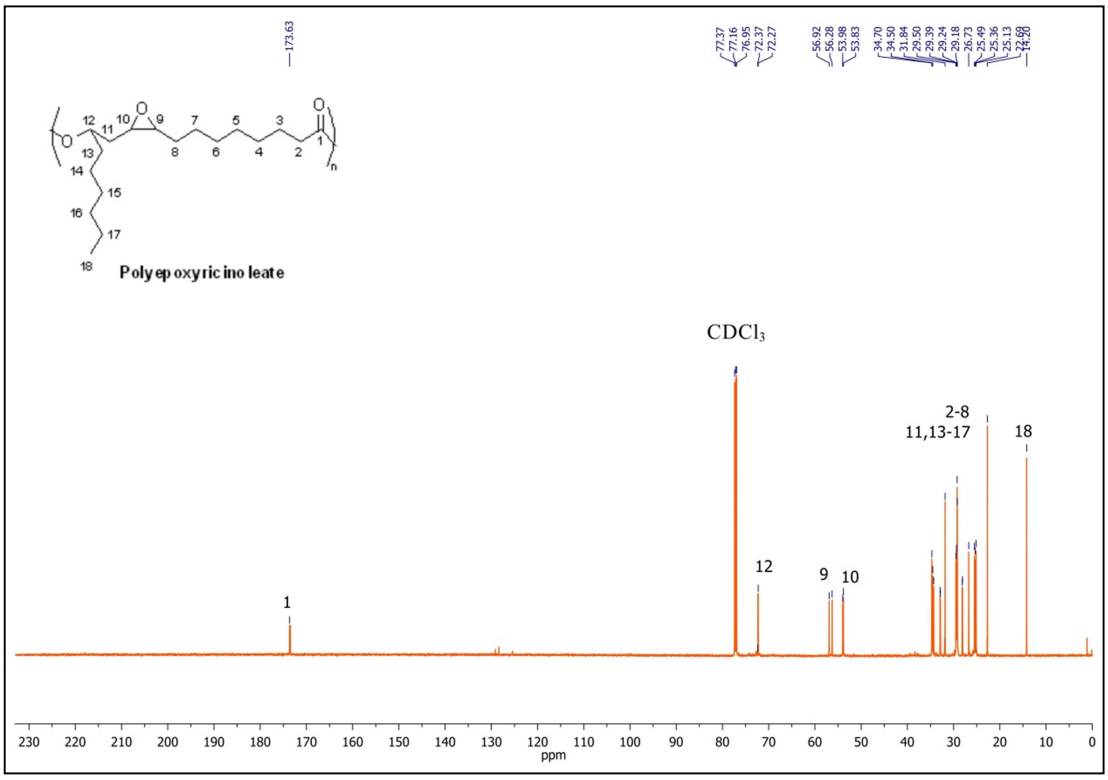


Figure 5.10: ^{13}C NMR spectrum of polyepoxyricinoleate.

5.2.3. FT-IR Spectroscopy of PRA-M, PRA-H and PER

FT-IR spectra of PRA-M and PRA-H are given in Figure 5.11. Weak band at 3450 cm^{-1} is assigned to overtone of the C=O ester stretch vibration. Stretching of =C-H (*cis*) gives medium band at 3012 cm^{-1}. Strong band at 2982 cm^{-1} belongs to –C-H (CH_2) asymmetric stretching and band at 2855 cm^{-1} belongs to –C-H (CH_2) symmetric stretching. Another strong band at 1730 cm^{-1} originates from –C=O (ester) stretching vibration. Band at 1464 cm^{-1} relates to bending (scissoring) vibration of –C-H (CH_2, CH_3). Weak band at 1417 cm^{-1} belongs to bending (rocking) vibration of =C-H (*cis*). Medium band of –C-H (CH_3) symmetric bending appears at 1377 cm^{-1}. Weak band at 1244 cm^{-1} and medium band at 1177 cm^{-1} belong to –C-O, -CH_2- stretching and bending. Weak band of –C-O stretching is visible at 1089 cm^{-1}.

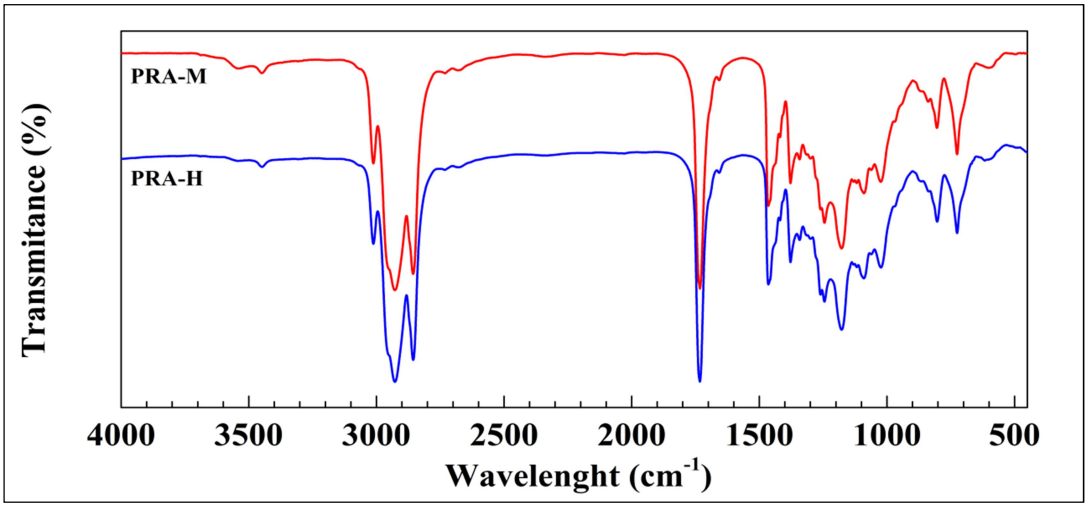


Figure 5.11: FT-IR spectra of PRA-M and PRA-H.

Polyepoxyricinoleate structure was also verified by FT-IR spectrum (Figure. 5.12). Band corresponding to stretching of =C-H (*cis*) at 3012 cm^{-1} disappeared confirming conversion of double bond into epoxide. Band of C-O asymmetric stretch of epoxide appeared at 830 cm^{-1}.

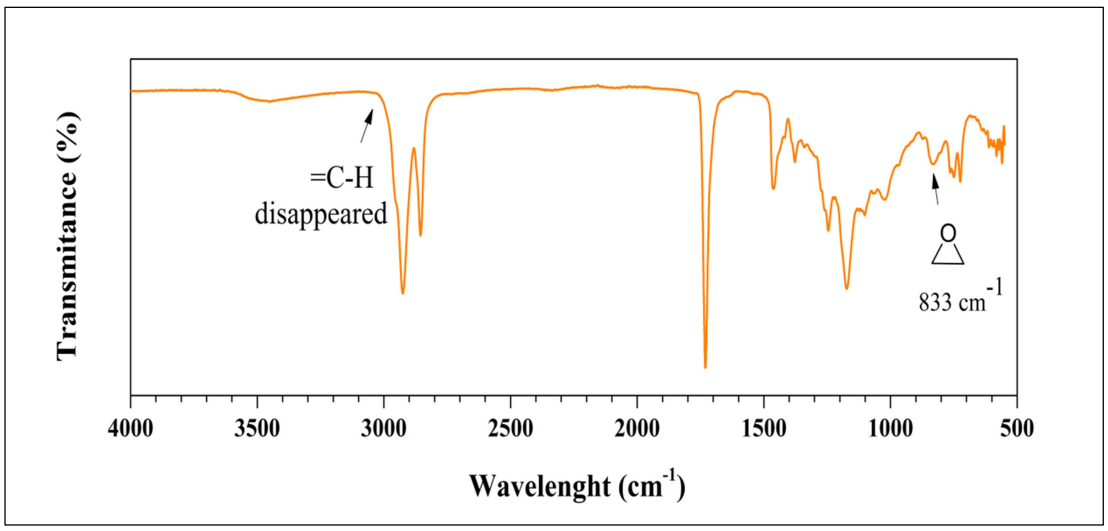


Figure 5.12: FT-IR spectrum of polyepoxyricinoleate.

5.2.4. DSC Analysis of PRA-M, PRA-H and PER

DSC scans of PRA-M and PRA-H were performed in order to determine thermal properties of polyricinoleates. Results are presented in Figure 5.13.

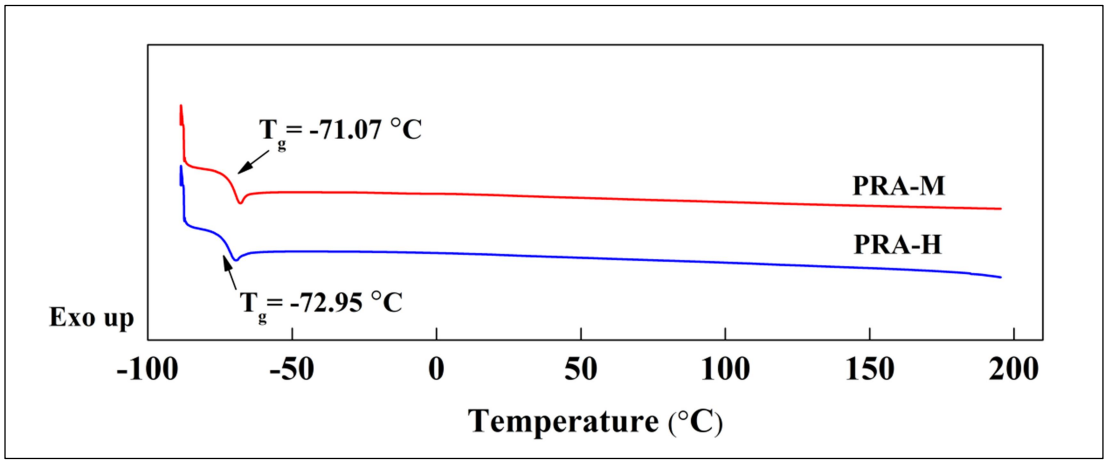


Figure 5.13: DSC scans of PRA-M and PRA-H polyricinoleates (2nd run).

Glass transition temperatures (T_g) of PRA-M and PRA-H are observed at -71.07ºC and -72.95ºC, respectively. Typically, polymers with higher molecular weight have higher T_g and reverse situation may originate from unusual polymer structure. Polyricinoleate main chain is aliphatic polyester with one dangling, aliphatic chain $–(CH_2)_5CH_3$ per each monomer unit. Dangling chains can create extra volume around and separates polymer chains from each other. Additionally, presence of *cis* double bonds causes twists on polymer backbone and prevents chain packing. In both cases, melting and crystallization peaks were not observed due to amorphous structure of polyricinoleates. Literature data confirm amorphous structure and correlation between T_g and molecular weight of polyricinoleate. Obtained results are consisted with literature data. Polyricinoleate of M_w = 100 600 $gmol^{-1}$ had fully amorphous structure and Tg = -74.80 ºC, while polyricinoleate of M_w = 8 000 $gmol^{-1}$ exhibited Tg at -49.4 ºC [80,86].

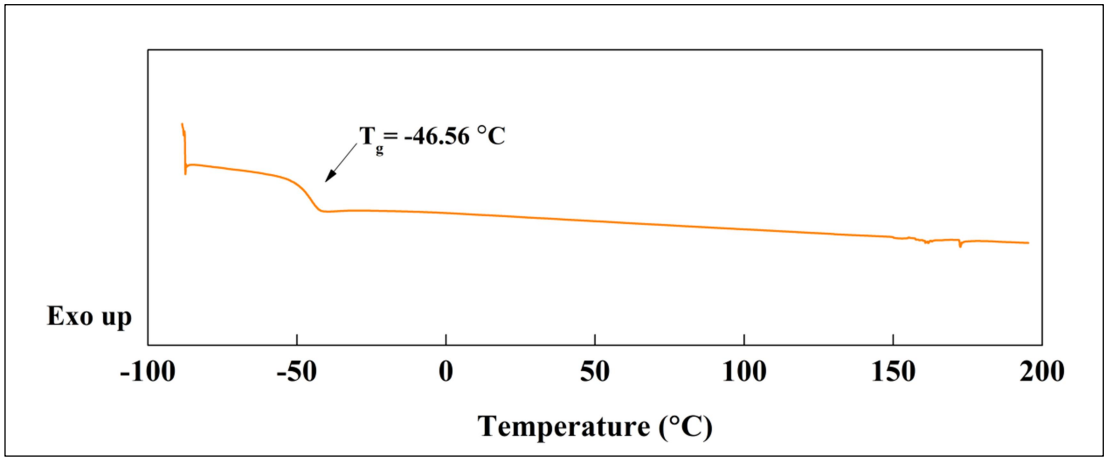


Figure 5.14: DSC scan of PER (2nd) run.

Similarly to polyricinoleate, polyepoxyricinoleate has fully amorphous structure and glass transition temperature (Tg) appears at -46.56ºC (Figure 5.14). Matsumura et al. [82] reported polyepoxyricinoleate of M_w = 186 000 $gmol^{-1}$ with T_g = -49.40ºC. Again, higher glass transition temperature of lower molecular weight polyepoxyricinoleate could be attributed to its structure – relatively long aliphatic side chain creating volume around polymer backbone and preventing chain packing.

5.2.5. TGA Analysis of PRA-M, PRA-H and PER

Thermogravimetric analysis was performed in order to determine thermal stability of polyricinoleates (Figure 5.15).

Polymers were thermally stable from 25ºC to about 300ºC, since almost no weight loss was observed. Thermal decomposition starts after exceeding 300ºC and has two stages. First decomposition stage occurs from approximately 300 ºC to 400 ºC. This significant weight loss may be attributed to scission of polyester main chain. Second degradation stage from 400 ºC to 500 ºC could be secondary chain scission of molecular chain as well as different chain scission pattern [88,89].

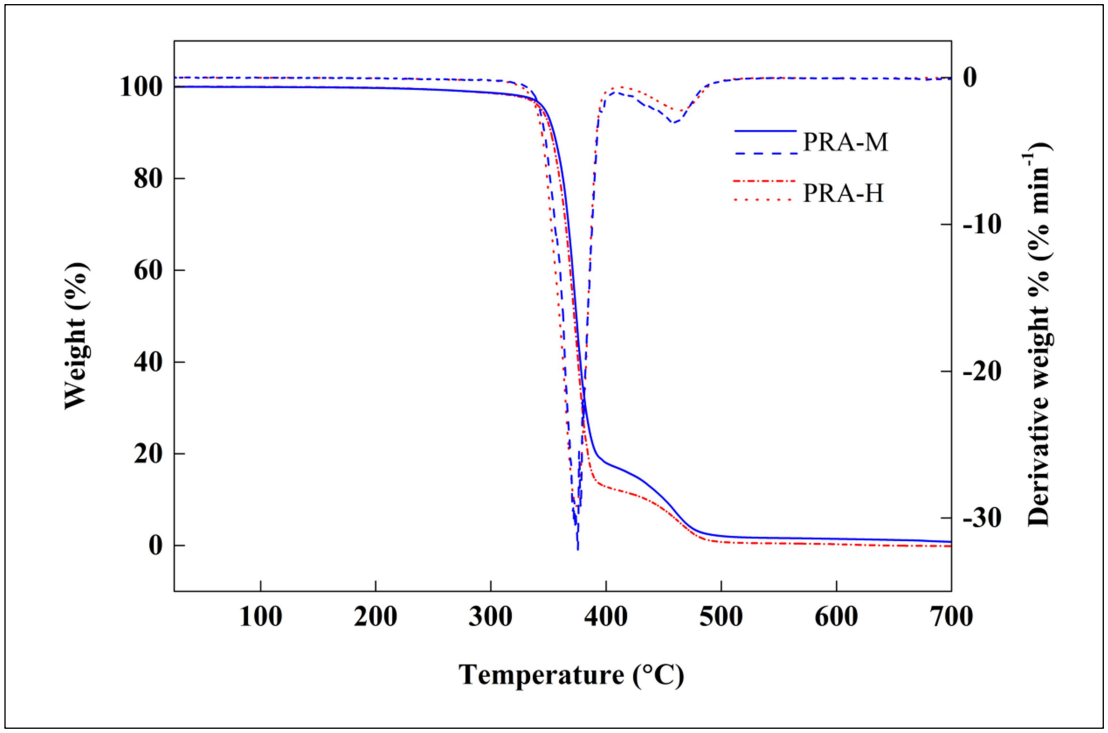


Figure 5.15: TGA scans of PRA-M and PRA-H polyricinoleates.

Thermal decomposition of PER is presented in Figure 5.16. Decomposition of polyepoxyricinoleate also has two stages. First small mass loss around 220ºC may come from any moisture loss or entrapped solvent remaining in the sample. Main chain scission with 88% of mass loss is observed in first decomposition stage from 300ºC to 400ºC and after second stage from 400ºC to 480ºC there was only 0.5% of mass residue.

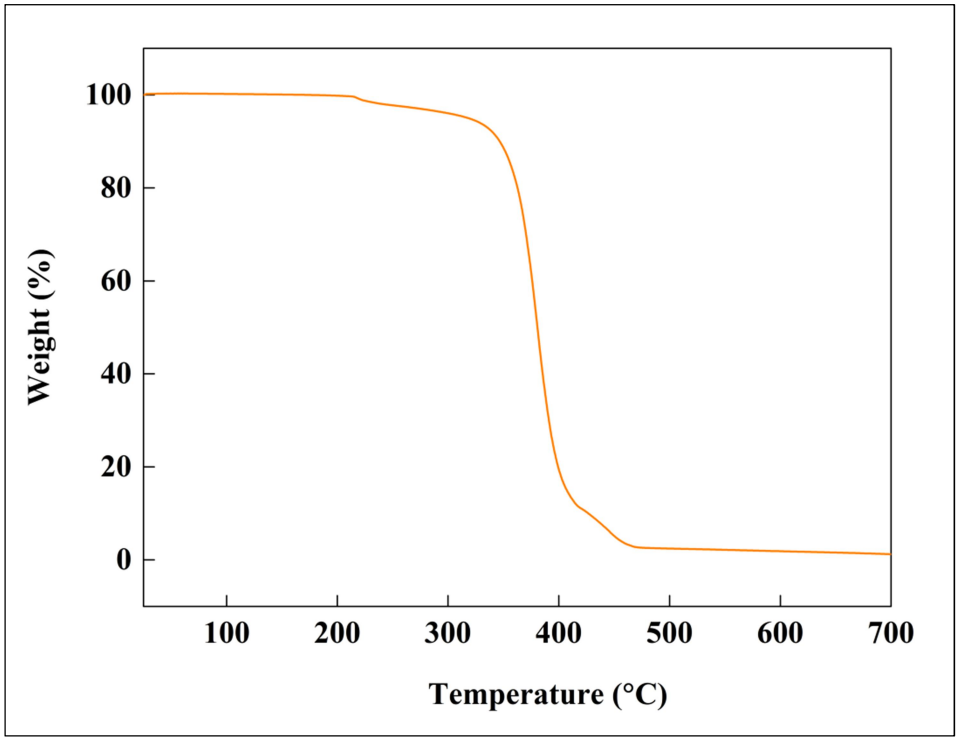


Figure 5.16: TGA scan of polyepoxyricinoleate (PER).

5.2.6. Rheology Measurements of RA, PRA-M, PRA-H and PER

Rheological properties of RA (pure ricinoleic acid), PRA-M, PRA-H and PER were performed at 37ºC to simulate physiological conditions.

5.2.6.1. Frequency Sweep – Measurement of Complex Viscosity

Frequency dependent complex viscosity values are given in Figure 5.17. RA and PRA-M samples show Newtonian behaviour at the experimental conditions. A Newtonian fluid is one that shows a linear relationship between shear stress and shear rate. In other words, the viscosity does not change with increasing shear rate. When we compare PRA-M and PRA-H samples, complex viscosity increased by 100 times with increasing of the molecular weight of PRA by ~2.5 fold. Polymer chains with higher molecular weight are more possible to tangle. The longer the polymer chain the higher the possibility of entanglement of polymer chains, which may be the reason for significant increase in viscosity between PRA-M and PRA-H.

For PRA-H and PER samples, complex viscosity is decreasing with increasing angular frequency which is caused by shearing of the polymer molecules. At low frequencies the slope of the curve goes to zero and a plateau region can be observed. At these low angular frequencies, the zero shear viscosity of a polymer melt can be determined directly using a frequency sweep. The zero shear viscosity is one of the most important material properties of polymers as it is directly proportional to the average molar mass (molecular weight). The zero shear viscosity values calculated by Carreau-Yasuda analysis are 981 Pa·s for PRA-H and 3358 Pa·s for PER.

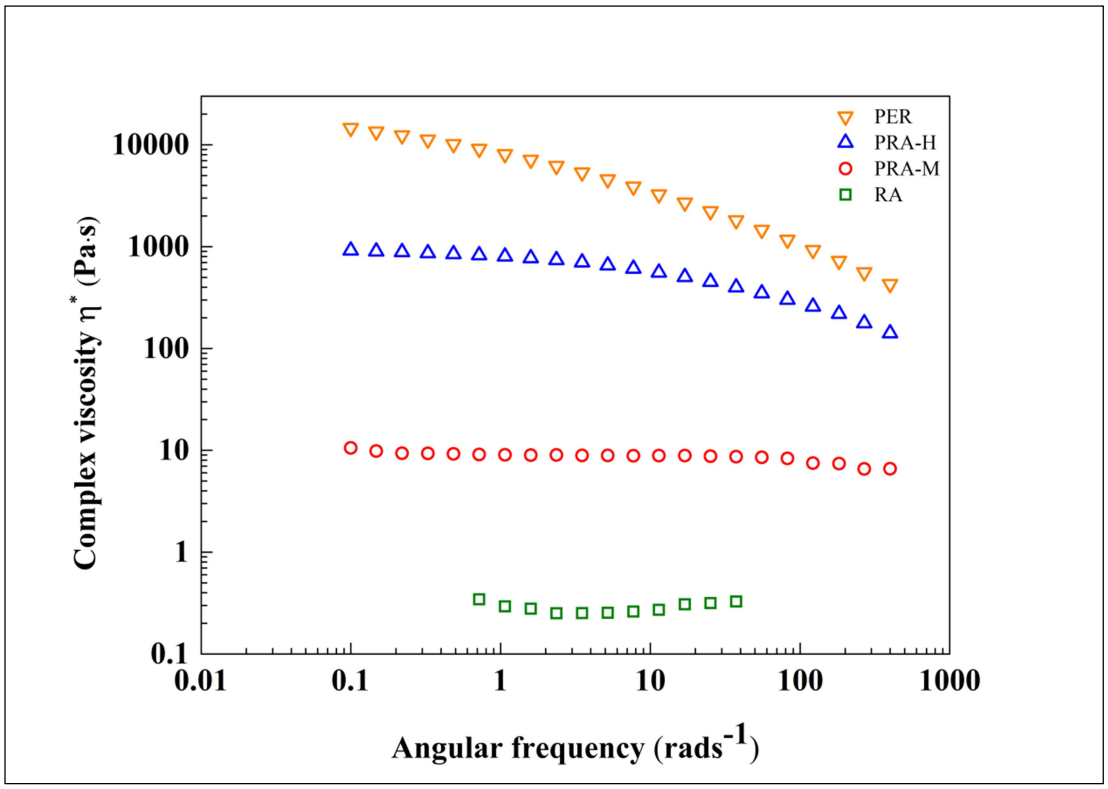


Figure 5.17: Frequency dependence of complex viscosity values.

5.2.6.2. Amplitude Sweep – Measurement of Storage and Loss Modulus

Results of the amplitude sweeps are shown in Figure 5.18. Samples showed liquid like behaviour due to G'' > G' and tanδ (which is loss factor and equal to G''G'$^{-1}$) values are above 1. For RA and PRA-M samples, loss factor values are far above 1000 (around 20000); so this samples show ideal viscous behaviour. PRA-H

and PER samples have a certain elastic portion which can be distinguished with rather higher G' values. Limits of the linear viscoelastic range are 28.3% for PRA-H and 24.2% for PER.

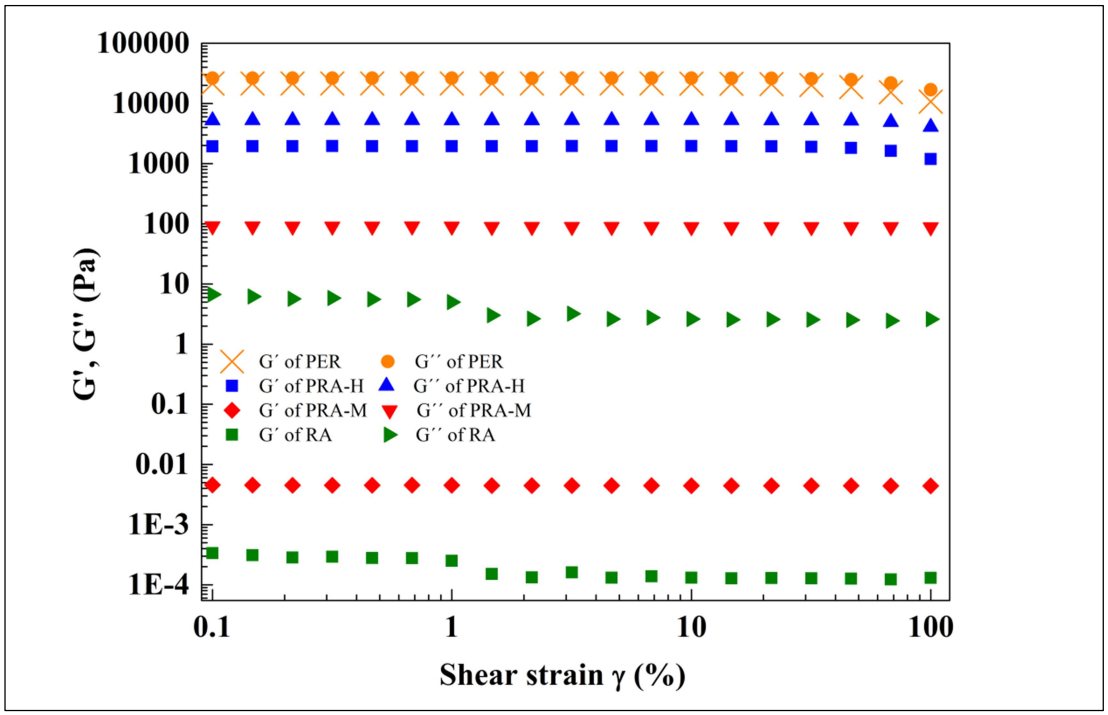


Figure 5.18: Amplitude sweep results of RA PRA-M, PRA-H and PER.

A strain value from linear viscoelastic range was selected from the amplitude sweep and frequency dependent behaviours of samples were investigated. After a certain frequency, G' values dominated G'' values and the elastic part plays a significant role during process of the sample. Cross-over points is 24.11 $rads^{-1}$ for PER and 214.12 $rads^{-1}$ for PRA-H (Figure 5.19).

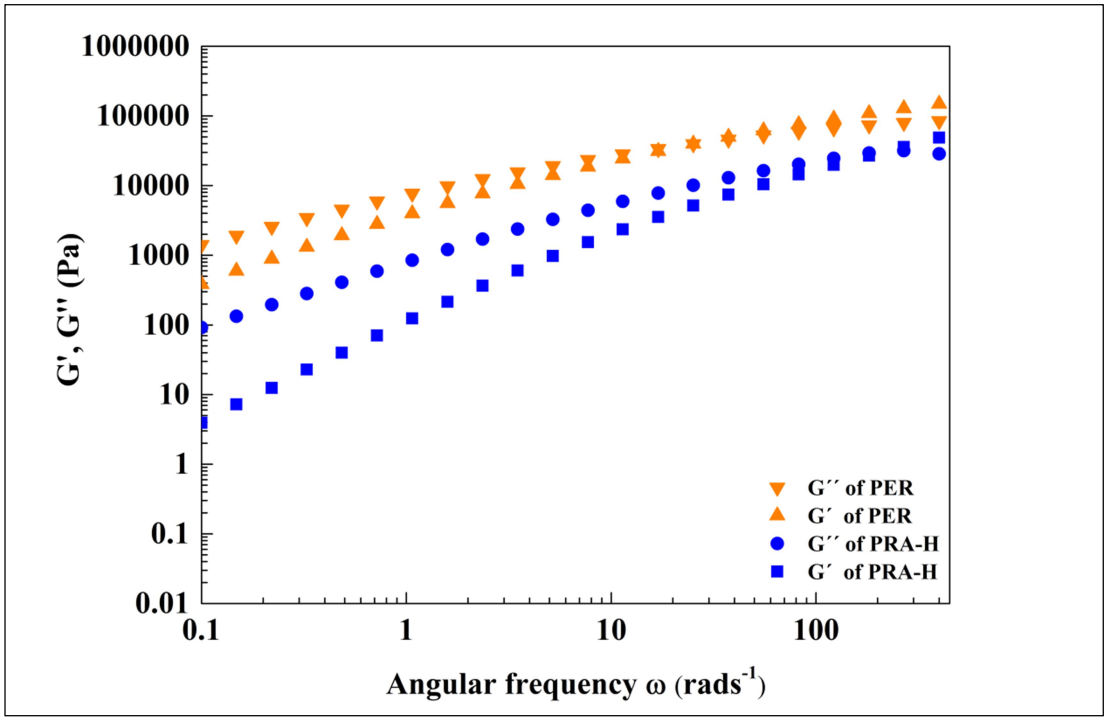


Figure 5.19: Frequency sweep of PRA-H and PER and calculated cross-over points.

5.3. Coating Properties of RA, PRA-M and PRA-H

Films of PRA-M and PRA-H polymers were prepared by solvent casting method in order to test coating properties of polyricinoleates. Films preparation is illustrated in Figure 5.20.

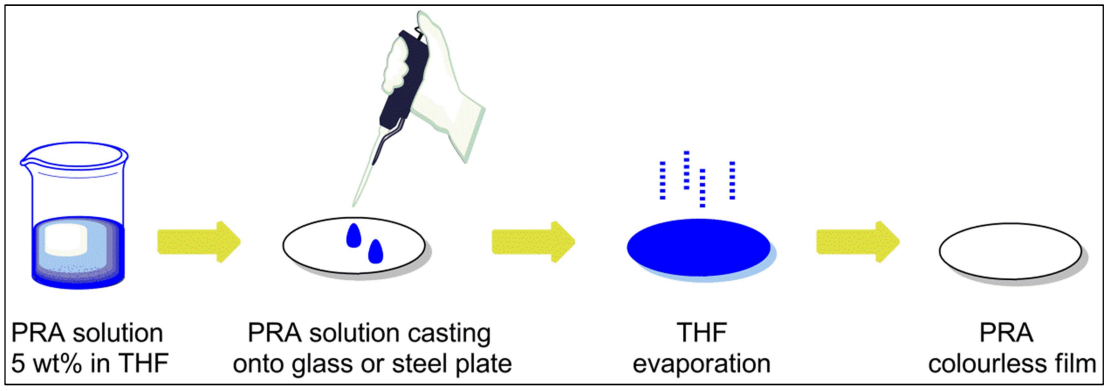


Figure 5.20: Preparation of RA, PRA-M and PRA-H films by solvent casting method.

In naked–eye observation RA, PRA-M and PRA-H formed thin, transparent and smooth coating by simple solvent casting. No surface roughness or film discontinuity was observed (Figure 5.21).

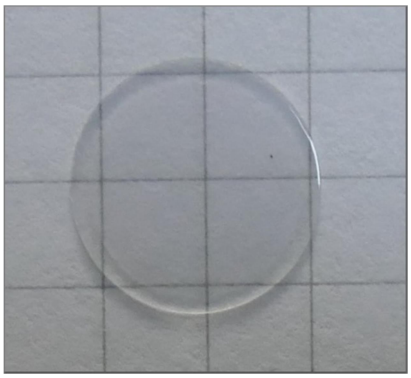


Figure 5.21: Glass plate covered with colourless PRA-H film.

5.3.1. SEM Observation of RA, PRA-M and PRA-H Films

To further investigate the surface properties of polyricinoleate films, surfaces coated with RA, PRA-M and PRA-H were investigated under SEM microscope (Figure 5.22).

Perfectly smooth and continuous surface of PRA-M and PRA-H was confirmed. SEM images of RA revealed that this film has irregular, scar like structures but again no film discontinuity was detected.

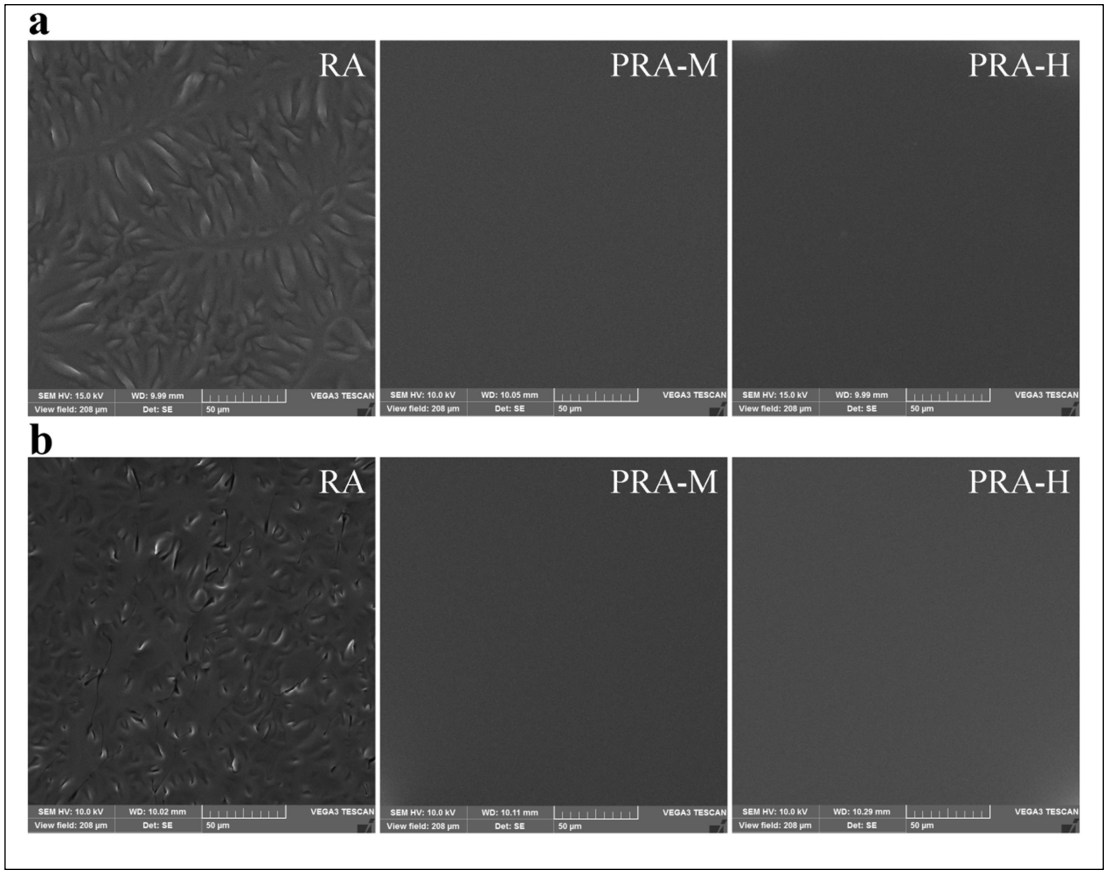


Figure 5.22: SEM micrographs of RA, PRA-M and PRA-H films on (a) glass cover slips and on (b) stainless steel plates.

5.3.2. AFM Observation of RA, PRA-M and PRA-H Films

Among the varying characterization methods for the measurement of surface roughness, AFM is the most ideal tool due to its excellent resolution and measurement in nanometre scale. Very few materials have atomically smooth surfaces. Usually, depending on material type, characteristic surface “landscape” with steeper gradients, cracks and pores can be observed [90,91].

AFM images of stainless steel plates covered with RA, PRA-M and PRA-H support SEM images and indicated a rougher surface for RA coated stainless steel plate with an average roughness of 157.36 nm (Figure 5.23). On the other hand, both PRA-M and PRA-H coated stainless steel showed a smoother surface with average roughness values of 68.39 and 57.36 nm, respectively.

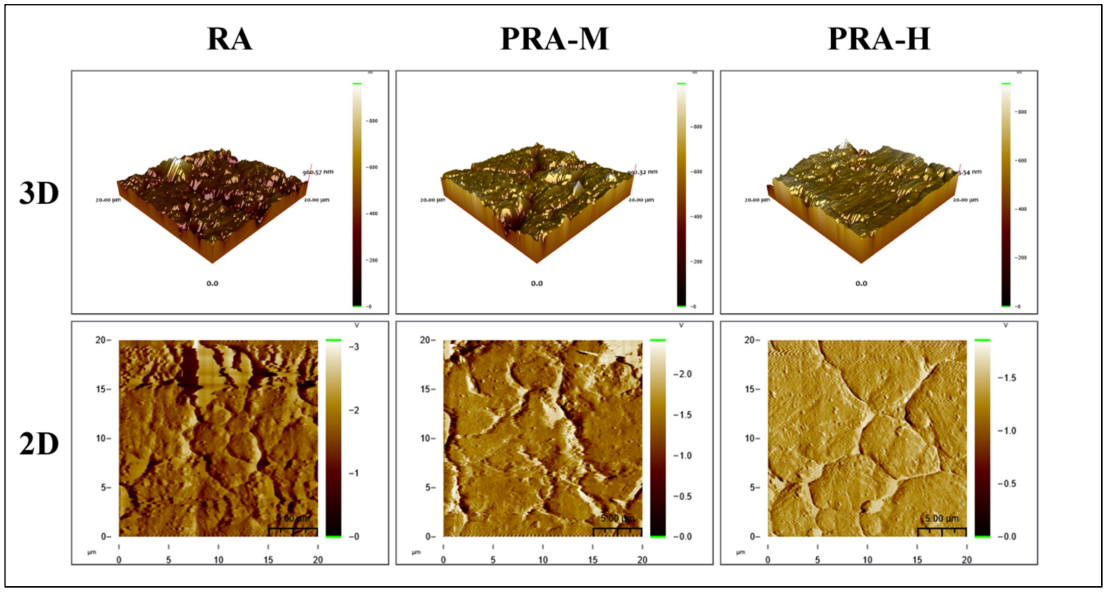


Figure 5.23: AFM images of RA, PRA-M and PRA-H coated stainless steel surfaces.

5.4. Antibacterial Properties of RA, PRA-M and PRA-H

The antibacterial activity of the RA, PRA-M and PRA-H samples were studied against *S. aureus* and *E. coli* via colony count assay. Complete inactivation of both *S. aureus* and *E. coli* has been observed for the RA coated samples (Figure 5.24a-d). Although the PRA-H samples showed some level of inhibition against *S. aureus* (Figure 5.24c), compared to the control samples, it is not statistically significant ($p<0.05$). Surprisingly, *S. aureus* counts were about 1 log higher compared to the control sample (Figure 5.24c).

For *E. coli*, no significant difference has been observed both for the PRA-M and PRA-H samples compared with the control sample (Figure 5.24d). Our studies evidenced that RA has a strong antibacterial activity against both *S. aureus* and *E. coli* while homopolymer PRA with two different molecular weights exhibited no significant inhibition of bacterial growth. Totaro et al. reported antimicrobial activity of poly(ricinoleic acid) (M_w = 8000 $gmol^{-1}$) against *S. aureus* and *E. coli*, with cell mortality rate of 100% and 45%, respectively [86]. To increase antibacterial effect of PRA they covalently bonded antimicrobial molecule (vinyl imidazolium salt) to polymer chain which increased *E. coli* mortality rate to 95%.

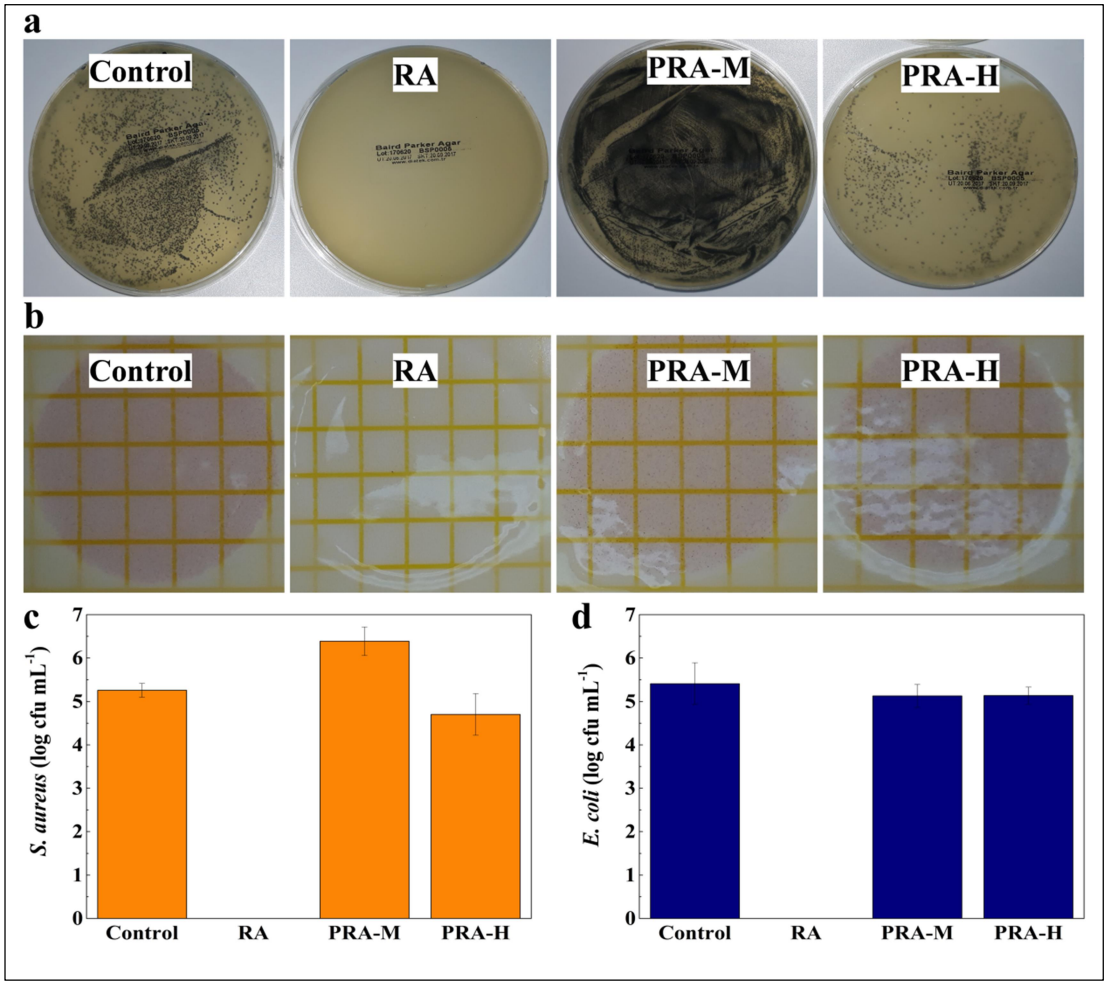


Figure 5.24: (a) Plates of S. aureus after 24 h of incubation at 37°C: Control, RA, PRA-M, PRA-H, (b) plates of E. coli after 24 h of incubation at 37°C: Control, RA, PRA-M, PRA-H, antibacterial activity against, (c) S. aureus, and (d) E. coli after 24 h of incubation at 37°C.

Antibacterial effect of RA is caused by its ability to interact with bacterial cell wall, encouraging denaturation and coagulation of proteins [92]. Long polymer chain could weaken these interactions and inhibit antibacterial affect. However, there are many factors such as surface chemistry, topography, roughness, mechanical properties and even polymer thickness that have influence on bacterial growth [93]. Surface topography of a biomaterial including surface roughness has key importance considering the interactions with biological objects such as bacteria, cells, proteins etc. [90]. For example, Braem *et al.* [94] reported that surface roughness and hydrophobicity are the main factors determining bacterial adhesion. They studied the relationship between surface topography and bacterial adhesion and concluded that porous coatings increase the risk on implant infection. In order to limit bacterial

adhesion and following biofilm formation, some surface modifications should be explored to promote more smooth surfaces [94,95]. Surfaces coated with PRA-M had higher roughness and could provide slightly more favourable conditions than PRA-H in case of *S. aureus*. On the other hand, this effect is not observed for *E. coli*.

5.5. Lap-Shear Adhesion Test

During preparation of polyricinoleates (PRAs) and polyepoxyricinoleate (PER) their ability of stick into different surfaces has been observed. Adhesion strength of PRAs and PER was measured by lap-shear test. First, lap-shear adhesion test was performed on different surfaces like glass, aluminium, paper and PET. Next, adhesive strength properties of PRAs and PER on ovine skin has been tested.

5.5.1. Lap-Shear Adhesion Test on Glass, Aluminium, Paper and PET

Lap shear adhesion test of PRA-M, PRA-H and PER show similar pattern on different materials (Figure 5.25) PRA-M exhibits the lowest adhesion on all materials. Adhesion force is 1.03 ± 0.23 kPa on glass plates, 1.75 ± 0.40 kPa on aluminium plates, and 1.24 ± 0.34 kPa and 1.95 kPa on paper and PET plates respectively.

Adhesion increased with polyricinoleate molecular weight. For PRA-H adhesion force is ~ 10 times higher compared to adhesion force of PRA-M and it is ~10 kPa on all materials. The highest adhesion force was detected for polyepoxyricinoleate (PER). On glass, aluminium and PET places adhesion force of PER was ~35 kPa. Increase of adhesion of PER on paper to ~ 44 kPa was observed, probably due to slightly more hydrophilic nature of PER which could increase interaction with paper substrate.

Adhesion strength of tested materials is comparable to some acrylic pressure sensitive adhesives which had adhesion strength of 11-190 kPa [96].

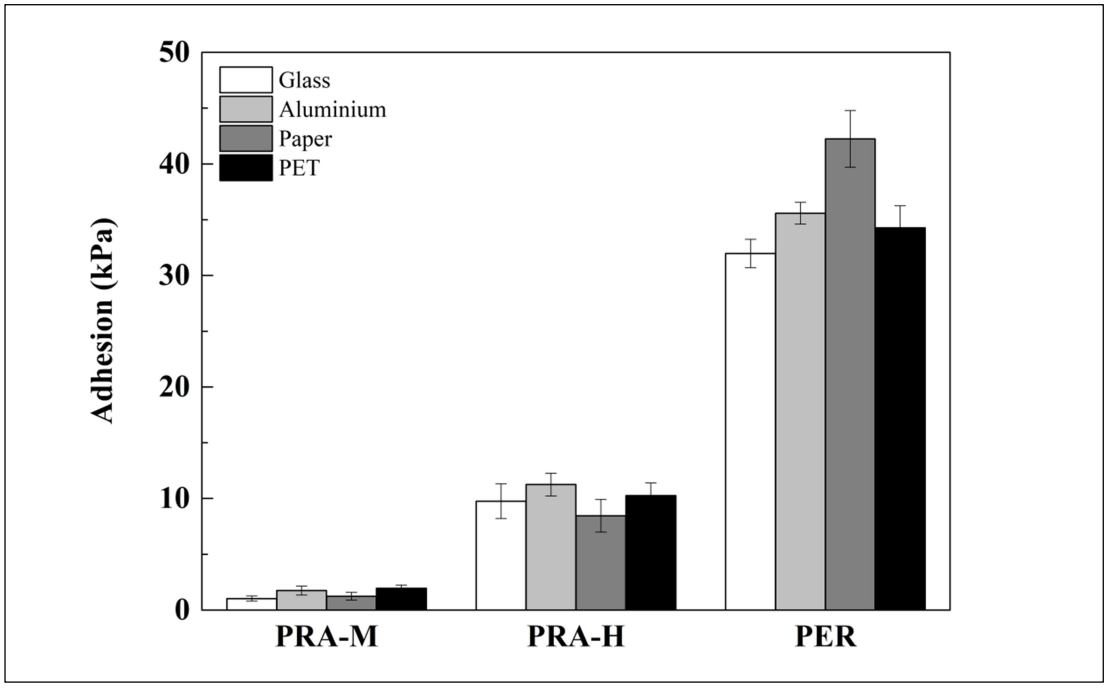


Figure 5.25: Lap shear strength of PRA-M, PRA-H and PER on different substrates.

Among all adhesion theories the theory of adsorption may most accurately describe adhesion phenomenon between organic and inorganic systems [97].

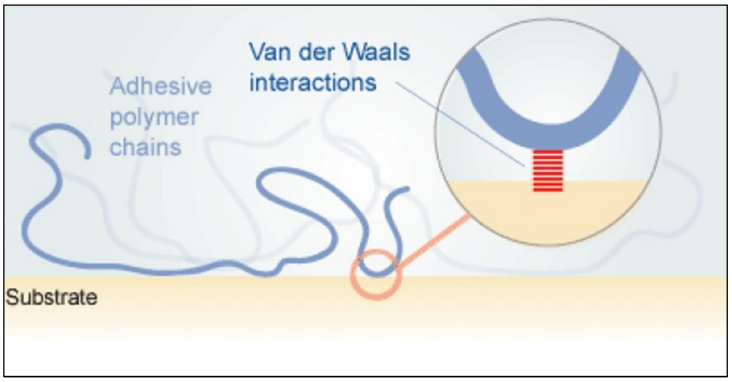


Figure 5.26: Schematic representation of Van der Waals interaction of adhesive polymer and substrate.

All tested polymers (PRA-M, PRA-H and PER) form a layer of viscous liquid on the surface of substrate and the bond could form because polymer being soft enough can wet the surface of the substrate. When polymer and substrate are close

enough, molecular interactions can contribute to adhesive strength (e.g. van deer Waals forces (see Figure 5.26) [97].

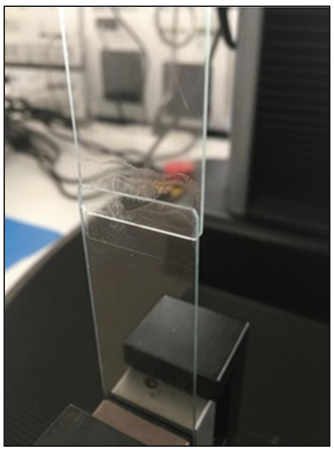


Figure 5.27: Lap-shear adhesion test of PRA-H on glass plates.

5.5.2. Lap-Shear Adhesion Test on Ovine Skin

Since PRA-H and PER had some adhesive properties on different substrates, its ability to adhere to tissue (ovine skin) has been determined (Figure 5.28 and Figure 5.29).

From lap shear adhesion test we could observe that both PRA-M and PRA-H showed low and very similar adhesion strength on ovine skin (570 ± 69 Pa and 624 ± 99 Pa for PRA-M and PRA-H respectively). In case of polyricinoleate molecular weight did not influence the adhesive strength and hydrophobic nature of the polymer seems to dominate. Adhesion strength of PER was ~ 1550 ± 74 Pa and this increase can be attributed to the presence of epoxide group on the polymer main chain.



Figure 5.28: Lap-shear adhesion test of PER on ovine skin.

In general, tissue adhesive polymers show wide range of adhesion strength. However, due to the differences in methodology and types of adherents, it is difficult to make direct comparison of obtained results and other reported studies in the literature.

For example hyaluronic acid/pluronic hydrogel showed maximum adhesion strength of 7.18 ± 0.93 kPa on mouse skin. On porcine skin, poly(ester urea) (poly(CA-Tyr-co-Leu)) showed adhesion strength of 9 kPa and PEG-$DOPA_4$ (poly(ethylene glycol)-L-3,4-dihydroxyphenylalanine) have adhesion strength of 35.1 ±12.5 kPa.

Generally some kind of cross-linking results in higher adhesion. Poly(dopamine-co-acrylate) cross-linked with horseradish peroxide showed adhesion of 76 ±13.4 kPa on porcine skin. Rfp-1 MAP (Mussel Adhesive Proteins) have adhesive strength of ~ 130 kPa after cross linking with $FeCl_3$ and ~200 kPa after cross-linking with $NaIO_3$ [98].

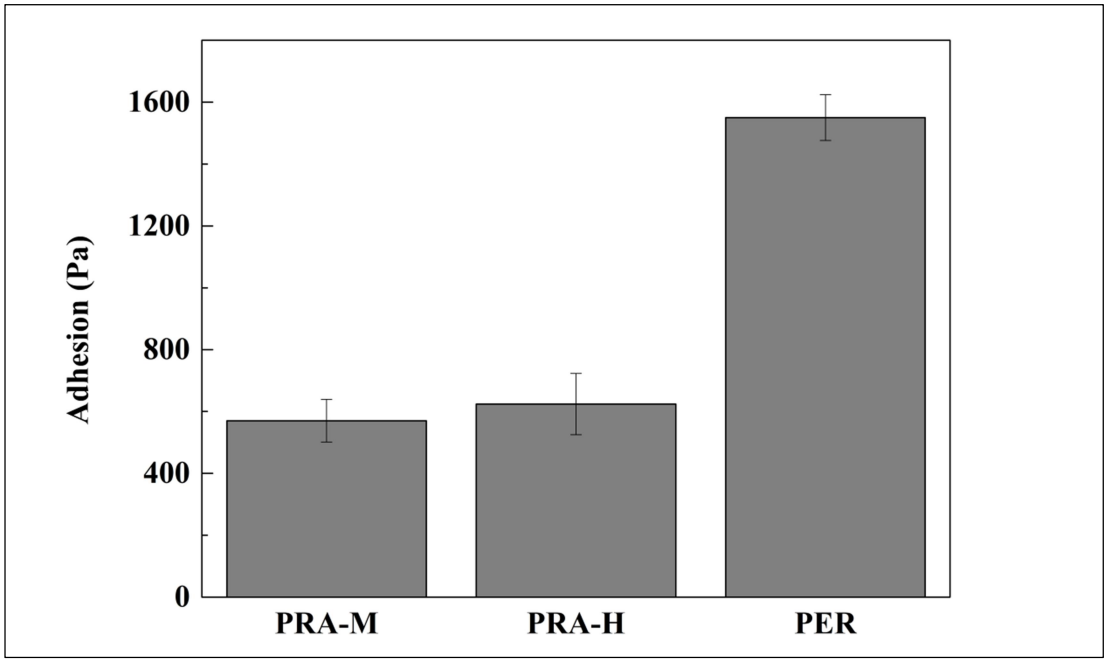


Figure 5.29: Lap shear strength of PRA-M, PRA-H and PER on ovine skin.

Also commercially available tissue adhesives reveal wide spectrum of adhesion strength. Using bovine pericardium as test substrate Dermabond® (Ethicon) had maximum lap shear strength of 181 ± 33.4 kPa and Tisseel^{TM} (Baxter) which is fibrin sealant had adhesive strength of 2.58 ± 1.76 kPa. On the other hand adhesion strength of PER is higher than adhesion strength of another commercial medical adhesive - CoSeal (Baxter) which has maximum adhesion strength in lap-shear test 0.6 ± 0.2 kPa when used for gluing two pieces of bovine pericardium [99,100].

5.6. *In Vitro* Degradation Study of PRA-M, PRA-H and PER

After 6 months of incubation, mass loss of PRA-M and PRA-H was 2.3% and 1.5% respectively (Figure 5.30). Polyricinoleates showed sustained *in vitro* degradation, most likely due to its hydrophobic nature and relatively high molecular weight. For comparison, *in vitro* hydrolytic degradation of PRA of M_w = 3 400 gmol^{-1} showed almost zero-order weight loss and after 60 days of incubation mass loss was about 40% [85]. Slow degradation could be advantageous for long-term medical applications especially for which stability is required. On the other hand

polyepoxyricinoleate showed 28.3% of weight loss after 6 months. This faster degradation of PER may be explained by the fact that the presence of polar epoxy group may ease contact of the otherwise hydrophobic polymer with buffer solution leading to faster degradation. To the best of our knowledge this is the first example of *in vitro* degradation study of medium and high molecular weight polyricinoleate and polyepoxyricinoleate.

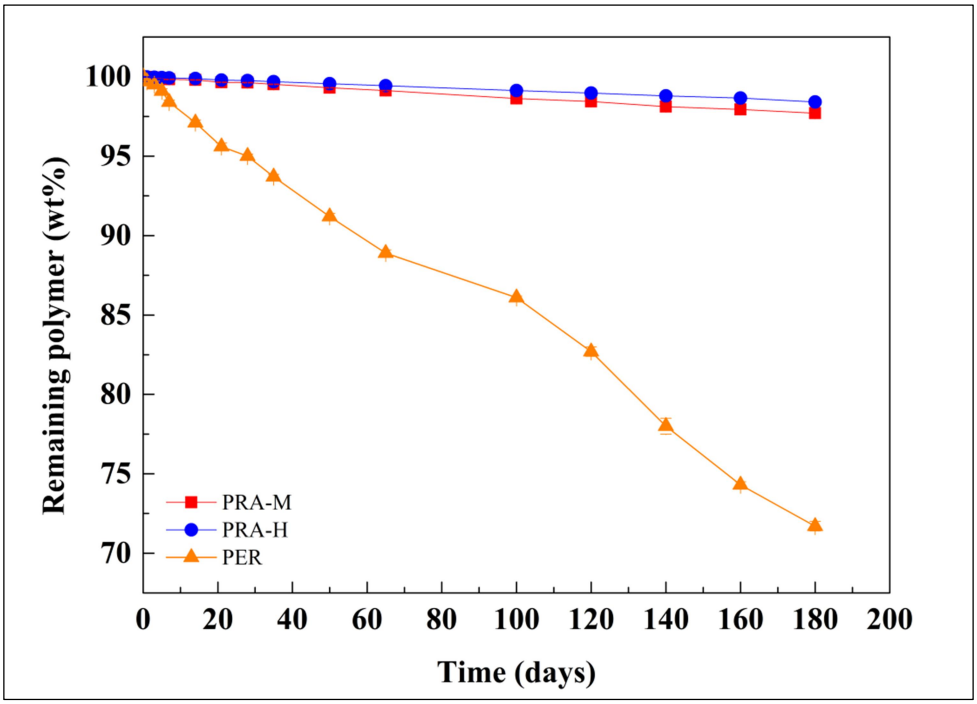


Figure 5.30: In vitro degradation of PRA-M, PRA-H and PER.

5.7. Whole Blood Clotting Time

Blood coagulation time *in vitro* for RA, PRA-M, PRA-H and PER was tested in order to get insight into its potential use *in vivo* (Figure 5.31 and Figure 5.32) when contact with blood may occur. Normal value of blood clotting time is in the range 8 – 15 minutes. Control blood samples and blood in contact with PRA-M, PRA-H and PER samples clotted after approximately 8-9 min. Blood clotting time increased to around 10 min. in the presence of RA. Despite slight differences, all samples are in the range of normal blood clotting time. This *in vitro* blood clotting time experiment shows that polyricinoleates and polyepoxyricinoleate do not affect blood clotting time and could have potential use *in vivo.*



Figure 5.31: Blood clotting experiment on glass plates covered with polymer (PRA-H sample).

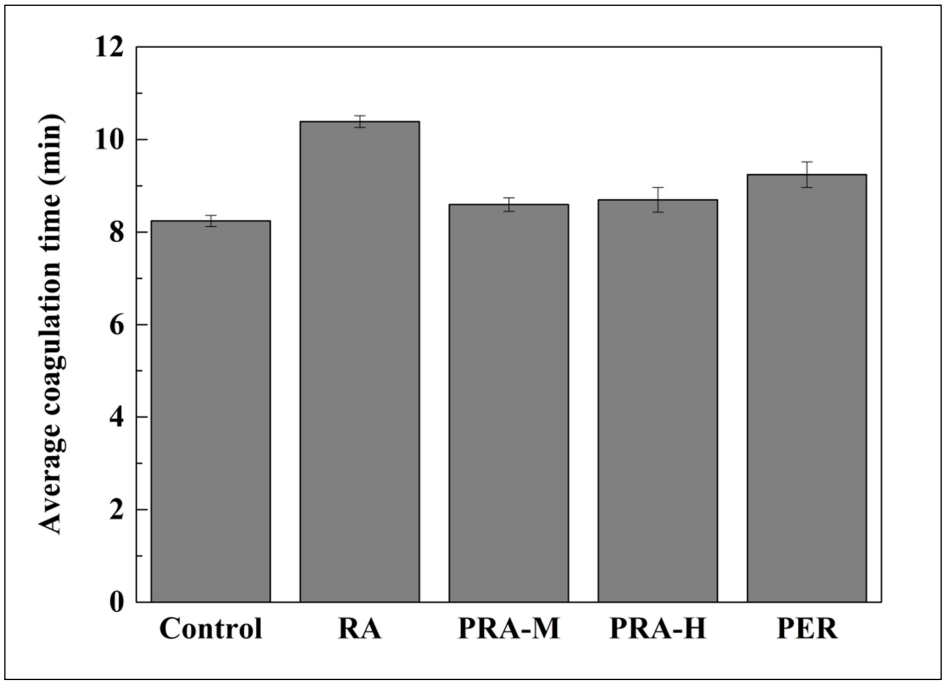


Figure 5.32: Average blood coagulation time in contract with RA, PRA-M, PRA-H and PER.

5.8. LDH Cytotoxicity Test

The LDH cytotoxicity assay was used to evaluate the cytotoxic properties of the materials. The LDH test was performed on day 1 and 3 (Figure 5.33). The LDH test was modified so cell viability was measured instead of relative toxicity.

After 1 day of incubation average cell viability was around 100% for PRA-M, PRA-H and PER samples and only 52% for RA. After 3 days average cell viability was the highest for PER material (90%) and for PRA-M and PRA-H was 83% and 85% respectively. In the presence of RA material average cell viability was 39% after 3 days. Good cell viability after 3 days makes polyricinoleate and polyepoxyricinoleate a promising material for *in vitro* application.

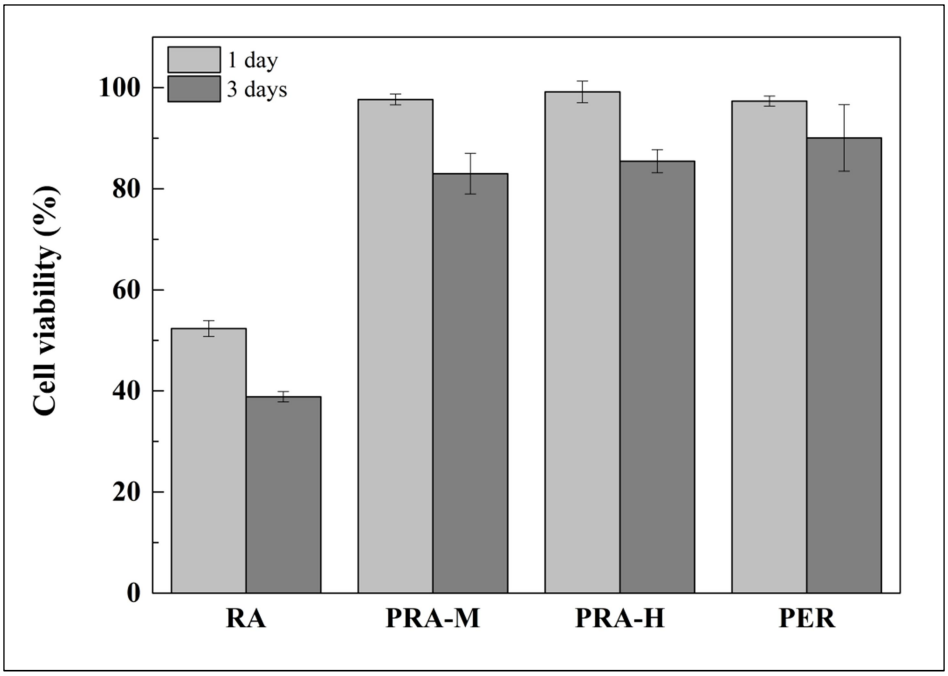


Figure 5.33: Cell viability after 1 and 3 days.

6. CONCLUSIONS

Vegetable oils are potential starting materials for synthesis of bio-based polymers. Ricinoleic acid has been widely used in polymer synthesis but mainly found application as a component of copolymers or polymeric blends. Few scientific reports mention synthesis of poly(ricinoleic acid) and final product has relatively low molecular weight.

On the other hand scientific research on ricinoleic acid high-molecular-weight homopolymer is limited due to high price of pure methyl ricinoleate (monomer) and lipase catalysts. High purity monomer is required to obtain high molecular weights because other mono functional fatty acids can untimely terminate growing polymer chain.

In the first part of this work, cost-effective synthesis of high-molecular-weight polyricinoleate is reported for the first time. High amount of methyl ricinoleate (monomer) was prepared from ordinary ricinoleic acid (80%) by simple liquid-liquid extraction method. Obtained monomer was of high purity (99.7% by GC). This could reduce the cost of monomer by at least 200 times when compared to price of ready monomer (according to prices for 2019). The use of commercial enzyme Lipozyme TL IM that could be reused for at least 2-3 times without significant decrease of polyricinoleate molecular weight could additionally reduce the cost of synthesis. This inexpensive route of synthesis of polyricinoleate could help reintroduce research on this topic.

In the second part of this work, various properties of polyricinoleates were analysed. Polyricinoleates have ability to form continuous coating on different surfaces prepared by simple solvent casting method. Antibacterial activity with direct contact to the surfaces indicated no significant activity of polyricinoleates against *E. coli* and *S. aureus*.

Polyepoxyricinoleate polymer was obtained by simple reaction of polyricinoleate with m-chloroperbenzoic acid. *In vitro* degradation experiment showed that after 6 months of incubation polyricinoleates showed good stability with only ~2% loss of their weight while polyepoxyricinoleate polymer was less stable with weight loss of ~28%. Lap-shear adhesion tests of polyricinoleates and polyepoxyricinoleate revealed that polyricinoleates and polyepoxyricinoleate have

some amount of adhesion strength on different substrates such as glass, aluminium, paper and PET. Polyepoxyricinoleate showed highest adhesion strength of all polymers with of max. 41 kPa on paper substrate. Lap-shear test performed on ovine skin showed that these polymers have relatively low adhesion to tested tissue. Again, polyepoxyricinoleate showed highest maximum adhesion strength of all polymers (~1500 Pa).

Whole blood clotting time tested *in vitro* in contact with polyricinoleates and polyepoxyricinoleate, demonstrated no significant influence of these polymers on blood clotting. Additionally, cytotoxicity assay showed good cell viability after 1 and 3 days of incubation of cells (3T3 mouse fibroblasts) in the presence of polyricinoleates and polyepoxyricinoleate.

Low cytotoxicity and the ability to form a continuous and smooth film layer even in such a small amount and long term in vitro stability could make polyricinoleates excellent candidate material for use as coatings for biomedical equipment e.g. coating of stainless steel stent, orthopaedic implants etc. Future studies should be also conducted to illustrate long-term interaction with biological subjects such as cell proliferation, bacterial and protein adhesion.

REFERENCES

[1] Ebnesajjad S., (2012), "Handbook of biopolymers and biodegradable plastics" 1st Edition, William Andrew.

[2] Meier M.A.R., Metzger J.O., Schubert U.S., (2007), "Plant oil renewable resources as green alternatives in polymer science" Chemical Society Reviews, 36 (11), 1788–1802.

[3] Xia Y., Larock R.C., (2010), "Vegetable oil-based polymeric materials: synthesis, properties, and applications" Green Chemistry, 12 (11), 1893–1909.

[4] Lligadas G., Ronda J.C., Galià M., Cádiz V., (2013), "Renewable polymeric materials from vegetable oils: a perspective" Materials Today, 16 (9), 337–343.

[5] Mutlu H., Meier M.A.R., (2010), "Castor oil as a renewable resource for the chemical industry" European Journal of Lipid Science and Technology, 112 (1), 10–30.

[6] Kemper T.G., (2005), "Bailey's Industrial Oil and Fat Products Edible Oil and Fat Products: Processing Technologies" 7th Edition, John Wiley & Sons.

[7] Farhat A.M., Bassam E.,A., Speight J.,G., (2005), "Handbook Of Industrial Chemistry: Organic Chemicals" 1st Edition, McGraw-Hill.

[8] Barnes D.J., Baldwin B.S., Braasch D.A., (2009), "Degradation of ricin in castor seed meal by temperature and chemical treatment" Industrial Crops and Products, 29 (2–3), 509–515.

[9] Kunduru K.R., Basu A., Haim Zada M., Domb A.J., (2015), "Castor Oil-Based Biodegradable Polyesters" Biomacromolecules, 16 (9), 2572–2587.

[10] Tallman K.A., Roschek B., Porter N.A., (2004), "Factors influencing the autoxidation of fatty acids: Effect of olefin geometry of the nonconjugated diene" Journal of the American Chemical Society, 126 (30), 9240–9247.

[11] Cakmakli B., Hazer B., Tekin I.O., Kizgut S., Koksal M., Menceloglu Y., (2004), "Synthesis and characterization of polymeric linseed oil grafted methyl methacrylate or styrene" Macromolecular Bioscience, 4 (7), 649–655.

[12] Çakmakli B., Hazer B., Tekin I.Ö., Cömert F.B., (2005), "Synthesis and characterization of polymeric soybean oil-g-methyl methacrylate (and n-butyl methacrylate) graft copolymers: Biocompatibility and bacterial adhesion" Biomacromolecules, 6 (3), 1750–1758.

[13] Cakmakli B., Hazer B., Acikgoz S., Can M., Comert F.B., (2007), "PMMA-multigraft copolymers derived from linseed oil, soybean oil, and linoleic acid: Protein adsorption and bacterial adherence" Journal of Applied Polymer Science, 105 (6), 3448–3457.

[14] Robertson M.L., Chang K., Gramlich W.M., Hillmyer M.A., (2010), "Toughening of polylactide with polymerized soybean oil" Macromolecules, 43 (4), 1807–1814.

[15] Li F., Larock R.C., (2003), "Synthesis, structure and properties of new tung oil - Styrene - Divinylbenzene copolymers prepared by thermal polymerization" Biomacromolecules, 4 (4), 1018–1025.

[16] Lu J., Khot S., Wool R.P., (2005), "New sheet molding compound resins from soybean oil. I. Synthesis and characterization" Polymer, 46 (1), 71–80.

[17] La Scala J., Wool R.,P., (2005), "Property analysis of triglyceride-based thermosets" Polymer, 46 (1), 61–69.

[18] Campanella A., La Scala J.J., Wool R.P., (2009), "The use of acrylated fatty acid methyl esters as styrene replacements in triglyceride-based thermosetting polymers" Polymer Engineering and Science, 49 (12), 2384–2392.

[19] Bonnaillie L.M., Wool R.P., (2007), "Thermosetting foam with a high bio-based content from acrylated epoxidized soybean oil and carbon dioxide" Journal of Applied Polymer Science, 105 (3), 1042–1052.

[20] Bunker S.P., Wool R.P., (2002), "Synthesis and characterization of monomers and polymers for adhesives from methyl oleate" Journal of Polymer Science, Part A: Polymer Chemistry, 40 (4), 451–458.

[21] Khot S.N., Lascala J.J., Can E., Morye S.S., Williams G.I., Palmese G.R., Kusefoglu S.H., Wool R.P., (2001), "Development and application of triglyceride-based polymers and composites" Journal of Applied Polymer Science, 82 (3), 703–723.

[22] Espinosa D.L.M., Ronda J.C., Galia M., Cadiz V., (2009), "A new route to acrylate oils: Crosslinking and properties of acrylate triglycerides from high oleic sunflower oil" Journal of Polymer Science, Part A: Polymer Chemistry, 47 (4), 1159–1167.

[23] Hui S.-P., Yoshimura T., Murai T., Chiba H., Kurosawa T., (2005), "Determination of Regioisomeric Hydroperoxides of Fatty Acid Cholesterol Esters Produced by Photosensitized Peroxidation Using HPLC." Analytical Sciences, 16 (10), 1023–1028.

[24] Samadi A., Martínez L.A., Miranda M.A., Morera I.M., (2004), "Mechanism of Lipid Peroxidation Photosensitized by Tiaprofenic Acid: Product Studies Using Linoleic Acid and 1,4-Cyclohexadienes as Model Substrates" Photochemistry and Photobiology, 73 (4), 359–365.

[25] Greer A., (2006), “Christopher Foote ’ s Discovery of Oxidation Reactions” Society, 39 (11), 797–804.

[26] Zhang P., Xin J., Zhang J., (2014), “Effects of catalyst type and reaction parameters on one-step acrylation of soybean oil” ACS Sustainable Chemistry and Engineering, 2 (2), 181–187.

[27] Wool R.P., Can E., Kusefoglu S., (2001), “Rigid , Thermosetting Liquid Molding Resins From Renewable Resources . I . Synthesis and Polymerization of Soy Oil Monoglyceride Maleates” Journal of Applied Polymer Science, 81, 69–77.

[28] Can E., Kusefoglu S., Wool R.P., (2002), “Rigid thermosetting liquid molding resins from renewable resources. II. Copolymers of soybean oil monoglyceride maleates with neopentyl glycol and bisphenol A maleates” Journal of Applied Polymer Science, 83 (5), 972–980.

[29] Li F., Larock R.C., (2000), “Thermosetting polymers from cationic copolymerization of tung oil: synthesis and characterization” Journal of Applied Polymer Science, 78 (5), 1044–1056.

[30] Li F., Larock R.C., (2002), “Novel polymeric materials from biological oils” Journal of Polymers and the Environment, 10 (1–2), 59–67.

[31] Li F., Hanson M.V., Larock R.C., (2001), “Soybean oil-divinylbenzene thermosetting polymers: Synthesis, structure, properties and their relationships” Polymer, 42 (4), 1567–1579.

[32] Li F., Larock R.C., (2001), “New soybean oil-styrene-divinylbenzene thermosetting copolymers. III. Tensile stress - strain behavior” Journal of Polymer Science, Part B: Polymer Physics, 39 (1), 60–77.

[33] Li F., Hasjim J., Larock R.C., (2003), “Synthesis, structure, and thermophysical and mechanical properties of new polymers prepared by the cationic copolymerization of corn oil, styrene, and divinylbenzene” Journal of Applied Polymer Science, 90 (7), 1830–1838.

[34] Andjelkovic D.D., Valverde M., Henna P., Li F., Larock R.C., (2005), “Novel thermosets prepared by cationic copolymerization of various vegetable oils - Synthesis and their structure-property relationships” Polymer, 46 (23), 9674–9685.

[35] Jin F.,-L., Park S.-J., (2008), “Thermomechanical behavior of epoxy resins modified with epoxidized vegetable oils” Polymer International, 57 (4), 577–583.

[36] Park S.J., Jin F.L., Lee J.R., (2004), “Synthesis and thermal properties of epoxidized vegetable oil” Macromolecular Rapid Communications, 25 (6), 724–727.

[37] Park S.J., Jin F.L., Lee J.R., (2004), “Effect of biodegradable epoxidized castor oil on physicochemical and mechanical properties of epoxy resins” Macromolecular Chemistry and Physics, 205 (15), 2048–2054.

[38] Banks R.L., Bailey G.C., (1964), “Olefin disproportionation” Industrial and Engineering Chemistry Product Research and Development, 3 (3), 170–173.

[39] Trnka T.M., Grubbs R.H., (2001), “The development of L2X2Ru=CHR olefin metathesis catalysts: an organometallic success story.” Accounts of Chemical Research, 34 (1), 18–29.

[40] Schrock R.R., Czekelius C., (2007), “Recent advances in the syntheses and applications of molybdenum and tungsten alkylidene and alkylidyne catalysts for the metathesis of alkenes and alkynes” Advanced Synthesis and Catalysis, 349 (1–2), 55–77.

[41] Schwab P., Grubbs R.H., Ziller J.,W., (2002), “ Synthesis and Applications of RuCl 2 (CHR‘)(PR 3) 2 : The Influence of the Alkylidene Moiety on Metathesis Activity ” Journal of the American Chemical Society, 118 (1), 100–110.

[42] Scholl M., Ding S., Lee C.W., Grubbs R.H., (1999), “Synthesis and activity of a new generation of ruthenium-based olefin metathesis catalysts coordinated with 1,3-dimesityl-4,5-dihydroimidazol-2-ylidene ligands.” Organic Letters, 1 (6), 953–6.

[43] Van Dam P.,B., Mittelmeijer M.C., Boelhouwer C., (1972), “Metathesis of unsaturated fatty acid esters by a homogeneous tungsten hexachloride-tetramethyltin catalyst” Journal of the Chemical Society, Chemical Communications, 0 (22), 1221–1222.

[44] Buchowicz W., Mol J.C., (1999), “Catalytic activity and selectivity of $Ru(=CHPh)Cl_2(PCy_3)_2$ in the metathesis of linear alkenes” Journal of Molecular Catalysis, 97–103.

[45] Refvik M.D., Larock R.C., Tian Q., (1999), “Ruthenium-catalyzed metathesis of vegetable oils” JAOCS, Journal of the American Oil Chemists’ Society, 76 (1), 93–98.

[46] Rybak A., Meier M.A.R., (2008), “Acyclic diene metathesis with a monomer from renewable resources: Control of molecular weight and one-step preparation of block copolymers” ChemSusChem, 1 (6), 542–547.

[47] Montero de Espinosa L., Meier M.A.R., Ronda J.C., Galià M., Cádiz V., (2010), “Phosphorus-Containing Renewable Polyester-Polyols via ADMET Polymerization: Synthesis, Functionalization, and Radical Crosslinking” Journal of Polymer Science Part A: Polymer Chemistry, 48 (1), 1649–1660.

[48] Fokou P.A., Meier M.A.R., (2008), “Acyclic triene metathesis polymerization with chain-stoppers: Molecular weight control in the synthesis of branched polymers” Macromolecular Rapid Communications, 29 (19), 1620–1625.

[49] Henna P., Larock R.C., (2009), “Novel thermosets obtained by the ring-opening metathesis polymerization of a functionalized vegetable oil and dicyclopentadiene” Journal of Applied Polymer Science, 112 (1), 1788–1797.

[50] Henna P.H., Larock R.C., (2007), “Rubbery thermosets by ring-opening metathesis polymerization of a functionalized castor oil and cyclooctene” Macromolecular Materials and Engineering, 292 (12), 1201–1209.

[51] Xia Y., Lu Y., Larock R.C., (2010), “Ring-opening metathesis polymerization (ROMP) of norbornenyl-functionalized fatty alcohols” Polymer, 51 (1), 53–61.

[52] Xia Y., Larock R.C., (2010), “Castor oil-based thermosets with varied crosslink densities prepared by ring-opening metathesis polymerization (ROMP)” Polymer, 51 (12), 2508–2514.

[53] Dutta N., Karak N., Dolui S.K., (2004), “Synthesis and characterization of polyester resins based on Nahar seed oil” Progress in Organic Coatings, 49 (2), 146–152.

[54] Petrović Z.S., Milić J., Xu Y., Cvetković I., (2010), “A chemical route to high molecular weight vegetable oil-based polyhydroxyalkanoate” Macromolecules, 43 (9), 4120–4125.

[55] Lenz R.W., Marchessault R.H., (2005), “Bacterial polyesters: Biosynthesis, biodegradable plastics and biotechnology” Biomacromolecules, 6 (1), 1–8.

[56] Hazer D.B., Hazer B., Kaymaz F., (2009), “Synthesis of microbial elastomers based on soybean oily acids. Biocompatibility studies” Biomedical Materials, 4 (3), 1-9.

[57] Islam M.R., Beg M.D.H., Jamari S.S., (2014), “Development of vegetable-oil-based polymers” Journal of Applied Polymer Science, 131 (18), 1-13.

[58] Fan X.D., Deng Y., Waterhouse J., Pfromm P., Carr W.W., (1999), “Development of an easily deinkable copy toner using soy-based copolyamides” Journal of Applied Polymer Science, 74 (6), 1563–1570.

[59] Deng Y., Fan X.D., Waterhouse J., (1999), “Synthesis and characterization of soy-based copolyamides with different α-amino acids” Journal of Applied Polymer Science, 73 (6), 1081–1088.

[60] Yeganeh H., Mehdizadeh M.R., (2004), “Synthesis and properties of isocyanate curable millable polyurethane elastomers based on castor oil as a renewable resource polyol” European Polymer Journal, 40 (6), 1233–1238.

[61] Petrovic Z.S., Cvetkovic I., Hong D., Wan X., Zhang W., Abraham T., Malsam J., (2008), "Polyester Polyols and Polyurethanes from Ricinoleic Acid" Journal of Applied Polymer Science, 108, 1184–1190.

[62] Somani K.P., Kansara S.S., Patel N.K., Rakshit A.K., (2003), "Castor oil based polyurethane adhesives for wood-to-wood bonding" International Journal of Adhesion and Adhesives, 23 (4), 269–275.

[63] Guo A., Cho Y., Petrović Z.S., (2000), "Structure and properties of halogenated and nonhalogenated soy-based polyols" Journal of Polymer Science, Part A: Polymer Chemistry, 38 (21), 3900–3910.

[64] Zlatanic A., Lava C., Zhang W., Petrovic Z.S., (2004), "Effect of structure on properties of polyols and polyurethanes based on different vegetable oils" Journal of Polymer Science Part B: Polymer Physics, 42 (5), 809–819.

[65] Petrovic Z.S., Guo A., Javni I., Cvetkovic I., Hong D.,P., (2007), "Polyurethane networks from polyols obtained by hydroformylation of soybean oil" Polymer International, 57, 275–281.

[66] Hojabri L., Kong X., Narine S.S., (2009), "Fatty Acid-Derived diisocyanate and biobased polyurethane produced from vegetable oil: Synthesis, polymerization, and characterization" Biomacromolecules, 10 (4), 884–891.

[67] Hojabri L., Kong X., Narine S.S., (2010), "Functional thermoplastics from linear diols and diisocyanates produced entirely from renewable lipid sources" Biomacromolecules, 11 (4), 911–918.

[68] Chandorkar Y., Madras G., Basu B., (2013), "Structure, tensile properties and cytotoxicity assessment of sebacic acid based biodegradable polyesters with ricinoleic acid" Journal of Materials Chemistry B, 1 (6), 865–875.

[69] Sokolsky-Papkov M., Langer R., Domb A.J., (2011), "Synthesis of aliphatic polyesters by polycondensation using inorganic acid as catalyst" Polymers for Advanced Technologies, 22 (5), 502–511.

[70] Vaisman B., Motiei M., Nyska A., Domb A.J., (2010), "Biocompatibility and safety evaluation of a ricinoleic acid-based poly(ester-anhydride) copolymer after implantation in rats" Journal of Biomedical Materials Research - Part A, 92 (2), 419–431.

[71] Krasko M.,Y., Domb A.J., (2007), "Pasty injectable biodegradable polymers derived from natural acids" J Biomed Mater Res A, 83 (4), 1138–1145.

[72] Fay F., Linossier I., Langlois V., Vallee-Rehel K., Krasko M.Y., Domb A.,J., (2007), "Protecting biodegradable coatings releasing antimicrobial agents" Journal of Applied Polymer Science, 106 (6), 3768–3777.

[73] Slivniak R., Domb A.J., (2005), "Lactic Acid and Ricinoleic Acid Based Copolyesters" Macromolecules, 38, 5545−5553.

[74] Slivniak R., Langer R., Domb A.J., (2005), “Lactic and ricinoleic acid based copolyesters stereocomplexation” Macromolecules, 38 (13), 5634–5639.

[75] Ickowicz D.E., Haim-Zada M., Abbas R., Touitou D., Nyska A., Golovanevski L., Weiniger C.F., Katzhendler J., Domb A.J., (2014), “Castor oil-citric acid copolyester for tissue augmentation” Polymers for Advanced Technologies, 25 (11), 1323–1328.

[76] Bharathi P., Moore J.S., (2000), “Controlled Synthesis of Hyperbranched Polymers by Slow Monomer Addition to a Core” Macromolecules, 33 (9), 3212–3218.

[77] Sathiskumar P.S., Chopra S., Madras G., (2012), “Investigation of biodegradable and biocompatible castor oil poly (mannitol-citric-sebacate) polyester as a drug carrier” Current Science, 102 (1), 97–104.

[78] Krasko M.Y., Shikanov A., Ezra A., Domb A.J., (2003), “Poly(ester anhydride)s Prepared by the Insertion of Ricinoleic Acid into Poly(sebacic acid)” Journal of Polymer Science Part A: Polymer Chemistry, 41, 1059–1069.

[79] Slivniak R., Domb A.J., (2005), “Macrolactones and polyesters from ricinoleic acid” Biomacromolecules, 6 (3), 1679–1688.

[80] Ebata H., Toshima K., Matsumura S., (2007), “Lipase-catalyzed synthesis and curing of high-molecular-weight polyricinoleate” Macromol Biosci, 7 (6), 798–803.

[81] Ebata H., Yasuda M., Toshima K., Matsumura S., (2008), “Poly (Ricinoleic Acid) Based Novel Thermosetting Elastomer” Journal of Oleo Science, 57 (6), 315–320.

[82] Kazariya A., Matsumura S., (2012), “Enzymatic Synthesis and Crosslinking of Novel High Molecular Weight Polyepoxyricinoleate” Polymers, 4 (4), 486–500.

[83] Berdeaux O., Christie W.W., Gunstone F.D., J.-L. S., (1997), “Large-scale synthesis of methyl cis-9, trans-11-octadecadienoate from methyl ricinoleate” Journal Of The American Oil Chemists Society, 74 (8), 1011–1015.

[84] Novak A., Clark G., Dupuy H., (1961), “Antimicrobial Activity of Some Ricinoleic and Oleic Acid Derivatives” Journal Of The American Oil Chemists Society, 38 (6), 321–324.

[85] Slivniak R., Ezra A., Domb A.J., (2006), “Hydrolytic Degradation and Drug Release of Ricinoleic Acid–Lactic Acid Copolyesters” Pharmaceutical Research, 23, 1306−1312.

[86] Totaro G., Cruciani L., Vannini M., Mazzola G., Di Gioia D., Celli A., Sisti L., (2014), "Synthesis of castor oil-derived polyesters with antimicrobial activity" European Polymer Journal, 56, 174–184.

[87] Awang R., Basri M., Ahmad S., Salleh A.,B., (2011), "Thermomyces lanuginosus Lipase-Catalyzed Esterification of 9,10-Dihydroxystearic Acid and Monohydric Alcohol" Journal of Oleo Science, 54 (5), 305–309.

[88] Chen S.C., Zhang X.M., Liu M., Ma J.P., Lu W.Y., Chen W.X., (2016), "Rheological characterization and thermal stability of different intrinsic viscosity poly(ethylene terephthalate) in air and nitrogen" International Polymer Processing, 31 (3), 292–300.

[89] Pohl H.A., (1951), "The Thermal Degradation of Polyesters" Journal of the American Chemical Society, 73 (12), 5660–5661.

[90] Li D., Zheng Q., Wang Y., Chen H., (2014), "Combining surface topography with polymer chemistry: Exploring new interfacial biological phenomena" Polymer Chemistry, 5 (1), 14–24.

[91] Assender H., Bliznyuk V., Porfyrakis K., (2002), "How Surface Topography Relates toMaterials' properties" Science, 297 (August), 973–976.

[92] Saastamoinen M., Fradinho M.,J., Santos A.,S., Miraglia N., (2012), "Forages and grazing in horse nutrition" 1st Edition, Wageningen Academic Publishers.

[93] Kolewe K.W., Zhu J., Mako N.R., Nonnenmann S.,S., Schiffman J.,D., (2018), "Bacterial Adhesion Is Affected by the Thickness and Stiffness of Poly(ethylene glycol) Hydrogels" ACS Applied Materials and Interfaces, 10 (3), 2275–2281.

[94] Braem A., Van Mellaert L., Mattheys T., Hofmans D., De Waelheyns E., Geris L., Anne J., Schrooten J., Vleugels J., (2014), "Staphylococcal biofilm growth on smooth and porous titanium coatings for biomedical applications" Journal of Biomedical Materials Research - Part A, 102 (1), 215–224.

[95] Harris L.G., Richards R.G., (2006), "Staphylococci and implant surfaces: a review" Injury, 37 (2), 3-14.

[96] Czech Z., Kowalczyk A., Kabatc J., Shao L., Bai Y., Swiderska J., (2013), "UV-initiated crosslinking of photoreactive acrylic pressure-sensitive adhesives using excimer-laser" Polymer Bulletin, 70 (2), 479–488.

[97] Ebnesajjad S., Landrock A.H., (2008), "Adhesives Technology Handbook" 2nd Edition, William Andrew.

[98] Bhagat V., Becker M.L., (2017), "Degradable Adhesives for Surgery and Tissue Engineering" Biomacromolecules, 18 (10), 3009–3039.

[99] Bochynska A.I., Hannink G., Verhoeven R., Grijpma D.W., Buma P., (2017), "Evaluation of novel biodegradable three-armed- and hyper-branched tissue adhesives in a meniscus explant model" Journal of Biomedical Materials Research - Part A, 105 (5), 1405–1411.

[100] Liu Y., Meng H., Konst S., Sarmiento R., Rajachar R., Lee B.P., (2014), "Injectable dopamine-modified poly(ethylene glycol) nanocomposite hydrogel with enhanced adhesive property and bioactivity" ACS Applied Materials and Interfaces, 6 (19), 16982–16992.

BIOGRAPHY

Magdalena Maria Tonta was born on April 27th, 1986 in Katowice, Poland. She started her chemistry education at Silesian University of Technology in Gliwice, Poland, in 2005. In 2009-2010 she studied at Institute of Chemical technology in Prague, Czech Republic. She received her M.S. in Chemistry from Silesian University of Technology in 2010. In 2013 she was registered as a Ph.D student to the Graduate School of Natural and Applied Sciences in Gebze Technical University, Turkey.

APPENDICES

Appendix A: Publications and Conference Proceedings

Tonta M. M., Sezer U. A, Olmez H., Gurek A. G., Sezer S., (2019), "Cost effective synthesis of Polyricinoleate: Investigation of coating characteristics, in vitro degradation and antibacterial activity". Journal of Applied Polymer Science, Accepted on 22 May 2019, doi: 10.1002/app.48172

Sahin Z. M., Alimli D., Tonta M. M., Kose M. E., Yilmaz F., (2017), "Highly sensitive and reusable mercury (II) sensor based on fluorescence quenching of pyrene moiety in polyacrylamide-based cryogel", Sensors and Actuators B: Chemical, 242, 362-368.

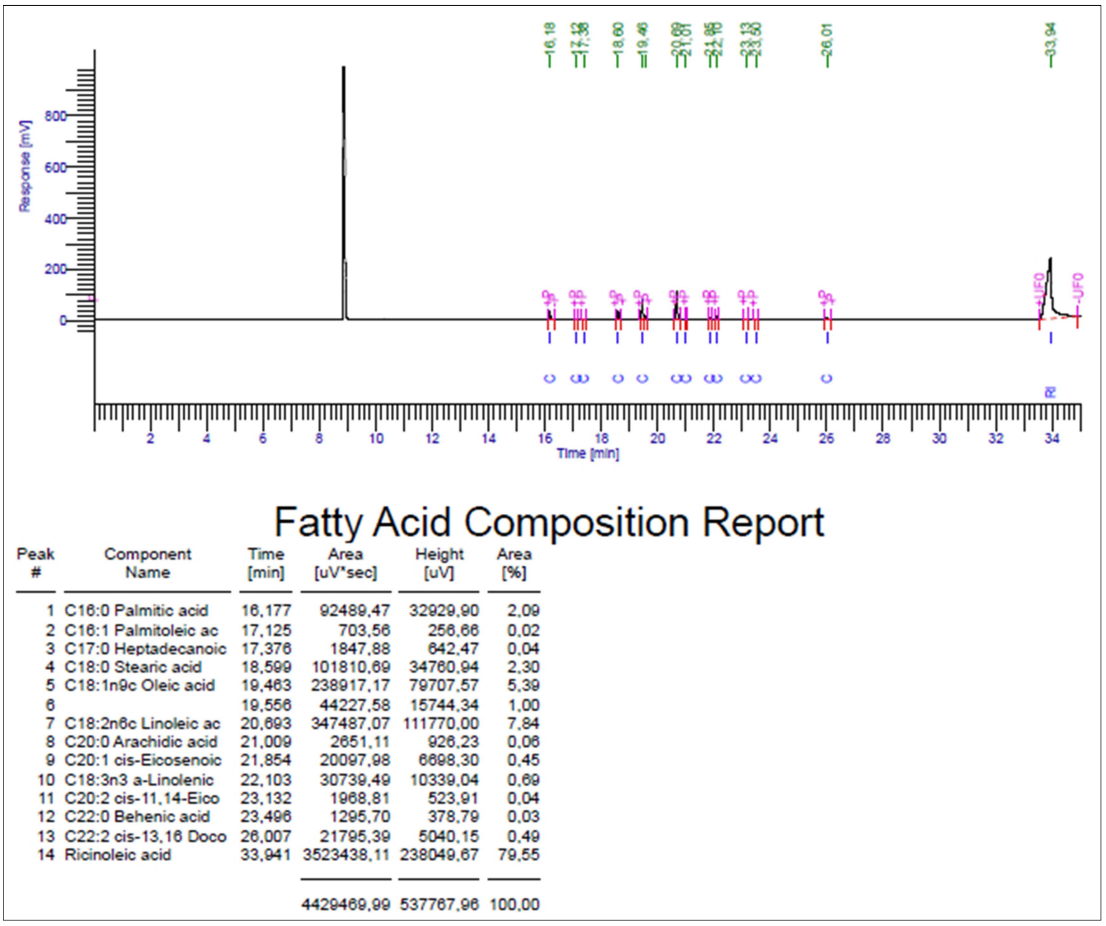
Yilmaz F., Sahin Z. M., Alimli D., Tonta M. M., Kose M. E. (2016), "Highly selective, sensitive and reusable Mercury (II) Sensor based on Fluorescence Quenching of Pyrene Moiety in Polyacrylamide Cryogel", EMN Meeting on Hydrogel Materials, Singapore, 9-13 May.

Yilmaz F., Sahin Z. M., Tonta M. M., (2015), "Raising the potential of polyacrylamide cryogel using click chemistry", APME, Yokohama, Japan, 18-22 October.

Tonta M. M., Yilmaz F., (2015), "Interpenetrated double network of PVA/PAAM cryogels". 5th Convention of Physical ChemistryNecmettin Erbakan University in Konya, Turkey, 16-19 May.

Sahin Z. M., Basmaz G., Tonta M. M., Ozturk N., (2015), Yilmaz F., (2015) "Preparation of redox-active polyacrylamide cryogels and their application as anion sensors". 5th Convention of Physical Chemistry Necmettin Erbakan University in Konya, Turkey, 16-19 May.

Appendix B: Characterization data



Fatty Acid Composition Report

Peak #	Component Name	Time [min]	Area [uV*sec]	Height [uV]	Area [%]
1	C16:0 Palmitic acid	16,177	92489,47	32929,90	2,09
2	C16:1 Palmitoleic ac	17,125	703,56	256,66	0,02
3	C17:0 Heptadecanoic	17,376	1847,88	642,47	0,04
4	C18:0 Stearic acid	18,599	101810,69	34760,94	2,30
5	C18:1n9c Oleic acid	19,463	238917,17	79707,57	5,39
6		19,556	44227,58	15744,34	1,00
7	C18:2n6c Linoleic ac	20,693	347487,07	111770,00	7,84
8	C20:0 Arachidic acid	21,009	2651,11	926,23	0,06
9	C20:1 cis-Eicosenoic	21,854	20097,98	6698,30	0,45
10	C18:3n3 a-Linolenic	22,103	30739,49	10339,04	0,69
11	C20:2 cis-11,14-Eico	23,132	1968,81	523,91	0,04
12	C22:0 Behenic acid	23,496	1295,70	378,79	0,03
13	C22:2 cis-13,16 Doco	26,007	21795,39	5040,15	0,49
14	Ricinoleic acid	33,941	3523438,11	238049,67	79,55
			4429469,99	537767,96	100,00

Figure B1.1: Fatty acids composition of FAME.

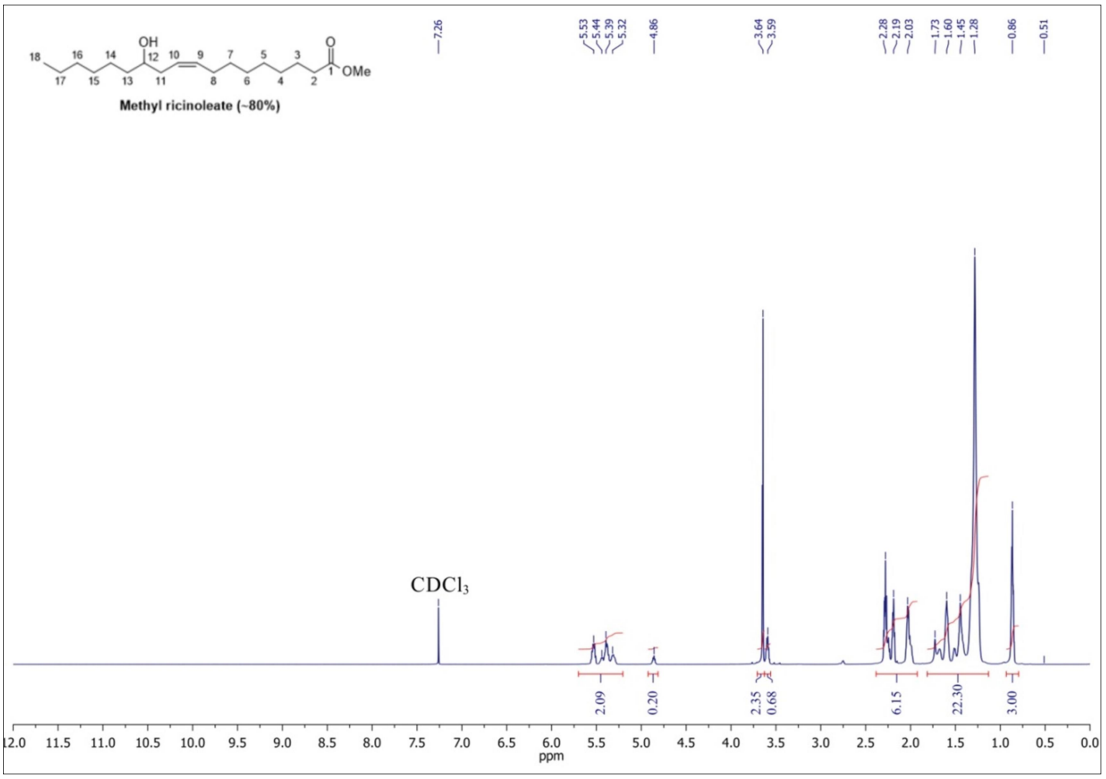


Figure B1.2: ^{1}H NMR spectrum of FAME.

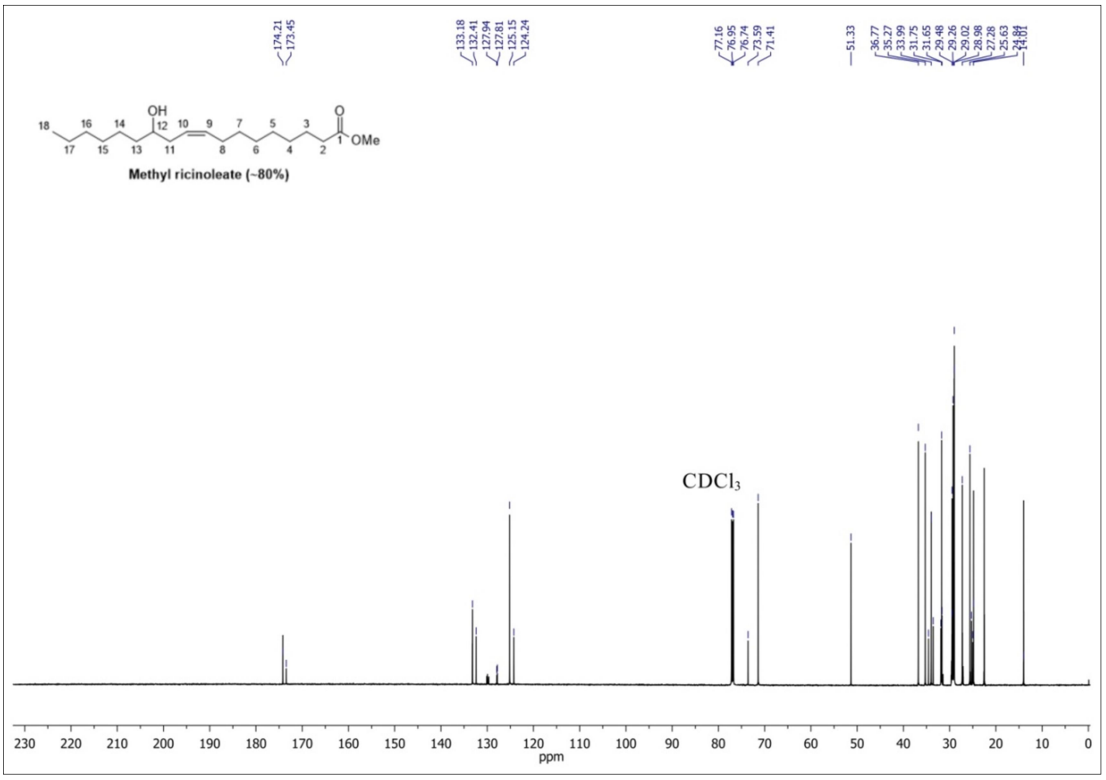


Figure B1.3: ^{13}C NMR spectrum of FAME.

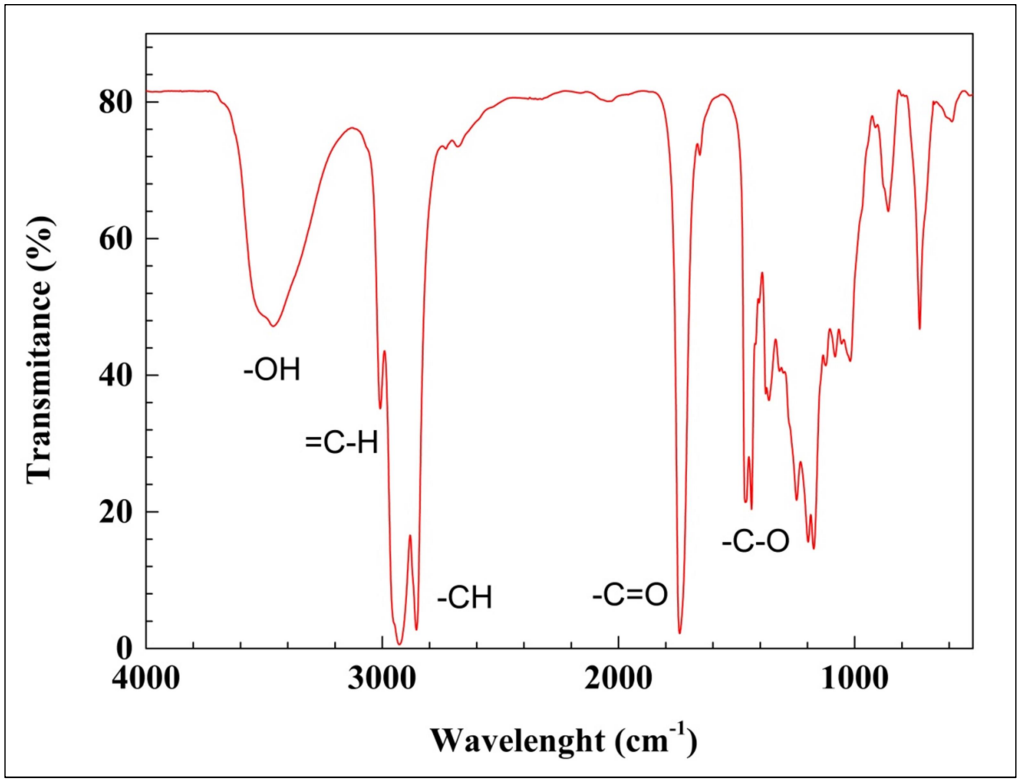


Figure B1.4: IR spectrum of FAME (Methyl ricinoleate 80%).

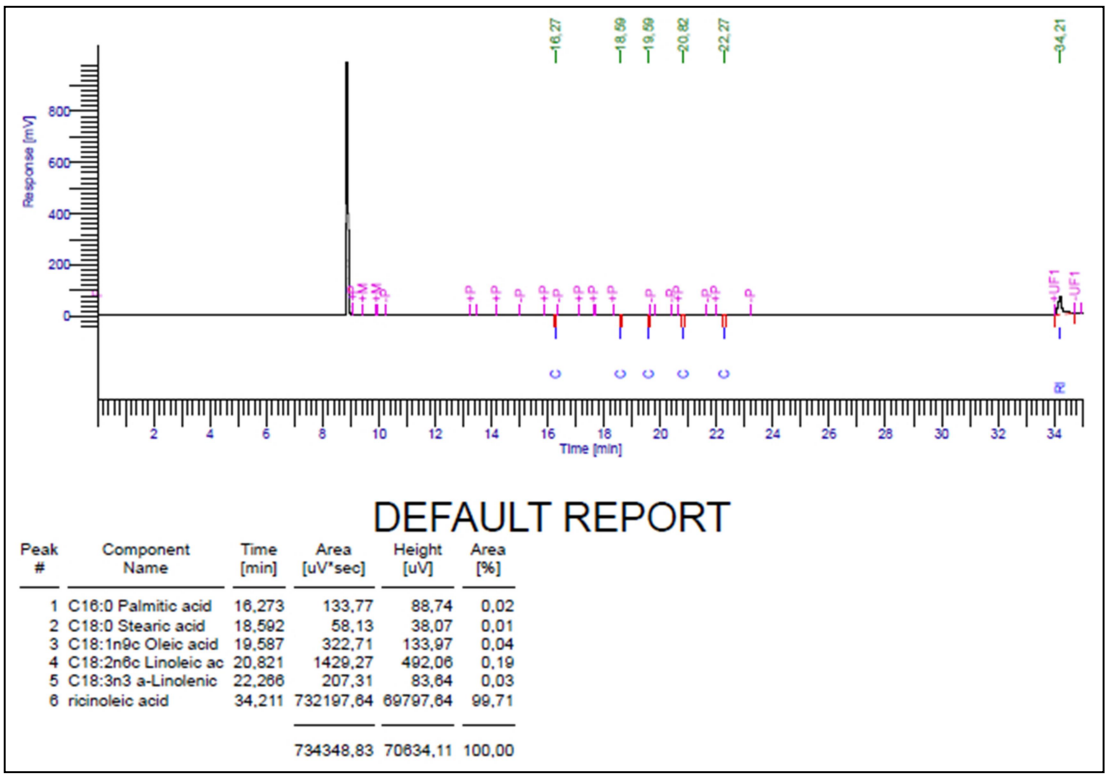


Figure B1.5: Fatty acids composition of pure methyl ricinoleate.

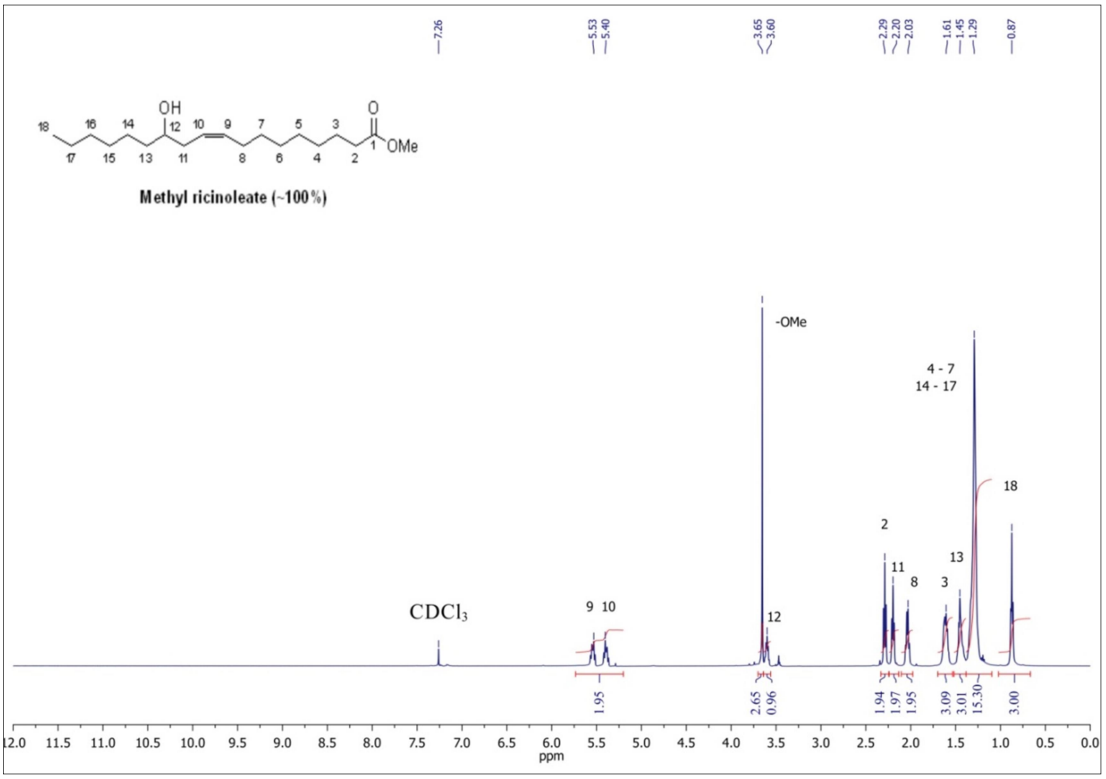


Figure B1.6: ^{1}H NMR spectrum of pure methyl ricinoleate.

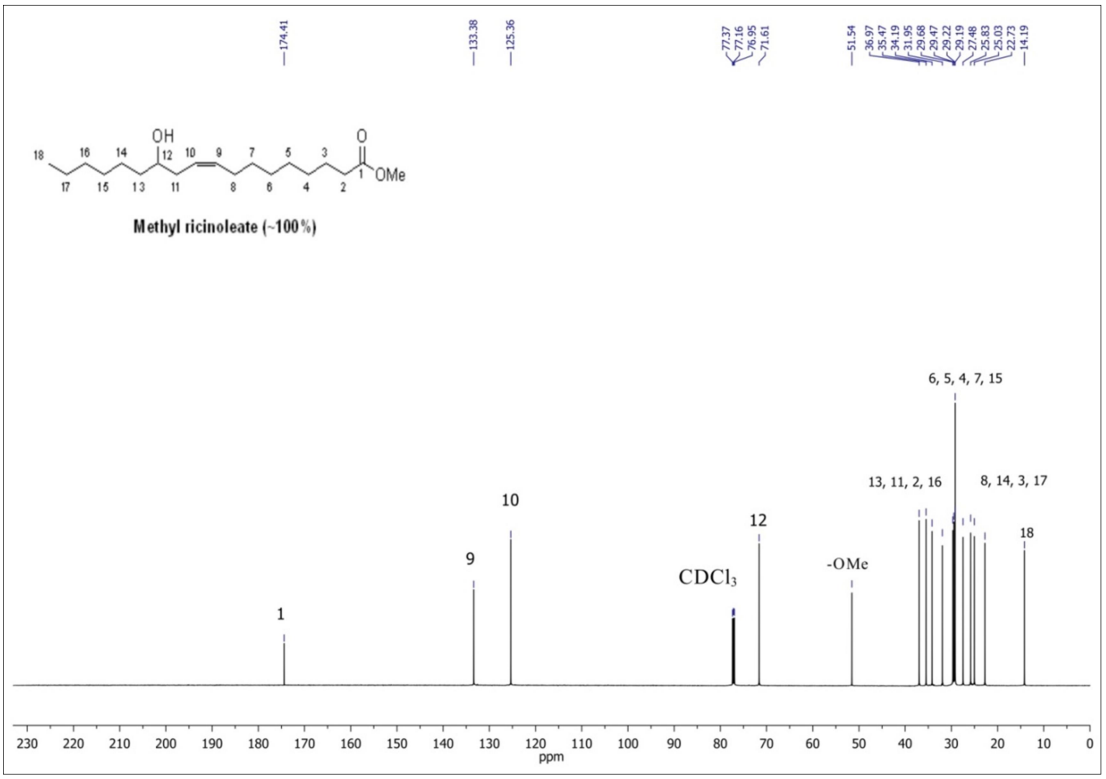


Figure B1.7: ^{13}C NMR spectrum of pure methyl ricinoleate.

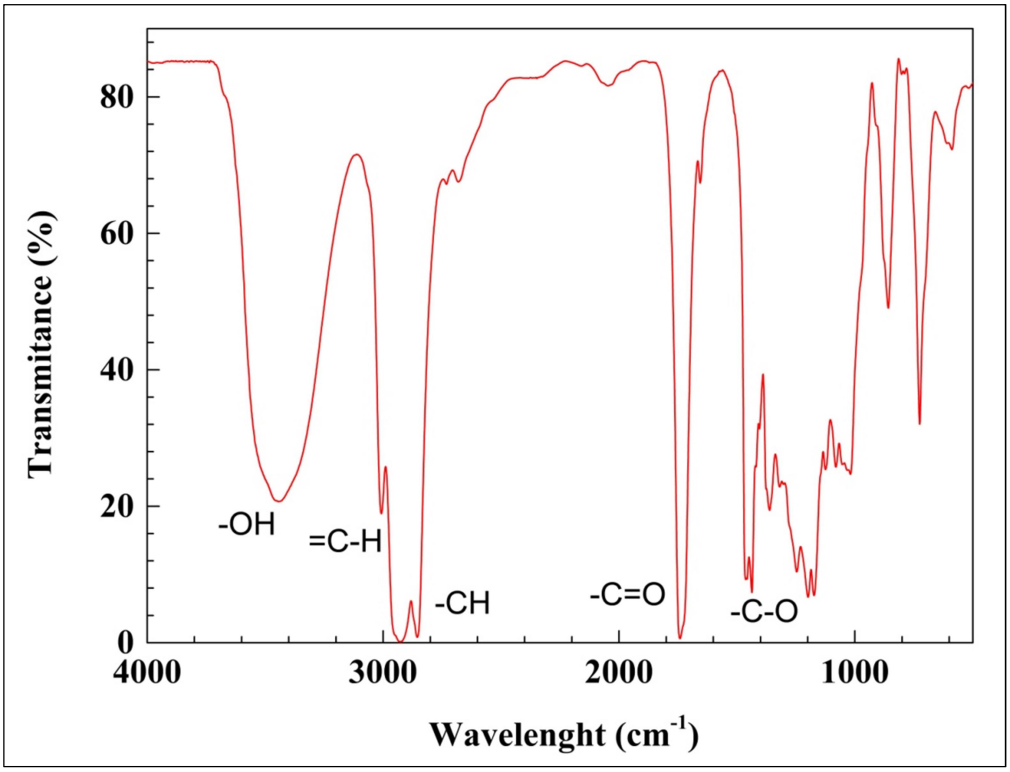


Figure B1.8: IR spectrum of pure methyl ricinoleate.

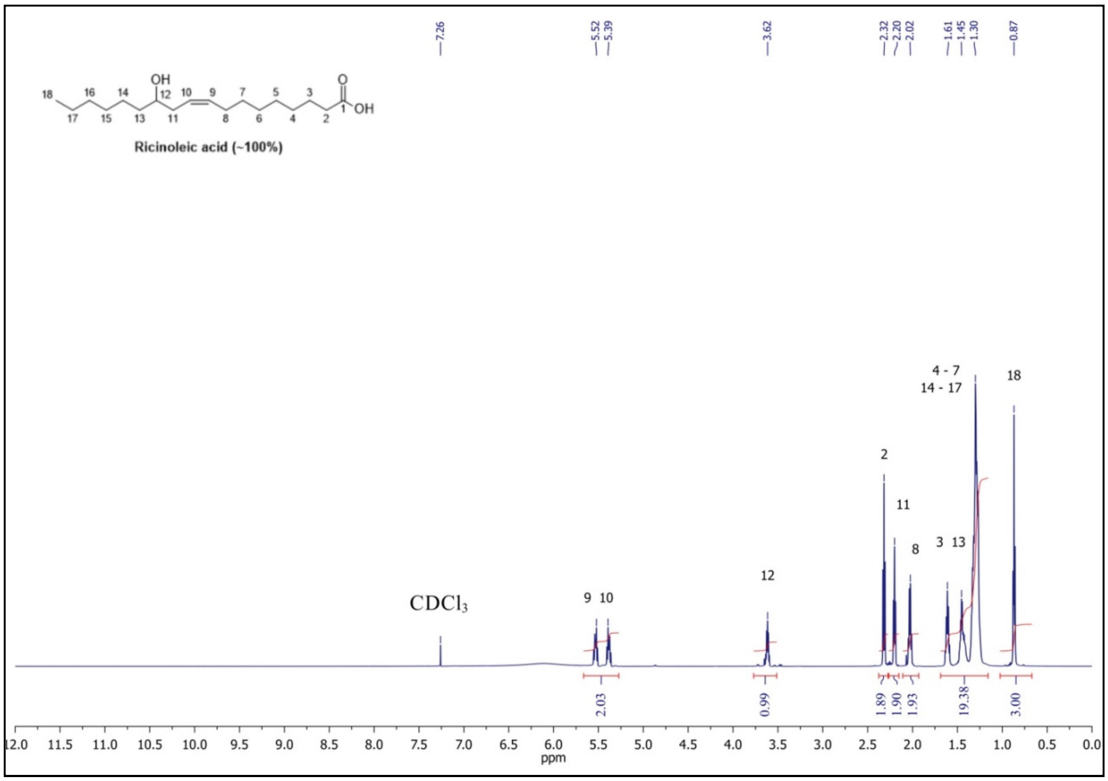


Figure B1.9: ^{1}H NMR spectrum of pure ricinoleic acid.

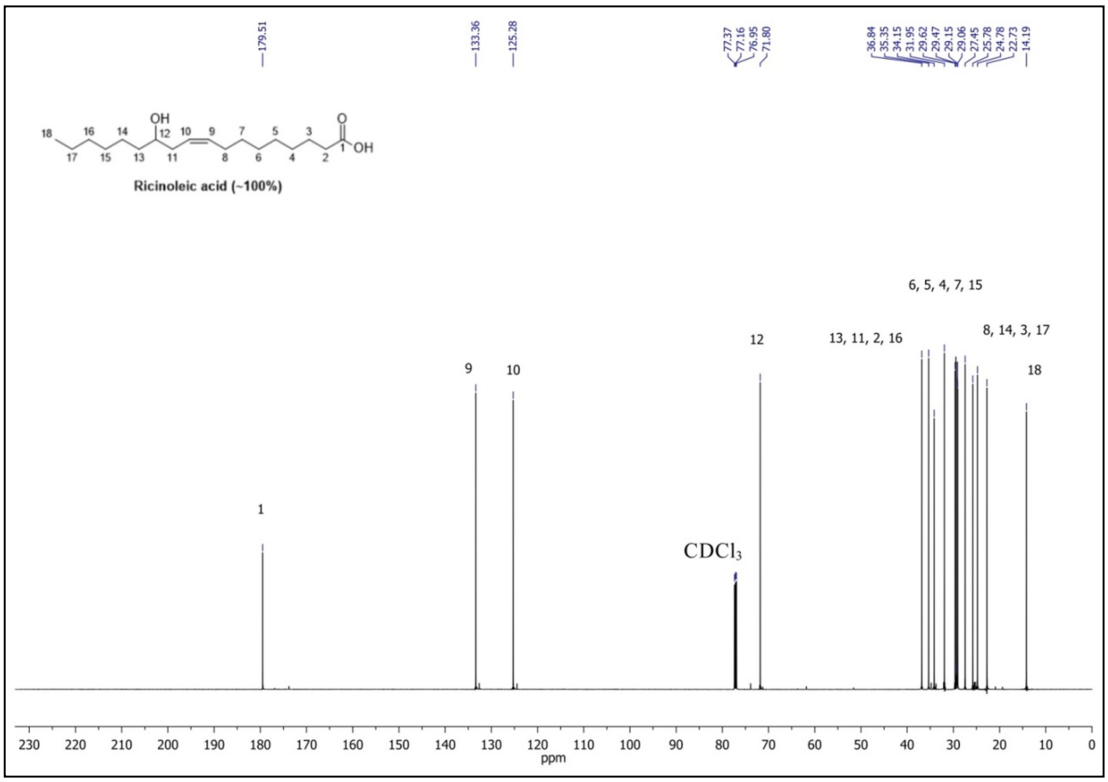


Figure B1.10: ^{13}C NMR spectrum of pure ricinoleic acid.

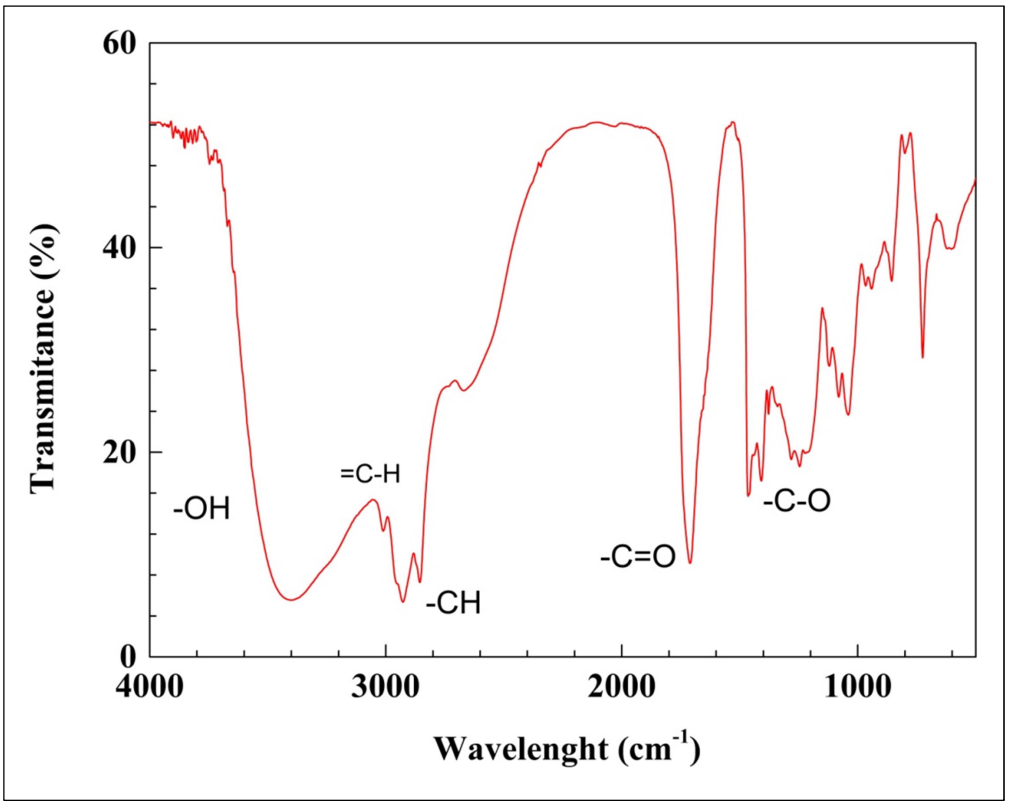


Figure B1.11: IR spectrum of pure ricinoleic acid.

^{1}H NMR and ^{13}C NMR spectra of all polymers were taken in order to confirm polyricinoleate structure. If not stated differently amount of enzyme is 100%wt relative to monomer.

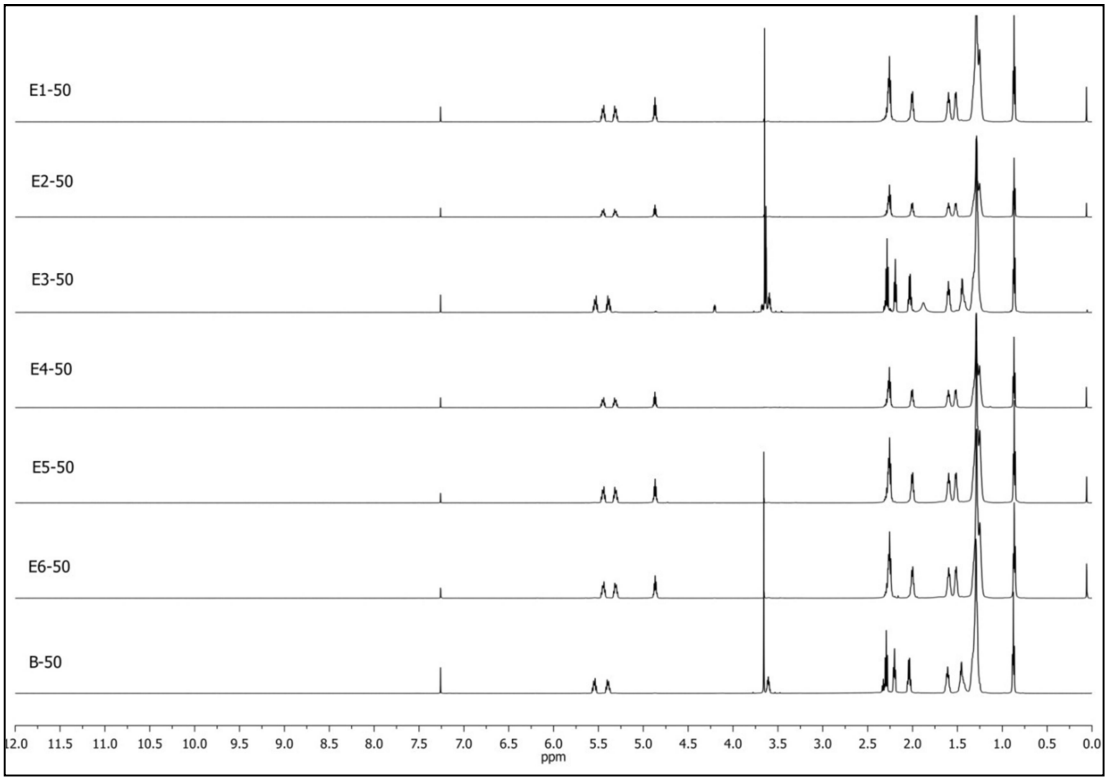


Figure B1.12: ^{1}H NMR spectra of polyricinoleates synthesized by various enzymes, for 7 days at 50°C.

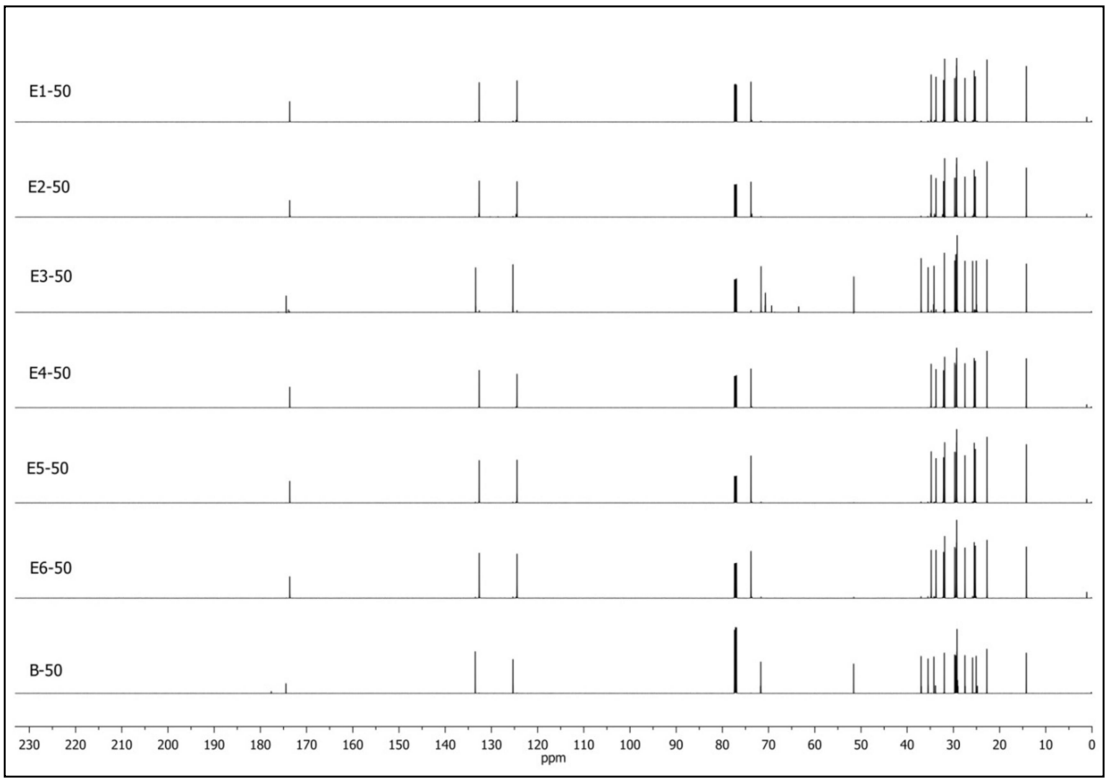


Figure B1.13: ^{13}C NMR spectra of polyricinoleates synthesized by various enzymes, for 7 days at 50°C.

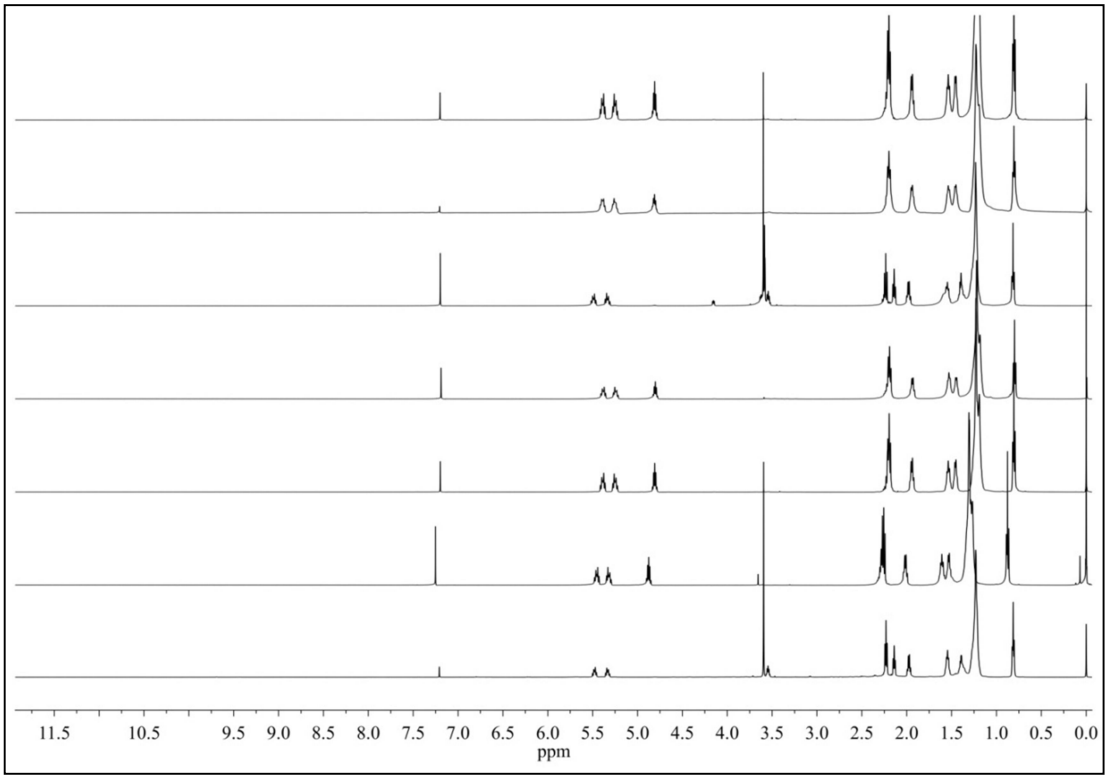


Figure B1.14: ^{1}H NMR spectra of polyricinoleates synthesized by various enzymes, for 7 days at 70°C.

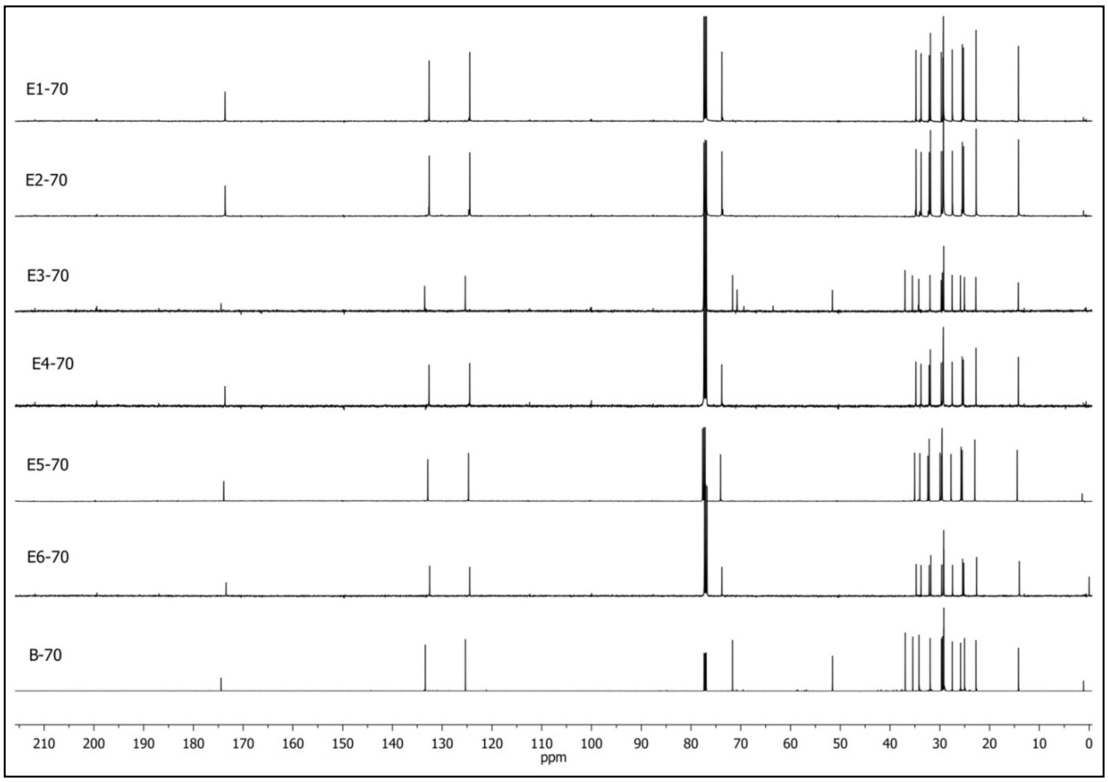


Figure B1.15: ^{13}C NMR spectra of polyricinoleates synthesized by various enzymes, for 7 days at 70°C.

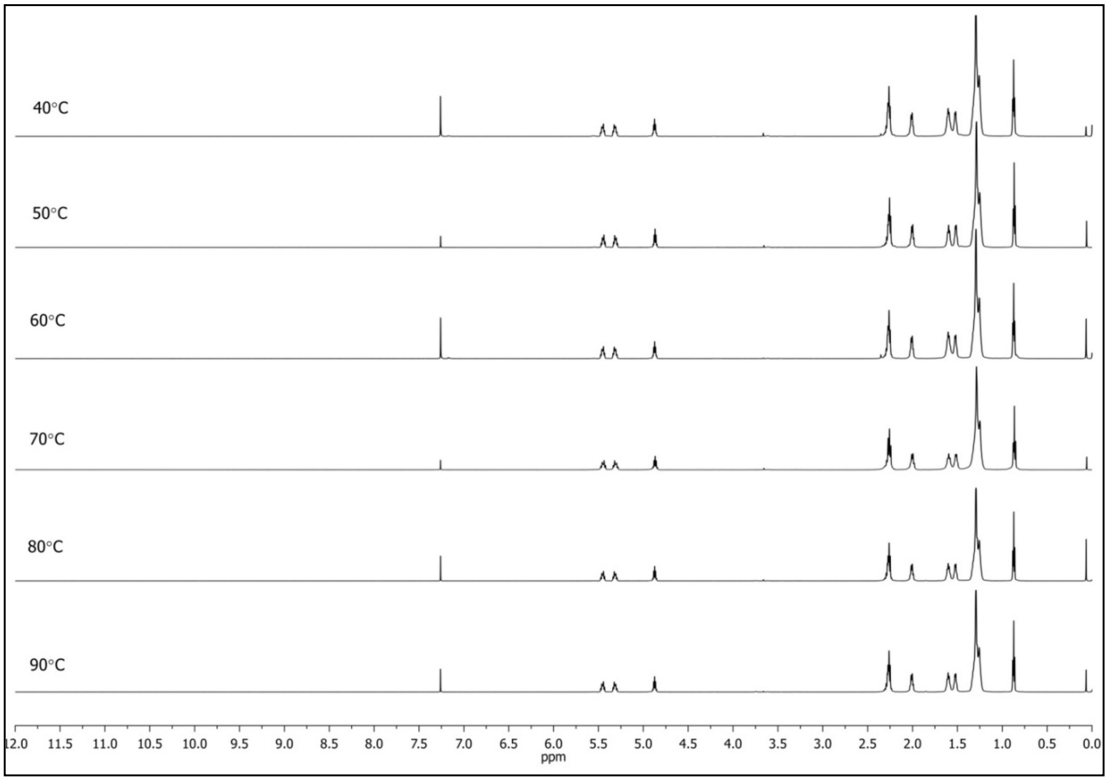


Figure B1.16: ^{1}H NMR spectra of polyricinoleates synthesized at various temperatures, for 7 days, in the presence of Lipozyme TL IM.

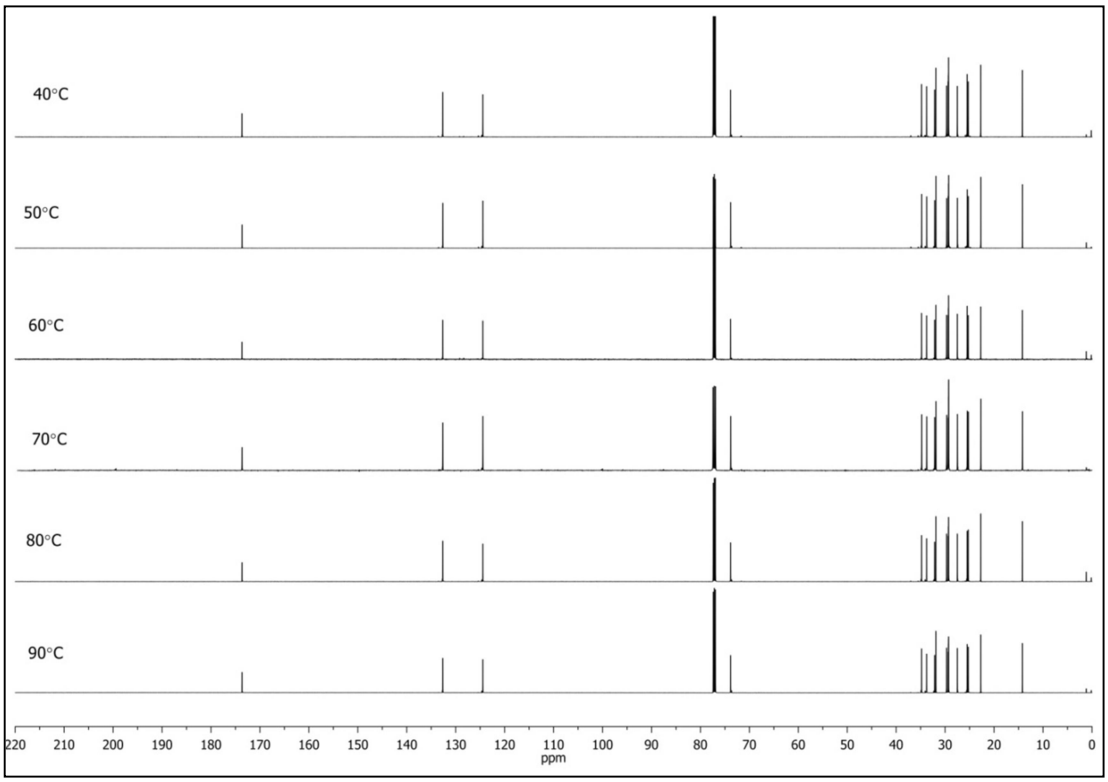


Figure B1.17: ^{13}C NMR spectra of polyricinoleates synthesized at various temperatures, for 7 days, in the presence of Lipozyme TL IM.

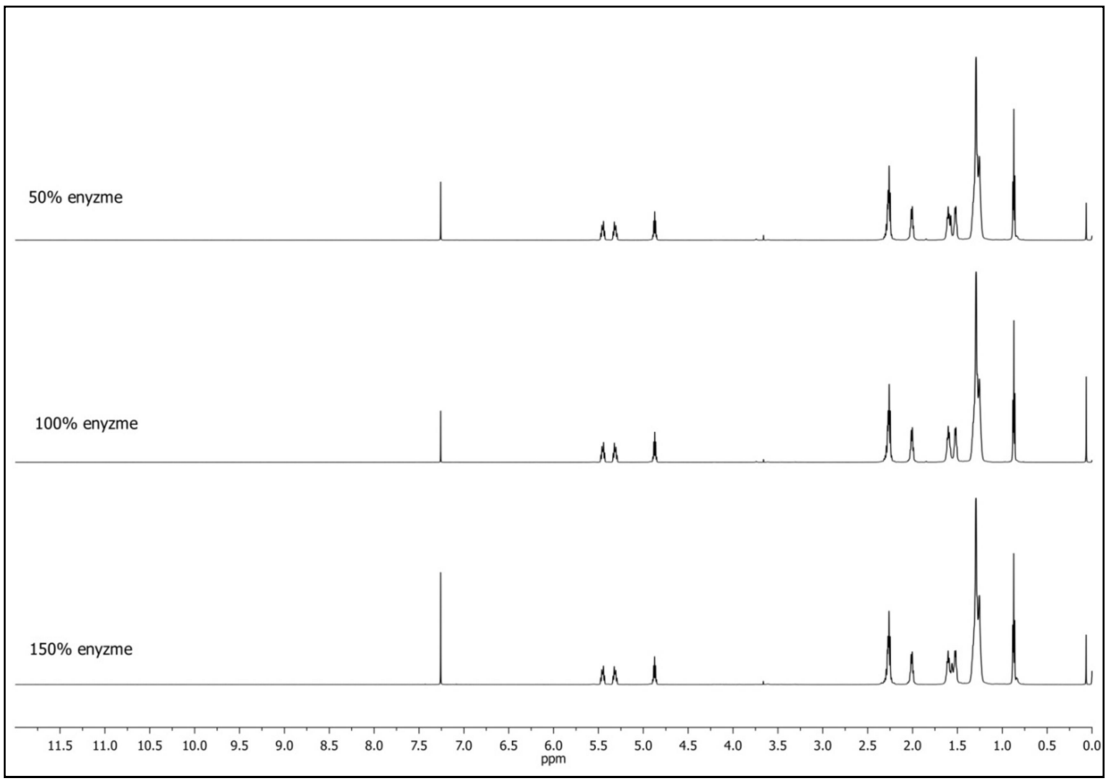


Figure B1.18: ^{1}H NMR spectra of polyricinoleates synthesized at enzyme/monomer ratios, for 7 days, in the presence of Lipozyme TL IM, at 80°C.

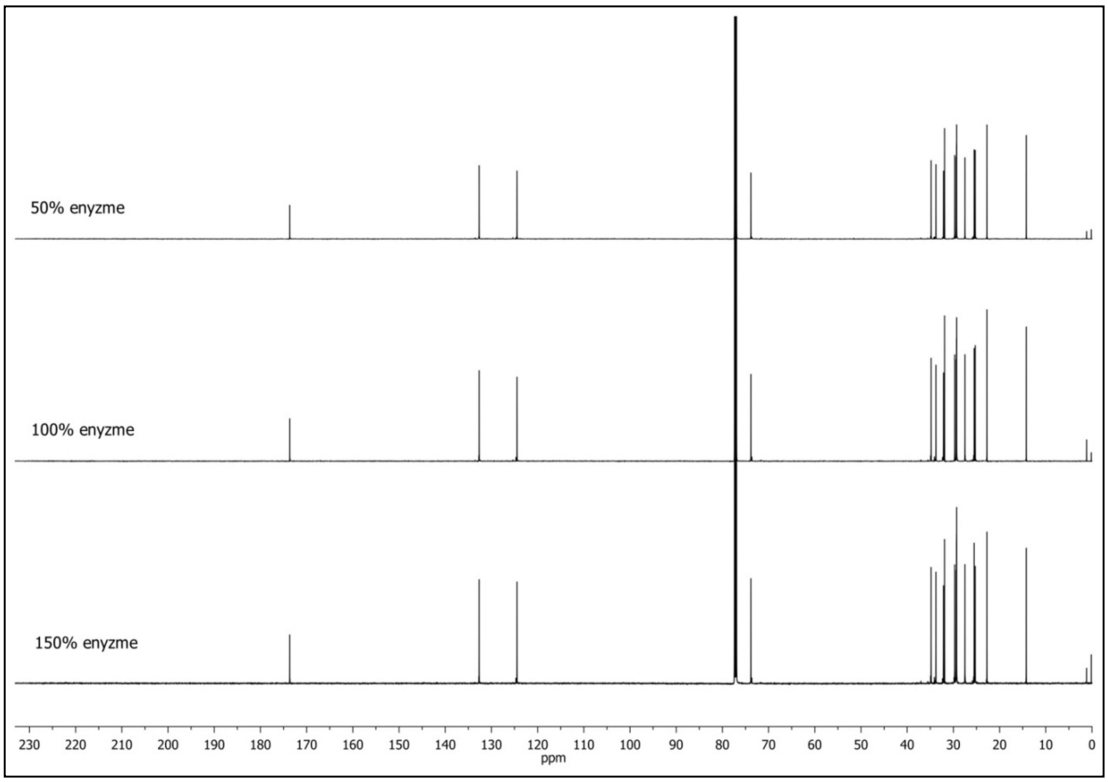


Figure B1.19: ^{13}C NMR spectra of polyricinoleates synthesized at enzyme/monomer ratios, for 7 days, in the presence of Lipozyme TL IM, at 80°C.

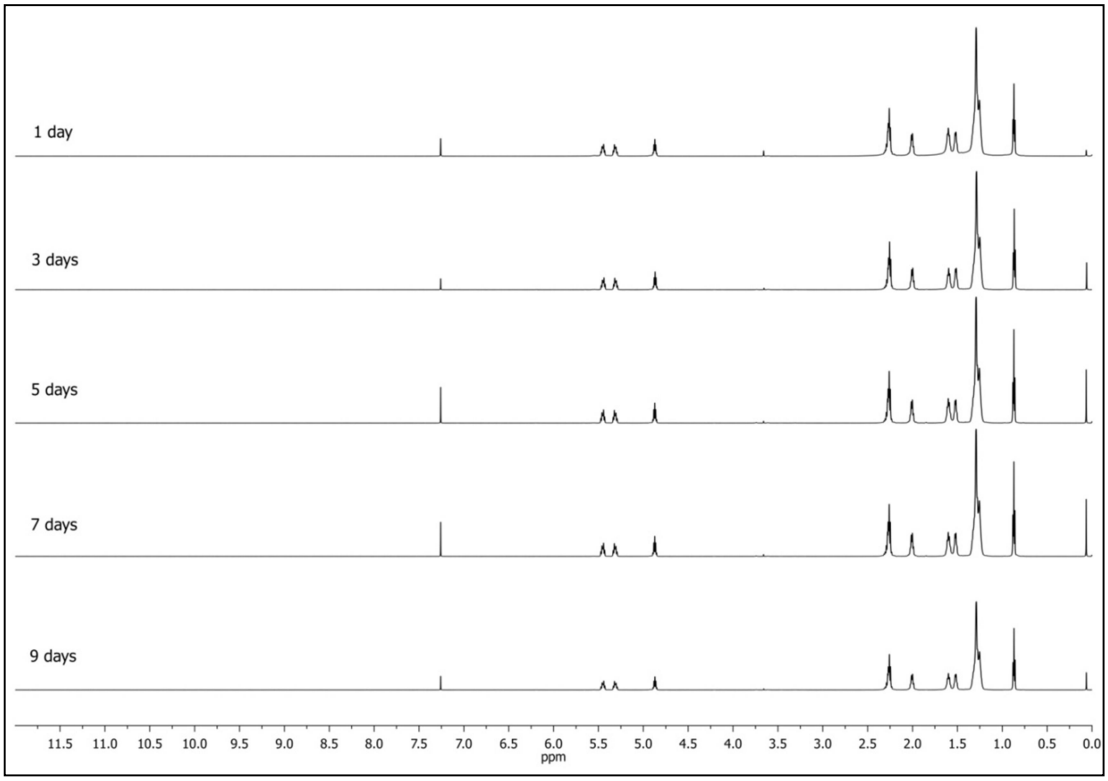


Figure B1.20: ^{1}H NMR spectra of polyricinoleates synthesized for various reaction times, in the presence of Lipozyme TL IM, at 80°C.

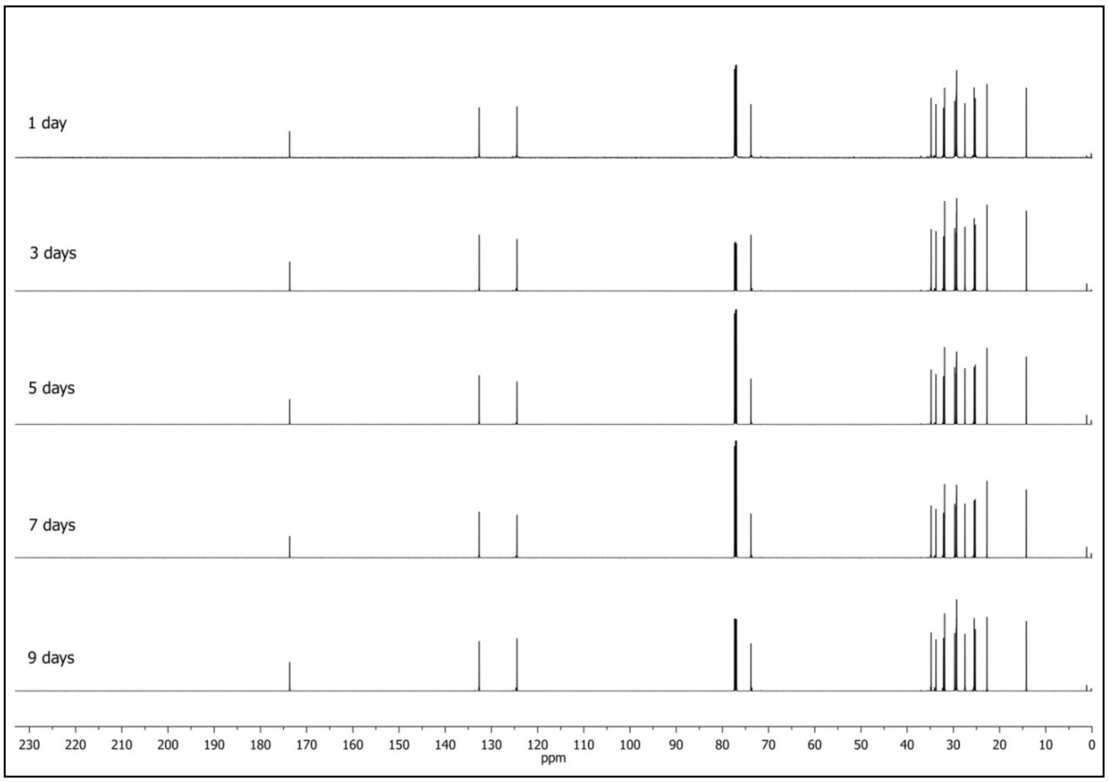


Figure B1.21: ^{13}C NMR spectra of polyricinoleates synthesized for varoius reaction times, in the presence of Lipozyme TL IM, at 80°C.